

2019

Beyond the Standard Model: Flavor Symmetry, Nonperturbative Unification, Quantum Gravity, and Dark Matter

Shikha Chaurasia

William & Mary - Arts & Sciences, shiksterz@gmail.com

Follow this and additional works at: <https://scholarworks.wm.edu/etd>



Part of the [Physics Commons](#)

Recommended Citation

Chaurasia, Shikha, "Beyond the Standard Model: Flavor Symmetry, Nonperturbative Unification, Quantum Gravity, and Dark Matter" (2019). *Dissertations, Theses, and Masters Projects*. William & Mary. Paper 1563898980.

<http://dx.doi.org/10.21220/s2-nr71-4303>

This Dissertation is brought to you for free and open access by the Theses, Dissertations, & Master Projects at W&M ScholarWorks. It has been accepted for inclusion in Dissertations, Theses, and Masters Projects by an authorized administrator of W&M ScholarWorks. For more information, please contact scholarworks@wm.edu.

Beyond the Standard Model: Flavor Symmetry, Nonperturbative Unification, Quantum Gravity, and Dark Matter

Shikha Chaurasia

Olney, Maryland

Master of Science, College of William & Mary, 2016
Bachelor of Science, College of Charleston, 2014

A Dissertation presented to the Graduate Faculty
of The College of William & Mary in Candidacy for the Degree of
Doctor of Philosophy

Department of Physics

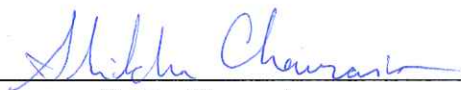
College of William & Mary
May 2019

©2019
Shikha Chaurasia
All rights reserved.

APPROVAL PAGE

This Dissertation is submitted in partial fulfillment of
the requirements for the degree of

Doctor of Philosophy



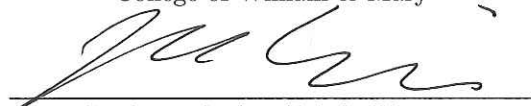
Shikha Chaurasia

Approved by the Committee March 2019



Committee Chair

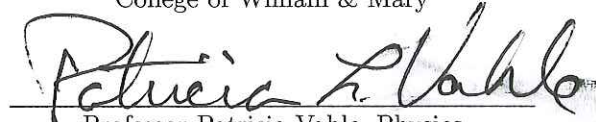
Professor Christopher Carone, Physics
College of William & Mary



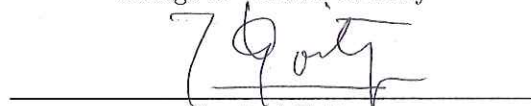
Professor Joshua Erlich, Physics
College of William & Mary



Professor Marc Sher, Physics
College of William & Mary



Professor Patricia Vahle, Physics
College of William & Mary



Dr. José Goity

Hampton University and Jefferson Laboratory

ABSTRACT

Despite the vast success of the Standard Model of particle physics, it is no secret that it also has its shortcomings, thus providing incentive to look beyond the Standard Model for solutions. In this thesis we focus in particular on a model of horizontal flavor symmetry, unification via a universal Landau pole, emergent gravity, and dark matter. First we explain the observed hierarchies in the elementary fermion mass spectrum via a model based on the double tetrahedral group, the smallest discrete subgroup of $SU(2)$, while relaxing previous assumptions of supersymmetry. A sequential symmetry breaking process results in a hierarchy in the Yukawa couplings. Just as the Standard Model raises questions on the origin of the fermion mass spectrum, it similarly raises questions on the origins of its gauge couplings. We have to look beyond the Standard Model for the possibility of a unified description of the electromagnetic, weak and strong forces. As an alternative to conventional unification, we assume the existence of a universal Landau pole in which the gauge couplings blow up at a common scale in the ultraviolet. We consider extensions of the minimal scenario, to see if there are cases that might be probed at a future hadron collider. Next we focus on gravity, the fourth fundamental force that has yet to be embedded in the Standard Model. We consider a model where gravity is an emergent phenomenon in which the graviton appears as a bound state of scalars. We show how this approach can accommodate an arbitrary metric. Lastly we turn to the issue of dark matter, a hypothetical form of matter believed to account for a large portion of the universe but with no place in the Standard Model. We specifically focus on fermionic dark matter that is charged under the simplest non-Abelian dark gauge group. Exotic, vector-like leptons that also transform under the dark gauge group can mix with standard model leptons and serve as a portal between the dark and visible sectors. We present a framework based on symmetries that allows the mixing between the dark and visible sectors to be non-negligible, while simultaneously suppressing unwanted flavor-changing processes. By extending the particle content and symmetries of the Standard Model, we can solve its various issues. In this thesis we seek to explain the observed hierarchies in the fermion mass spectrum, provide a unified description of the three gauge couplings, generalize a model of emergent gravity, and create a model that gives rise to dark matter via a vector-like fermion portal.

TABLE OF CONTENTS

Acknowledgments	iii
Dedication	iv
List of Tables	v
List of Figures	vi
 CHAPTER	
1 Introduction	2
2 Flavor from the double tetrahedral group without supersymmetry	19
2.1 Introduction	20
2.2 Typical Yukawa textures from T-prime symmetry	24
2.3 Numerical analysis	29
2.4 Direct lower bounds on the flavor scale	35
2.5 Nonsupersymmetric models	40
2.6 Conclusions	43
3 Universal Landau Pole and Physics below the 100 TeV Scale	45
3.1 Introduction	46
3.2 One vector-like generation	49
3.3 Next-to-minimal possibilities	56
3.4 Model building issues	59
3.5 Conclusions	64

4	Curved Backgrounds in Emergent Gravity	66
4.1	Introduction	67
4.2	Emergent Gravity with Curved Backgrounds	70
4.3	Discussion and Conclusions	82
5	Dark sector portal with vector-like leptons and flavor sequestering	85
5.1	Introduction	86
5.2	The Model	90
5.3	Flavor sequestering	100
5.4	Phenomenology	105
5.4.1	Relic Density	105
5.4.2	Direct Detection	109
5.5	Conclusions	115
6	Conclusions	117
	Bibliography	120
	Vita	133

ACKNOWLEDGMENTS

I would like to thank my advisor, Dr. Christopher D. Carone, for his continuous support, guidance and encouragement in my classwork and research. He has been an excellent and patient mentor to me and really helped me grow as a scientist. I would also like to thank Dr. Joshua Erlich for inviting me to work with him and his student, Yiyu Zhou, which allowed me to broaden the scope of my research. I extend my gratitude to the collaborators I have had during my Ph.D., including Savannah Vasquez, Jack Donahue, and Tangereen Claringbold.

I am grateful for the friends I have made in the physics department, whose constant companionship became a source of comfort and joy throughout my time at William & Mary. Thanks also to my significant other, simply for being there. I would not be here without my family, who helped me realize my passion for physics, and supported me throughout my life. And last but not least I should probably thank my feline friend, whose ridiculous entity brought me back to earth when I was deep in the world of physics.

Dedicated to my loving parents.

LIST OF TABLES

2.1	Fit parameters and observables for a flavor scale of $M_F = 10^6$ GeV.	32
2.2	Fit parameters and observables for $M_F = 10^{18}$ GeV.	34
2.3	Lower bounds on the flavor scale.	37
2.4	Lower bound on M_F for the largest flavor-changing decays.	39
3.1	Numerical results for the scale of the vector-like matter m_V and the blow-up scale Λ for the minimal Landau pole scenario and a model with the same one-loop (but differing two-loop) beta functions as the minimal scenario.	54
3.2	Solutions for m_V and Λ , for a variety of next-to-minimal heavy matter sectors, for $m_{susy} \leq m_V$	58
3.3	Solutions for m_V and Λ , for a variety of next-to-minimal heavy matter sectors, for $m_{susy} \geq m_V$	60
3.4	Results for the next-to-minimal $(3, 2, 0, 2)$ scenario with $m_V = m_{susy}$ taking into account the effect of the additional SU(2) gauge group.	62

LIST OF FIGURES

1.1	Running of the Standard Model gauge couplings.	9
2.1	Minimum $\tilde{\chi}^2$ values as a function of the flavor scale, for two different model assumptions.	31
3.1	The dependence of the Weinberg angle and the third coupling constant on the mass of the vector-like generation in the minimal Landau pole scenario.	54
4.1	Leading large- N diagrams that give rise to the emergent gravitational interaction.	76
4.2	Feynman diagrams for our current theory.	77
4.3	Redefined theory where the matter field can scatter off of itself and the background field.	80
5.1	Qualitative picture of dark matter annihilation to a charged lepton-anti-lepton pair.	95
5.2	Regions of the dark gauge coupling - dark matter mass plane which produce the desired dark matter relic density band, for fixed choices of the dark gauge boson mass and mixing angle.	108
5.3	Self energies leading to kinetic mixing between the dark gauge boson and hypercharge after $SU(2)_D$ is spontaneously broken.	110
5.4	The Feynman diagram for the scattering of dark matter particles off of protons through kinetic mixing of the dark matter boson and the photon.	112
5.5	Upper bound on the fractional mass splitting of the vector-like leptons as a function of the mass of the dark matter particle, for fixed values of the dark gauge boson and coupling.	114

BEYOND THE STANDARD MODEL: FLAVOR SYMMETRY, NONPERTURBATIVE
UNIFICATION, QUANTUM GRAVITY, AND DARK MATTER

CHAPTER 1

Introduction

The Standard Model (SM) of particle physics describes how the elementary particles interact in the presence of electromagnetic, weak and strong forces. Although it has very successfully provided experimental predictions and lived up to experimental results, it leaves some phenomena unexplained and does not provide a unified description of all four fundamental interactions. Thus we have to look beyond the Standard Model for answers. Here we touch on some of the Standard Model's shortcomings and the models we have developed to explain phenomena that have yet to be resolved.

The SM particle content contains three generations of fermions whose representations in the $SU(3)_c \times SU(2)_L \times U(1)_Y$ gauge group are given by

$$Q_L (\mathbf{3}, \mathbf{2})_{1/6}, \quad u_R (\mathbf{3}, \mathbf{1})_{2/3}, \quad d_R (\mathbf{3}, \mathbf{1})_{-1/3}, \quad L_L (\mathbf{1}, \mathbf{2})_{-1/2}, \quad e_R (\mathbf{1}, \mathbf{1})_{-1}, \quad (1.1)$$

where we have suppressed generation indices. The up-type quarks, down-type quarks and

charged leptons have the same quantum numbers but different masses [1]:

$$\begin{aligned}
m_u &= 2.2 \text{ MeV}, & m_c &= 1.275 \text{ GeV}, & m_t &= 173 \text{ GeV}; \\
m_d &= 4.7 \text{ MeV}, & m_s &= 95 \text{ MeV}, & m_b &= 4.18 \text{ GeV}; \\
m_e &= 0.511 \text{ MeV}, & m_\mu &= 106 \text{ MeV}, & m_\tau &= 1.777 \text{ GeV}.
\end{aligned}
\tag{1.2}$$

Furthermore, the quark mass ratios renormalized at the grand unified scale are given approximately by

$$m_d :: m_s :: m_b = \lambda^4 :: \lambda^2 :: 1, \quad \text{while} \quad m_u :: m_c :: m_t = \lambda^8 :: \lambda^4 :: 1, \tag{1.3}$$

where $\lambda \approx 0.22$ is the Cabibbo angle [2]. This observation poses a number of questions; for instance, why are there three generations of quarks and leptons (as opposed to some other number)? And what is the origin of the charged fermion masses and the hierarchies in the spectrum? Evidently the down-type quark masses are similar in magnitude to the charged lepton masses, while the up-type quark masses are much more hierarchical; the third generation up-type quark is much larger in mass than the third generation particles of the other families. The Standard Model's inability to explain these observations is the flavor problem of particle physics.

The fermion masses arise from the Yukawa interactions,

$$\mathcal{L}_Y = -Y_{ij}^d \overline{Q}_{Li} \phi d_{Rj} - Y_{ij}^u \overline{Q}_{Li} \tilde{\phi} u_{Rj} - Y_{ij}^e \overline{L}_{Li} \phi e_{Rj} + \text{h.c.}, \tag{1.4}$$

where ϕ is the Higgs field, the scalar field responsible for breaking the $SU(2)_L \times U(1)_Y$ symmetry, $\tilde{\phi} = i\sigma_2 \phi^*$, i, j are generation indices and $Y^{u,d,\ell}$ are complex 3×3 matrices. When ϕ acquires a vacuum expectation value (vev), $\langle \phi \rangle = (0, v/\sqrt{2})$, the charged fermions gain masses. For the quark sector we identify unitary matrices V_{qL} and V_{qR} that diagonalize

the mass matrices such that

$$M_q^{\text{diag}} = V_{qL} M_q V_{qR}^\dagger, \quad q = u, d, \quad M_q = \frac{v}{\sqrt{2}} Y_q. \quad (1.5)$$

The quark mass eigenstates $q^{(0)}$ are subsequently given by $q_{Li}^{(0)} = (V_{qL})_{ij} q_{Lj}$ and $q_{Ri}^{(0)} = (V_{qR})_{ij} q_{Rj}$. In the basis in which the masses are diagonal, the charged current weak interactions are not,

$$\mathcal{L}_{W^\pm}^q = -\frac{g}{\sqrt{2}} \overline{u_{Li}^{(0)}} \gamma^\mu W_\mu^+ (V_{uL} V_{dL}^\dagger)_{ij} d_{Lj}^{(0)} + \text{h.c.}, \quad (1.6)$$

where g is the $SU(2)_W$ gauge coupling. Hence the charged weak gauge bosons W^\pm couple to the mass eigenstates of different generations, and this is the only instance of interactions that change quark flavor in the Standard Model. The discrepancy between the flavor and mass bases is represented by V_{CKM} , the 3×3 unitary Cabibbo-Kobayashi-Maskawa (CKM) matrix [1]:

$$V_{\text{CKM}} \equiv V_{uL} V_{dL}^\dagger = \begin{pmatrix} V_{ud} & V_{us} & V_{ub} \\ V_{cd} & V_{cs} & V_{cb} \\ V_{td} & V_{ts} & V_{tb} \end{pmatrix} \approx \begin{pmatrix} 1 & 0.2 & 0.004 \\ 0.2 & 1 & 0.04 \\ 0.008 & 0.04 & 1 \end{pmatrix}, \quad (1.7)$$

where the second matrix in the Eq. (1.7) only displays approximate magnitudes. The CKM matrix is nearly diagonal, parameterized by three mixing angles (the largest one being the Cabibbo angle), and the phase responsible for all CP -violating phenomena in flavor-changing processes. The CKM matrix elements have been well measured, as they are fundamental parameters of the Standard Model. But what is the origin of the hierarchies in the CKM matrix? This is another question posed by the flavor problem of the standard model.

It is a possibility that the observed hierarchy of fermion masses and mixing angles originates from the spontaneous breaking of a new horizontal flavor symmetry, G_F . Ideally only the Yukawa couplings for the third generation are allowed by the horizontal symmetry, thereby accounting for the large, order-one top quark Yukawa coupling. The horizontal symmetry is sequentially broken at energy scales μ_i through a series of nested subgroups H_i , such that

$$G_F \xrightarrow{\mu_1} H_1 \xrightarrow{\mu_2} H_2 \xrightarrow{\mu_3} \dots \quad \text{for } \mu_1 > \mu_2 > \mu_3. \quad (1.8)$$

Here $\mu_i \equiv \langle \phi_i \rangle / M_F$, where ϕ_i is the flavon field whose vev breaks H_{i-1} to H_i , and M_F is the ultraviolet cutoff of G_F [3]. The hierarchical structure of the Yukawa couplings is achieved on account of the differing energy scales that are associated with the various stages of symmetry breaking $\langle \phi_i \rangle$. Of course, a model with a horizontal symmetry is successful if it yields Yukawa textures that are phenomenologically viable.

The literature contains many studies in which a horizontal symmetry is introduced to obtain the hierarchical structure of the fermion masses. Models have been proposed with Abelian [5, 6] and non-Abelian [7, 8, 9, 10, 11] continuous and discrete symmetries. One type of particularly successful model considered in the literature assumes the continuous, global symmetry $G_F = U(2)$ [12, 13, 14]. These models involve fields in **1**, **2** and **3** dimensional representations (reps), with quarks and leptons embedded into $\mathbf{2} \oplus \mathbf{1}$ dimensional reps. This allows for an order-one top quark Yukawa coupling, as the third generation fields are treated differently. A set of flavons (the symmetry-breaking fields) appears in all three of these representations. The $U(2)$ group contains the multiplication rule $\mathbf{2} \otimes \mathbf{2} = \mathbf{3} \oplus \mathbf{1}$, which results in a symmetric and antisymmetric decomposition of the Yukawa matrices

for first and second generation fields so that the Yukawa sector takes the form:

$$Y_{U,D,E} \sim \left(\begin{array}{c|c} S_{ab} + A_{ab} & \phi_a \\ \hline \phi_a & 1 \end{array} \right). \quad (1.9)$$

Here ϕ_a , S_{ab} and A_{ab} are a set of flavon fields, where ϕ is a U(2) doublet, S is a symmetric U(2) triplet and A is an antisymmetric U(2) singlet. The U(2) symmetry is broken to a U(1) subgroup that rotates all first generation fields by a phase. This forbids Yukawa couplings involving first generation fields. The residual U(1) symmetry is broken at a lower scale to nothing; this sequential symmetry breaking produces a hierarchy in the Yukawa couplings.

Although a horizontal U(2) symmetry explains the observed hierarchy of fermion masses, it is not the most minimal symmetry. In Refs. [3, 4], Aranda, Carone and Lebed consider the smallest discrete flavor group that predicts the same form of the Yukawa textures. This is accomplished by assuming the symmetry $G_F = T' \times Z_3$ and the breaking pattern

$$T' \times Z_3 \xrightarrow{\epsilon} Z_3^D \xrightarrow{\epsilon'} \text{nothing}. \quad (1.10)$$

Here Z_3 is a discrete Abelian subgroup of U(1) and T' is the double tetrahedral group, the smallest discrete subgroup of SU(2) with **1**, **2** and **3** dimensional reps and the multiplication rule $\mathbf{2} \otimes \mathbf{2} = \mathbf{3} \oplus \mathbf{1}$. T' contains 24 elements: 12 elements that correspond to the 12 proper rotations that take a regular tetrahedron into coincidence with itself, while the remaining 12 elements result from a rotation by 2π of the first set, which produces a factor of -1 in the even-dimensional reps. The $T' \times Z_3$ flavor group contains the diagonal Z_3^D subgroup, which is responsible for rotating all first-generation matter fields by a phase. When the $T' \times Z_3$ symmetry is broken to Z_3^D , it is assumed that the doublet and triplet

flavons ϕ and S acquire the vevs

$$\frac{\langle\phi\rangle}{M_F} \sim \begin{pmatrix} 0 \\ \epsilon \end{pmatrix}, \quad \frac{\langle S\rangle}{M_F} \sim \begin{pmatrix} 0 & 0 \\ 0 & \epsilon \end{pmatrix}. \quad (1.11)$$

Yukawa couplings involving first generation fields are generated after the Z_3^D symmetry is broken at a lower scale by the flavon A :

$$\frac{\langle A\rangle}{M_F} \sim \begin{pmatrix} 0 & \epsilon' \\ -\epsilon' & 0 \end{pmatrix}, \quad (1.12)$$

where $\epsilon' < \epsilon$. The sequential symmetry breaking in Eq. (1.10) yields the following Yukawa textures for the up quarks, down quarks and leptons:

$$Y_U = \begin{pmatrix} 0 & u_1\epsilon'\rho & 0 \\ -u_1\epsilon'\rho & u_2\epsilon\rho & u_3\epsilon \\ 0 & u_4\epsilon & u_5 \end{pmatrix}, \quad Y_D = \begin{pmatrix} 0 & d_1\epsilon' & 0 \\ -d_1\epsilon' & d_2\epsilon & d_3\epsilon \\ 0 & d_4\epsilon & d_5 \end{pmatrix} \xi, \quad Y_E = \begin{pmatrix} 0 & \ell_1\epsilon' & 0 \\ -\ell_1\epsilon' & \ell_2\epsilon & \ell_3\epsilon \\ 0 & \ell_4\epsilon & \ell_5 \end{pmatrix} \xi. \quad (1.13)$$

Here u_i , d_i and ℓ_i are undetermined $\mathcal{O}(1)$ operator coefficients that can be determined by a global fit. Alas the $T' \times Z_3$ flavor symmetry by itself cannot explain the discrepancies between the hierarchies within Y_U , Y_D and Y_E (see Eq. (1.3)). To accommodate for this we include the additional suppression factors ρ and ξ , which arise via additional symmetries. In the original supersymmetric $T' \times Z_3$ models in Refs. [3, 4], the most elegant origin for these suppression factors were obtained by working in the context of an SU(5) grand unification.

Previous studies by Aranda, Carone and Lebed have utilized the double tetrahe-

dral group to build flavor models that provide a successful description of charged fermion masses and the CKM mixing elements. However these theories were constructed nearly two decades ago, back when it was assumed that weak-scale supersymmetry was the likely solution to the hierarchy problem. However the LHC has yet to produce any results that would confirm the existence of supersymmetry, thereby reducing confidence in supersymmetry as a key ingredient in tackling issues raised by the standard model. Instead we ask the question, how well do the T' flavor models in Refs. [3, 4] work if there is no supersymmetry below the Planck scale?

In our study discussed in Chapter 2, we numerically evolve the Yukawa matrices in Eq. (2.13) using the one-loop, nonsupersymmetric renormalization groups equations (RGEs). The RGEs are run down from the flavor scale, M_F , to the weak scale, m_Z (the mass of the Z boson). The flavor scale is varied from the TeV scale to the Planck scale, M_{Pl} , and the Yukawa matrices are diagonalized at the weak scale. We perform global fits to the charged fermion masses and the CKM angles. Our results indicate that T' models without supersymmetry provide viable phenomenological results for a wide range of M_F , with a preference for values closer to the TeV scale than the Planck scale. However the feasibility of $M_F \sim M_{Pl}$ is consistent with the possibility that there is no new physics between the weak and gravitational scales. The lowest M_F are further constrained by flavor-changing-neutral-current (FCNC) processes that receive contributions from physical components of the flavon fields, thus providing indirect probes of the model.

In building flavor models, we aim to explain the origin of the Yukawa couplings. Similarly we may also attempt to explain the origins of the Standard Model's gauge couplings, α_1 , α_2 and α_3 , which characterize the strength of the electromagnetic, weak and strong forces. The coupling constants are dependent on the energy scale, μ , at which one observes

them, and the running of the couplings is encoded in the renormalization group equations:

$$\frac{dg_i}{dt} = \frac{g_i}{16\pi^2} \left[b_i g_i^2 + \frac{1}{16\pi^2} \left(\sum_{j=1} b_{ij} g_i^2 g_j^2 - \sum_{j=U,D,E} a_{ij} g_i^2 \text{tr}[Y_j Y_j^\dagger] \right) \right], \quad (1.14)$$

where $t = \ln \mu$ is the log of the renormalization scale, $\alpha_i = g_i^2/4\pi$, b_i and b_{ij} are the beta function coefficients and a_{ij} are the coefficients for the Yukawa matrices Y_i (though in practice only the top quark Yukawa coupling needs to be taken into account since it is significantly larger than the other Yukawa couplings). The evolution of the Standard Model RGE's from the weak scale to the Planck scale is given in Fig. 1.1.

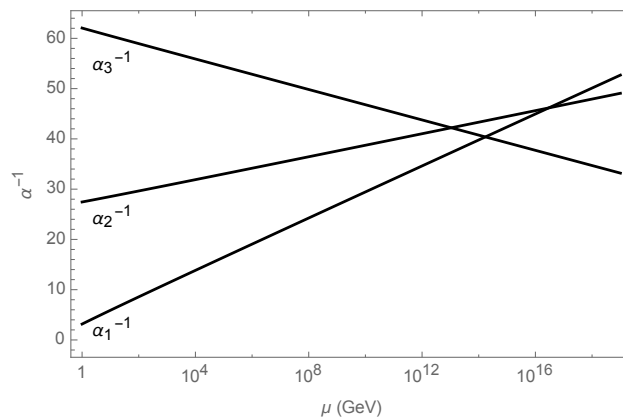


FIG. 1.1: Running of the Standard Model gauge couplings from the weak scale to the Planck scale.

Fig. 1.1 is suggestive of unification, and with additional physics beyond the Standard Model it is possible that the gauge couplings meet at a high scale. In this case hypercharge would be unified with the strong and weak forces, which would explain why fundamental particles carry electric charges that appear to be exact multiples of $1/3$ of the elementary charge, as opposed to other arbitrary numbers. Charge quantization can be addressed through the introduction of a grand unified theory (GUT) in which the SM gauge group is embedded in a larger underlying gauge group (such as $SU(5)$) with a single gauge coupling constant [15]. Quarks and leptons are placed together in irreducible representations of the

underlying group and are related by its symmetries. For instance if we embed the SM in $SU(5)$, the fermions fit neatly into its anomaly-free chiral $\bar{5} \oplus 10$ representation. The underlying group is then broken to $SU(3) \times SU(2) \times U(1)$ at some high scale, typically in the $10^{14} - 10^{16}$ GeV range [16]. Above this scale all fermions and their interactions would appear very much alike, and thus the electromagnetic, weak and strong forces would all come together (up to normalization factors) at the GUT scale.

Although a tantalizing idea, grand unified theories have their shortcomings as well. Many GUT models explicitly break the baryon number symmetry, allowing protons to decay, in contradiction with current experimental evidence [17]. In supersymmetric GUT models, an extreme fine-tuning of parameters is required to produce a large mass splitting in Higgs multiplets, called the “doublet-triplet splitting problem” [18], to keep the SM Higgs doublet much lighter than the GUT scale. However, there is an alternative framework in which the gauge couplings assume a common value at a high energy scale without calling for conventional grand unification. Instead we assume the existence of a universal Landau pole in which the gauge couplings blow up at a common scale Λ in the ultraviolet:

$$\alpha_1^{-1}(\Lambda) = \alpha_2^{-1}(\Lambda) = \alpha_3^{-1}(\Lambda) = 0. \quad (1.15)$$

A universal Landau pole may arise in models with composite gauge bosons. For instance, the QED Lagrangian with radiative corrections contains the terms

$$\mathcal{L} \supset -\frac{1}{4}Z(\mu)F^{\mu\nu}F_{\mu\nu} + g_0 A^\mu \bar{\psi} \gamma_\mu \psi. \quad (1.16)$$

If the photon were composite, we would expect the photon’s wave-function renormalization factor to vanish at the compositeness scale, i.e., $Z(\Lambda_{\text{comp}}) = 0$, indicating that the photon has become nondynamical. Redefining the fields and couplings so that the gauge field’s

kinetic term retains its canonical form,

$$\mathcal{L} \supset -\frac{1}{4}F^{\mu\nu}F_{\mu\nu} + \frac{g_0}{\sqrt{Z(\mu)}}A^\mu\bar{\psi}\gamma_\mu\psi, \quad (1.17)$$

the gauge coupling is given by $g(\mu) = g_0/\sqrt{Z(\mu)}$, which blows up as the wave-function renormalization factor goes to zero at the compositeness scale. This gives plausibility to the boundary condition in Eq. (1.15).

For a universal Landau pole to be achieved all the gauge couplings must be asymptotically non-free, but since this is not the case for the SU(3) coupling in the minimal supersymmetric standard model (MSSM), additional matter is necessary. The simplest implementation of this idea is presented in Ref. [18], in which the MSSM is augmented by an additional vector-like generation of matter fields at the TeV scale. In Chapter 3 of this thesis we revisit this minimal scenario and find extensions that produce more viable phenomenological results.

There are two scales to consider: the scale of the new vector-like matter, m_V , and the susy-breaking scale, m_{susy} . In the previous literature the two scales were set equal to one another [18], although we allow them to vary independently in our study. For a given choice of m_V and m_{susy} , we fix the blow-up scale Λ by the requirement that the correct value of the fine structure constant at the weak scale is reproduced. We then compute the weak scale values of α_3^{-1} and the Weinberg angle $\sin^2\theta_W$ up to theoretical uncertainties. A viable solution is obtained if a value of m_V and m_{susy} can be found in which both $\sin^2\theta_W(m_Z)$ and $\alpha_3^{-1}(m_Z)$ are consistent with the data.

At the Landau pole in Eq. (1.15) the gauge couplings are in the non-perturbative regime, where the RGEs cannot be trusted. Instead we impose the boundary condition $\alpha_1(\Lambda) = \alpha_2(\Lambda) = \alpha_3(\Lambda) = 10$, values that are barely perturbative. This still effectively results in a Landau pole since for $\alpha(\Lambda) = 10$ and $\alpha(\Lambda_{\text{actual}}) = \infty$, there is negligible

difference between Λ and Λ_{actual} , as the couplings rapidly increase as the renormalization scale is increased. To determine the theoretical uncertainty we vary α_i independently between 1 and 100 at the blow-up scale and find that the low-energy coupling constants are nearly independent of the precise choice of boundary conditions, as long as the couplings are large at Λ . This insensitivity is due to the existence of an infrared fixed point in the RGE for the ratios of the gauge couplings [19].

As the minimal scenario described above was studied more than two decades ago, we reproduce it with up-to-date experimental data, but find that it requires values of either m_V or m_{susy} that are in some tension with current LHC bounds. Thus we consider extensions of the minimal scenario, particularly by including a small number of additional complete SU(5) multiplets of vector-like matter, as this is known to preserve successful unification. This leads to solutions for m_V that are beyond the reach of the LHC, but potentially within reach of a 100 TeV future hadron collider for some choices of m_{susy} . We consider the possibility that the new matter fields transform under an additional gauge group that is constrained by the same ultraviolet boundary condition. In that case the heavy fields could fall in irreducible representations of the new gauge group, explaining the multiplicity of new particles required to achieve the Landau pole. We explore the consequences of the heavy matter sector being vector-like or chiral under the new gauge group.

We have discussed scenarios in which the three gauge couplings unify, but there is a fourth fundamental force to consider: gravity. The electromagnetic, weak and strong forces are successfully described in a quantum mechanical framework, while our current understanding of gravity is based on Einstein's general theory of relativity, which is derived within the framework of classical physics. To unify gravity with the other forces we would first need to find a consistent quantum mechanical description.

Quantizing gravity necessitates the existence of a force-carrying particle akin to the

photon of the electromagnetic interaction; this can be accomplished with the introduction of the spin-two massless graviton. But when applying standard protocols of quantum field theory to the graviton, the resulting theory is not renormalizable and consequently the predictivity of the theory is lost. In a renormalizable theory there exists a finite number of relevant parameters, capable of being measured via experiment, which encodes all the physics of the theory at a particular energy scale. For instance in quantum electrodynamics these parameters are the mass and charge of the electron. Then the number of divergences are finite and may be absorbed into the renormalization of these parameters. In the case of gravity the number of divergences is not finite [20]. The Einstein-Hilbert term is given by

$$S_{EH} = \frac{1}{16\pi G_N} \int d^D x \mathcal{R} \sqrt{-g} = \frac{1}{2\kappa^2} \int d^D x \mathcal{R} \sqrt{-g} \quad (1.18)$$

where G_N is Newton's gravitational constant, κ is related to the d-dimensional Planck length, $g = \det(|g_{\mu\nu}|)$ is the determinant of the metric tensor and \mathcal{R} is the Ricci (curvature) scalar of general relativity. To expand the gravitational action around flat space we write $g_{\mu\nu} = \eta_{\mu\nu} + \kappa h_{\mu\nu}$, where $\eta_{\mu\nu}$ is the flat-space metric and $h_{\mu\nu}$ is a perturbation about it. Then an expansion in the action results in an infinite series of the form

$$S_{EH} \sim \frac{1}{2} \sum_{n=0}^{\infty} \int d^D x (\partial h)^2 (\kappa h)^n, \quad (1.19)$$

where κ^2 has units of $[L]^{D-2}$ and so is not dimensionless for $D > 2$ [20]. Each term in the expansion receives divergent loop contributions involving lower order terms, requiring an ever-increasing number of counterterms to cancel the divergences. Accordingly we would need to specify an infinite set of parameters before the theory is fixed, wherein the process of renormalization fails.

Besides nonrenormalizability, quantum gravity also faces the problem of time. Quan-

tum mechanics takes the flow of time to be universal and absolute, as it acts as an independent background through which states evolve. The Hamiltonian operator is responsible for generating infinitesimal translations of quantum states through time. In contrast general relativity assumes that time is a dynamical variable. But this would require the Hamiltonian to vanish, producing an absence of dynamics of quantum states.

String theory has commonly been called upon to resolve some of these issues. It introduces a new length scale, related to the string tension, at which particles are no longer pointlike. Oscillations of the string manifest themselves as new symmetries (particularly supersymmetry) that reduce the infinite parameters to a finite set. However as it was pointed out above there is an increasing loss of confidence in supersymmetry, as the LHC has yet to produce any results that confirm its existence. Furthermore, string theory introduces a huge number of ground state vacua, perhaps $\sim 10^{500}$ [21], so there is a price to pay in making quantum gravity finite. Thus we focus on another possibility: the emergence of gravity as the effective description of a massless composite spin-two state.

The possibility of emergent long-range interactions in quantum field theory is not limited to gravity. In Ref. [22], Bjorken argued that a four-fermion interaction of the form $\mathcal{L}_{int} = G_F(\bar{\psi}\gamma^\mu\psi)(\bar{\psi}\gamma_\mu\psi)$ gives rise to a massless spin-one composite state with interactions akin to the photon in electrodynamics. During the development of the theory of the strong sector, it was briefly considered that quantum chromodynamics emerged as consequence of color confinement imposed via a constraint of vanishing color current, rather than the other way around [24, 25]. Since the Standard Model provided a successful description of the electroweak and strong interactions, the existence of emergent gauge interactions was no longer necessary to explain existing phenomena. However the Standard Model has yet to successfully incorporate general relativity, and so the paradigm of emergent gravity remains compelling. Much of the activity in this area has been inspired by Ref. [26], in which Sakharov pointed out that the dynamics of spacetime emerge in a generally

covariant quantum field theory which contains a covariant regulator to resolve infinities in perturbation theory. The regularized effective action for the spacetime metric contains the Einstein-Hilbert term, even if no such term is present at tree level.

In Ref. [27], Carone, Erlich and Vaman were motivated by the observation that gauge interactions can emerge from a constraint of vanishing current and studied the possibility that by analogy gravitational interactions emerge via a constraint of vanishing energy-momentum tensor. They created a scalar field theory with a vanishing energy-momentum tensor that has a perturbative low-energy description, and demonstrated that the scattering of scalar particles includes a massless spin-two pole, corresponding to the exchange of a massless composite graviton that couples to matter as in Einstein gravity. Dimensional regularization is used as a placeholder for a generally covariant, physical regulator, and the gravitational coupling is determined by this regularization. The problem of time is addressed by allowing for certain scalar fields to play the role of the physical clock and rulers by a gauge-fixing condition analogous to the static-gauge condition in string theory.

In Chapter 4 we generalize this model of emergent gravity; the theory in the previous study assumed a flat-space metric, while we study the consequences of a model with a general field-space metric for the scalar fields that play the role of clock and rulers. A field redefinition cannot take a curved-space metric to a flat-space one, so the theory with a general field-space metric is genuinely inequivalent to the flat-space version in the previous study. The static-gauge configuration satisfies the classical equations of motion, with all other fields sitting at the minimum of the potential and with the emergent spacetime metric equal to the field-space metric. Thus there is a natural perturbative expansion about this classical background. We write the curved-space metric as an expansion about the Minkowski metric, $G_{\mu\nu} = \eta_{\mu\nu} + \tilde{H}_{\mu\nu}$, where $\tilde{H}_{\mu\nu}$ determines the background spacetime, and we show that scattering off this background spacetime is as in general relativity.

Although the quantization of gravity remains an open question, classical general rela-

tivity continues to be an excellent description of the universe at macroscopic scales provided that one additional ingredient is assumed: dark matter, a hypothetical form of matter that does not directly interact with observable electromagnetic radiation but believed to account for approximately 85% of the total matter in the universe [28]. Yet this mystery has no place in the Standard Model, despite a variety of astrophysical phenomena implying its existence. The primary evidence for dark matter arises from galactic rotation curves, which illustrate how the orbital velocity of visible stars and gas in a galaxy varies with their distance from the galaxy’s center. From Kepler’s Second Law, it is expected that the rotational velocities of stars in spiral galaxies would decrease with distance from the galactic center; however the rotational velocities have been observed to remain flat with increasing distance. This inconsistency suggests that each galaxy is surrounded by significant amounts of non-luminous matter (dark matter).

The primary candidate for dark matter is some new sort of elementary particle that has yet to be discovered; candidates include weakly-interacting massive particles (WIMPs), axions (hypothetical particles postulated to resolve the strong charge-parity problem in quantum chromodynamics), sterile neutrinos (heavy neutrinos without electroweak quantum numbers that are motivated to explain the observed neutrino masses), and in supersymmetric models, the LSP (lightest supersymmetric partner). There are many experiments aimed at detecting dark matter, divided into two classes: direct detection experiments (including LUX [29], XENON [30], CDMS [31]), which observe the effects of dark matter collisions with atomic nuclei within a detector, and indirect detection experiments (including PAMELA [32] and IceCube [33]), which search for the products from the annihilation or decay of dark matter particles in the galaxy, including excessive bursts of gamma rays, positrons or antiprotons.

All dark matter models have to annihilate a sufficient amount of dark matter so that the correct relic density is obtained. Dark matter “freezes out” when its interactions prob-

ability per unit time falls below the expansion rate of the universe [34]. The literature contains many diverse dark matter models which reproduce the desired relic density, although they all usually contain three components: the visible sector that at a minimum includes all the standard model fields, the dark sector which consists of a collection of fields that communicate very weakly with the visible sector, and the messenger or portal sector which enables a coupling between the previous two sectors. Dark matter models have been proposed with Abelian and non-Abelian symmetries; see Refs. [35, 36, 37, 38, 39] for examples of the former and Refs. [40, 41, 42, 43, 44, 45, 46] for the latter. There are a wide variety of proposed portals between the dark and visible sectors, including kinetic mixing portals, Higgs portals, and vector-like fermion portals.

In Chapter 5 we consider fermionic dark matter that is charged under the simplest non-Abelian dark gauge group, and focus on the case where the vector-like fermion portal is dominant. Such a portal consists of vector-like fermions that are charged under the dark gauge group but contain the quantum numbers of some standard model particle (in our case, the right-handed electron), so that communication between the dark and visible sectors can occur via mass mixing. In our model, the dark gauge boson couples to a vector-like state that mixes with standard model leptons after the dark and visible gauge symmetries of the theory are spontaneously broken. However, lepton-flavor-violating processes emerge when the vector-like lepton mixes with all three standard model flavors. Consequently, there are bounds on vector-like heavy leptons that exceed 100 TeV [47]. But to obtain a sufficient dark matter annihilation cross section to a standard model lepton, the mixing angle cannot be too small, which implies that the vector-like leptons cannot be arbitrarily heavy. To work around the stringent lower bounds on heavy vector-like leptons that arise from lepton-flavor-violating processes, we identify a mechanism, based on discrete symmetries, that we call “flavor sequestering.” This allows for mixing between the vector-like leptons and a single standard model lepton flavor exclusively (the remaining standard

model lepton flavors may only mix with each other). Thus lepton flavor violation is suppressed, providing for vector-like fermion portal sectors that are lighter. Then the mixing angle between the vector-like lepton and the chosen lepton flavor can be large enough so that an adequate scattering cross section is obtained from dark matter annihilation to a lepton-anti-lepton pair. The vector-like fermion portal we present is renormalizeable and completely specified; we explicitly investigate the flavor structure dictating the mixing between the exotic and standard model fields and the resulting phenomenology. Specifically, we look for regions of parameter space that successfully reproduce the dark matter relic density and satisfy current direct detection bounds.

To recap: this thesis addresses a variety of issues that are not resolved by the Standard Model. In Chapter 2, we explain the observed hierarchies in the elementary fermion mass spectrum via a model based on the double tetrahedral group, a subgroup of $SU(2)$, without relying on supersymmetry. In Chapter 3, we consider an alternative to conventional unification in which the electromagnetic, weak and strong couplings blow up at a common Landau pole and consider extensions of the minimal scenario, to see if there are cases that might be probed at a future 100 TeV collider. In Chapter 4, we turn to the issue of quantum gravity, generalizing a composite graviton model to the case of curved spacetime backgrounds. In Chapter 5, we consider a model with fermionic dark matter that communicates with the Standard Model via a vector-like fermion portal. We present a framework based on symmetries that allows the mixing between the dark and visible sectors to be non-negligible, while simultaneously suppressing unwanted flavor-changing processes. Lastly we summarize our conclusions in Chapter 6.

CHAPTER 2

Flavor from the double tetrahedral group without supersymmetry ¹

In this chapter we consider a class of previous flavor models, relaxing the assumption of supersymmetry and allowing the flavor scale to float anywhere between the weak and Planck scales. We perform global fits to the charged fermion masses and CKM angles, and consider the dependence of the results on the unknown mass scale of the flavor sector. We find that the typical Yukawa textures in these models provide a good description of the data over a wide range of flavor scales, with a preference for those that approach the lower bounds allowed by flavor-changing-neutral-current constraints. Nevertheless, the possibility that the flavor scale and Planck scale are identified remains viable. We present models that demonstrate how the assumed textures can arise most simply in a non-supersymmetric framework.

¹Work previously published in C. D. Carone, S. Chaurasia and S. Vasquez, “Flavor from the double tetrahedral group without supersymmetry,” *Phys. Rev. D* **95**, no. 1, 015025 (2017) [arXiv:1611.00784 [hep-ph]].

2.1 Introduction

There is a vast literature on models that attempt to explain the observed hierarchy of fermion masses by means of horizontal symmetries. In this chapter, we revisit one such model, proposed by Aranda, Carone and Lebed, based on the double tetrahedral group T' [3, 4]. Prior to this work, it had been shown that supersymmetric grand unified theories with $U(2)$ flavor symmetry predict simple forms for the Yukawa matrices, ones that provide a successful description of charged fermion masses and the Cabibbo-Kobayashi-Maskawa (CKM) mixing matrix [12, 14]. The authors of Ref. [3, 4] posed a simple question: What is the smallest discrete flavor group that predicts the same form for the Yukawa textures? The answer to this question was determined by the specific group theoretic properties of $U(2)$ that were utilized in the most successful $U(2)$ models [14]:

1. $U(2)$ models involved fields in **1**, **2** and **3** dimensional representations (reps). Matter fields of the three generations were embedded into $\mathbf{2} \oplus \mathbf{1}$ dimensional reps; the fact that the third generation fields were treated differently allowed the model to accommodate an order one (*i.e.*, a flavor-group-invariant) top quark Yukawa coupling. The flavor-symmetry-breaking fields, called flavons, appeared in all three of these representations.
2. In each Yukawa matrix, the two-by-two block associated with the first two generations decomposed into an antisymmetric and symmetric part. These followed from the couplings of the **1** and **3**-dimensional flavon fields, respectively, due to the group multiplication rule

$$\mathbf{2} \otimes \mathbf{2} = \mathbf{3} \oplus \mathbf{1} . \tag{2.1}$$

3. The $U(2)$ symmetry was broken to a $U(1)$ subgroup that rotated all first generation fields by a phase. This $U(1)$ symmetry was subsequently broken at a lower energy scale than that of the original $U(2)$ symmetry. Since Yukawa couplings emerge as a ratio of

a symmetry-breaking scale to a cut off, the sequential breaking of the flavor symmetry explains why the Yukawa couplings associated with first generation were smaller than those of the heavier generations.

The group T' is special in that it is the smallest discrete group that has **1**, **2** and **3**-dimensional representations, as well as the multiplication rule $\mathbf{2} \otimes \mathbf{2} = \mathbf{3} \oplus \mathbf{1}$. We will briefly review the representations and multiplication rules for T' symmetry in Sec. 2.2. Following Ref [3, 4], the appropriate symmetry breaking sequence is achieved if the flavor group includes an Abelian factor, so that $G_F = T' \times Z_3$. Then the breaking pattern of the U(2) model

$$U(2) \xrightarrow{\epsilon} U(1) \xrightarrow{\epsilon'} \text{nothing}, \quad (2.2)$$

is mimicked by

$$T' \times Z_3 \xrightarrow{\epsilon} Z_3^D \xrightarrow{\epsilon'} \text{nothing}. \quad (2.3)$$

Here we have indicated the scale of each symmetry breaking via the dimensionless parameters ϵ and ϵ' , which represent the ratio of a symmetry-breaking vacuum expectation value (vev) to the cut off of the effective theory. We refer to the cut off as the flavor scale, M_F , henceforth. A useful way to understand the connection between Eq. (2.2) and (2.3) is to consider the $SU(2) \times U(1)$ subgroup of U(2); The T' factor is a subgroup of the SU(2) factor while Z_3 is a subgroup of the U(1). The Z_3 factor remaining after the first step in the symmetry-breaking chain in Eq. (2.3) also transforms all first generation fields by a phase and will be specified later. The $T' \times Z_3$ model defined in this way reproduces the successful Yukawa textures of the U(2) models, but with a much smaller symmetry group. For other productive applications of T' symmetry in flavor model building, we refer the reader to Ref. [48].

The T' models of Refs. [3, 4] were constructed more than 16 years ago, when it was

widely assumed that weak-scale supersymmetry was the likely solution to the gauge hierarchy problem. The numerical study of the Yukawa textures in these references assumed supersymmetric renormalization group equations to relate the predictions of the theory at the flavor scale M_F to those at observable energies. Superpartners were taken to have masses just above the electroweak scale, while M_F was identified with the scale of supersymmetric grand unification, $\sim 2 \times 10^{16}$ GeV. The latter choice was motivated by the most elegant T' models, which were formulated in the context of an $SU(5)$ grand unified theory. Some of the essential features of the Yukawa textures followed from the combined restrictions of the flavor and grand unified symmetries.

At the present moment, however, the status of weak-scale supersymmetry as a necessary ingredient in model building is far less certain. The latest data from the LHC has found no evidence for supersymmetry. Of course, this may simply mean that the scale of the superpartner masses is slightly higher than what one might prefer from the perspective of naturalness; this interpretation would have little effect on the results of Refs. [3, 4]. On the other hand, the LHC may be hinting that there is no necessary connection between the weak scale and the scale of supersymmetry breaking. In this case, one might entertain the possibility that the supersymmetry breaking scale is associated with the only higher physical mass scale whose existence is well established: the Planck scale. For example, it has been suggested in Ref. [49] that the shallowness of the Higgs potential may be explained by Planck-scale supersymmetry breaking, assuming that supersymmetry is still relevant for a quantum gravitational completion. This latter assumption itself has been challenged in Ref. [50], where it has been noted that there are consistent string theories that are fundamentally non-supersymmetric and whose low-energy limit could include the standard model. Whether supersymmetry is broken at the Planck scale, or not present at any scale, one might attempt to address the hierarchy between the weak scale and Planck scale, for example, by anthropic selection, or by Higgs field relaxation [51], or by mechanisms not yet

known. Alternatively, one might pursue the idea that quantum gravitational physics does not contribute to scalar field quadratic divergences in the way that one expects naively from effective field theory arguments [52]. In this chapter, we remain completely agnostic on the issue of naturalness. We instead investigate a question that can be addressed in a more definitive and quantitative way: how well do the T' flavor models in Refs. [3, 4] work if there is no supersymmetry below the Planck scale?

We begin our study by assuming a standard form for the Yukawa textures expected in models with $T' \times Z_3$ symmetry and perform a global fit to the charged fermion masses and CKM elements assuming that the predictions at the flavor scale M_F are related to those at the weak scale via non-supersymmetric renormalization group equations¹. In the absence of supersymmetry, we no longer have gauge coupling unification and therefore do not consider grand unified embeddings. The flavor scale is taken as a free parameter that may vary anywhere from the TeV scale to the Planck scale. By study of the goodness of these fits, we consider whether there is any preference for a higher or lower flavor scale within the specified range. If one were to find acceptable results for values of M_F near the Planck scale, one might conclude that the model is consistent with a minimal scenario in which there are no other energy scales of physical relevance other than the weak and the Planck scale. On the other hand, if one were to find acceptable results for M_F closer to the lower bounds from flavor-changing-neutral-current processes, then one might obtain interesting predictions for observable indirect effects of heavy particles associated with the flavor sector.

The chapter is organized as follows. In the next section, we briefly review the flavor models of interest and present a parameterization of the Yukawa matrix textures that

¹Note that we do not consider neutrino physics in the present work due to the additional model dependence affecting that sector of the theory. For example, the structure of the theory is different depending on whether neutrino masses are Dirac or Majorana, whether the Majorana masses arise via a seesaw mechanism or via coupling to electroweak triplet Higgs fields, and whether additional neutral fermions are present with which the neutrinos can mix. We reserve such a study for future work.

typically arise in these models at the flavor scale M_F . In Sec. 2.3, we study the predictions that follow from these textures by a non-supersymmetric renormalization group analysis, including global fits to the current data on charged fermion masses and CKM elements. In Sec. 2.4, we point out the largest indirect effects of heavy flavor-sector particles on flavor-changing-neutral current processes in the case where M_F is low. In Sec. 3.4, we address model building issues: supersymmetric models have two Higgs doublets (in order to cancel anomalies) and have a superpotential that is constrained by holomorphicity; these requirements are absent in the non-supersymmetric case. Hence, in this section we show how the textures assumed in Sec. 2.3 may arise in non-supersymmetric T' models. In the final section, we summarize our conclusions.

2.2 Typical Yukawa textures from T-prime symmetry

The group T' is discussed at length in Ref. [4]. Here we summarize only the most basic properties relevant to the present discussion: The group has 24 elements. This includes 12 elements that correspond to the 12 proper rotations that take a regular tetrahedron into coincidence with itself, with choices of Euler angles that are less than 2π . The remaining 12 elements are the first set times an element called R that corresponds to a 2π rotation. As we indicated earlier, T' has **1**, **2** and **3**-dimensional representations, that we specify more precisely below. For odd-dimensional representations, R acts trivially and the action of the group T' is not distinguishable from that of the tetrahedral group T . For the even-dimensional representations, however, R acts non-trivially; this reflects the fact that T' is a subgroup of $SU(2)$ and that spinors flip sign under a rotation by 2π .

The complete list of T' representations is as follows: there is a trivial singlet, $\mathbf{1}^0$, two non-trivial singlets, $\mathbf{1}^\pm$, three doublets, $\mathbf{2}^0$ and $\mathbf{2}^\pm$, and one one triplet, $\mathbf{3}$. The different singlet and doublet representations are distinguished by how they transform under a Z_3

subgroup, generated by the group element called g_9 in Ref. [4]. This is indicated by the triality superscript; when we multiply representations, trialities add under addition modulo three. Keeping this in mind, the rules for multiplying representations are then specified by

$$\begin{aligned}
\mathbf{1} \otimes \mathbf{R} &= \mathbf{R} \otimes \mathbf{1} \text{ for any rep } \mathbf{R}, \\
\mathbf{2} \otimes \mathbf{2} &= \mathbf{3} \oplus \mathbf{1}, \\
\mathbf{2} \otimes \mathbf{3} &= \mathbf{3} \otimes \mathbf{2} = \mathbf{2}^0 \oplus \mathbf{2}^+ \oplus \mathbf{2}^-, \\
\mathbf{3} \otimes \mathbf{3} &= \mathbf{3} \oplus \mathbf{3} \oplus \mathbf{1}^0 \oplus \mathbf{1}^+ \oplus \mathbf{1}^-.
\end{aligned} \tag{2.4}$$

As we indicated in the Introduction, the models of interest are based on the flavor group $G_F = T' \times Z_3$, which includes a Z_3 subgroup that rotates all first-generation matter fields by a phase. We now identify that subgroup. In the models of Ref. [4], the first two generations are assigned to the $\mathbf{2}^0$ representation², in which the element g_9 is given by

$$g_9(\mathbf{2}^0) = \begin{pmatrix} \eta^2 & 0 \\ 0 & \eta \end{pmatrix}, \tag{2.5}$$

where $\eta \equiv e^{2\pi i/3}$. However, the matter fields may also transform under the Z_3 factor that commutes with T' . We represent charge assignments under this Z_3 by an additional triality index 0, + and −, corresponding to the phase rotations 1, η and η^2 . The diagonal subgroup of the Z_3 subgroup generated by g_9 and the Z_3 factor that commutes with T' is the intermediate symmetry that we desire; we call this subgroup Z_3^D . If we assign the first

²This choice is motivated by the cancelation of discrete gauge anomalies. See Ref. [4] for details.

two generations to the rep $\mathbf{2}^{0-}$, then the action of Z_3^D is through powers of the product

$$g_9(\mathbf{2}^0) \cdot \eta^2 = \begin{pmatrix} \eta & 0 \\ 0 & 1 \end{pmatrix}, \quad (2.6)$$

which provides the desired first generation phase rotation.

Assigning the three generations of matter fields to the $T' \times Z_3$ reps $\mathbf{2}^{0-} \oplus \mathbf{1}^{00}$ yields the following transformation properties of the Yukawa matrices:

$$Y_{U,D,E} \sim \begin{pmatrix} [\mathbf{3}^- \oplus \mathbf{1}^{0-}] & [\mathbf{2}^{0+}] \\ [\mathbf{2}^{0+}] & [\mathbf{1}^{00}] \end{pmatrix}. \quad (2.7)$$

The models of interest include a set of flavon fields, A_{ab} , ϕ_{ab} and S_{ab} , which transform as $\mathbf{1}^{0-}$, $\mathbf{2}^{0+}$ and $\mathbf{3}^-$, respectively. When the $T' \times Z_3$ symmetry is broken to Z_3^D , the doublet and triplet flavons acquire the VEVs

$$\frac{\langle \phi \rangle}{M_F} \sim \begin{pmatrix} 0 \\ \epsilon \end{pmatrix}, \quad \frac{\langle S \rangle}{M_F} \sim \begin{pmatrix} 0 & 0 \\ 0 & \epsilon \end{pmatrix}, \quad (2.8)$$

where we use \sim when we omit possible order one factors. This is the most general pattern of non-vanishing entries that is consistent with the unbroken Z_3^D symmetry defined by Eq. (2.6). Yukawa couplings involving first-generation fields are generated only after the Z_3^D symmetry is broken at a lower scale; in analogy to the U(2) models of Ref. [12, 14], it is assumed that this is accomplished solely through the vev of the flavon A_{ab} ,

$$\frac{\langle A \rangle}{M_F} \sim \begin{pmatrix} 0 & \epsilon' \\ -\epsilon' & 0 \end{pmatrix}, \quad (2.9)$$

where $\epsilon' < \epsilon$. This sequential breaking $T' \times Z_3 \xrightarrow{\epsilon} Z_3^D \xrightarrow{\epsilon'} \text{nothing}$ yields a Yukawa texture for the up quarks, down quarks and leptons of the form

$$Y_{U,D,E} \sim \begin{pmatrix} 0 & \epsilon' & 0 \\ -\epsilon' & \epsilon & \epsilon \\ 0 & \epsilon & 1 \end{pmatrix}, \quad (2.10)$$

where we've suppressed $\mathcal{O}(1)$ operator coefficients.

The forms of the Yukawa matrices obtained in Eq. (2.10) are inadequate, given the known differences between the up-, down- and charged-lepton masses. The top quark Yukawa coupling is of order one, while the all others are substantially smaller, suggesting an additional overall suppression factor is desirable in Y_D and Y_E . Moreover, the hierarchy of quark masses is more extreme in the up-quark sector than in the down; for example, the quark mass ratios renormalized at the supersymmetric grand unified scale are given approximately by [2]

$$m_d :: m_s :: m_b = \lambda^4 :: \lambda^2 :: 1 \quad \text{while} \quad m_u :: m_c :: m_t = \lambda^8 :: \lambda^4 :: 1, \quad (2.11)$$

where $\lambda \approx 0.22$ is the Cabibbo angle. This suggest that an additional suppression in the 1-2 block of Y_U is also desirable. We call these suppression factors ρ and ξ , which modify the textures of Eq. (2.10) as follows:

$$Y_U \sim \begin{pmatrix} 0 & \epsilon' \rho & 0 \\ -\epsilon' \rho & \epsilon \rho & \epsilon \\ 0 & \epsilon & 1 \end{pmatrix}, \quad Y_D \sim \begin{pmatrix} 0 & \epsilon' & 0 \\ -\epsilon' & \epsilon & \epsilon \\ 0 & \epsilon & 1 \end{pmatrix} \xi, \quad Y_E \sim \begin{pmatrix} 0 & \epsilon' & 0 \\ -\epsilon' & \epsilon & \epsilon \\ 0 & \epsilon & 1 \end{pmatrix} \xi. \quad (2.12)$$

Clearly, the smallness of ρ and ξ does not follow directly from the assumed flavor symmetry

breaking, but requires additional symmetries and/or dynamics. In the U(2) models of Refs. [12, 14] and the T' models of Refs. [3, 4], ξ is assumed to arise from mixing in the Higgs sector of the theory, while the origin of ρ is understood in terms of a grand unified embedding. Flavon charge assignments under the unified gauge group can cause Yukawa entries to arise at higher order in $1/M_F$ than they would otherwise. In the non-supersymmetric T' models that we discuss in Sec. 3.4, we will neither have an extended Higgs sector nor a grand unified embedding; we will, however, show how ρ and ξ may arise simply by a small extension of the flavor symmetry.

All other differences between Y_U , Y_D and Y_E can now be accommodated by the choice of the undetermined $\mathcal{O}(1)$ operator coefficients, identified according to naive dimensional analysis. We generally require these to be between $1/3$ and 3 in magnitude; the precise range is a matter of taste, but our choice is consistent with the assumptions of Refs. [3, 4]. Variations in the operator coefficients are then sufficient, for example, to account for differences between Y_D and Y_E that are attributed to group theoretic factors of 3 in grand unified theories [53]. We parameterize the Yukawa matrices in terms of coefficients u_i , d_i and ℓ_i as follows:

$$Y_U = \begin{pmatrix} 0 & u_1\epsilon'\rho & 0 \\ -u_1\epsilon'\rho & u_2\epsilon\rho & u_3\epsilon \\ 0 & u_4\epsilon & u_5 \end{pmatrix}, \quad Y_D = \begin{pmatrix} 0 & d_1\epsilon' & 0 \\ -d_1\epsilon' & d_2\epsilon & d_3\epsilon \\ 0 & d_4\epsilon & d_5 \end{pmatrix} \xi, \quad Y_E = \begin{pmatrix} 0 & \ell_1\epsilon' & 0 \\ -\ell_1\epsilon' & \ell_2\epsilon & \ell_3\epsilon \\ 0 & \ell_4\epsilon & \ell_5 \end{pmatrix} \xi. \quad (2.13)$$

These forms will be used to define the Yukawa matrices at the flavor scale M_F in the numerical study presented in the following section.

2.3 Numerical analysis

We numerically evolve the Yukawa matrices in Eq. (2.13), using the one-loop, non-supersymmetric renormalization group equations (RGEs). The flavor scale M_F is taken to be variable, while the scale of observable energies is chosen to be the mass of the Z boson, m_Z . We omit all weak-scale threshold corrections. The RGEs are given by [54]

$$\frac{dg_i}{dt} = \frac{b_i^{\text{SM}}}{16\pi^2} g_i^3, \quad (2.14)$$

$$\frac{dY_U}{dt} = \frac{1}{16\pi^2} \left(-\sum_i c_i^{\text{SM}} g_i^2 + \frac{3}{2} Y_U Y_U^\dagger - \frac{3}{2} Y_D Y_D^\dagger + Y_2(S) \right) Y_U, \quad (2.15)$$

$$\frac{dY_D}{dt} = \frac{1}{16\pi^2} \left(-\sum_i c_i^{\text{SM}} g_i^2 + \frac{3}{2} Y_D Y_D^\dagger - \frac{3}{2} Y_U Y_U^\dagger + Y_2(S) \right) Y_D, \quad (2.16)$$

$$\frac{dY_E}{dt} = \frac{1}{16\pi^2} \left(-\sum_i c_i^{\prime\text{SM}} g_i^2 + \frac{3}{2} Y_E Y_E^\dagger + Y_2(S) \right) Y_E, \quad (2.17)$$

where

$$Y_2(S) = \text{Tr}[3 Y_U Y_U^\dagger + 3 Y_D Y_D^\dagger + Y_E Y_E^\dagger]. \quad (2.18)$$

Here, the g_i are the gauge couplings, Y_U , Y_D and Y_E are the Yukawa matrices, and $t = \ln \mu$ is the log of the renormalization scale. The SU(5) normalization of g_1 is assumed. In the absence of supersymmetry [54],

$$b_i^{\text{SM}} = \left(\frac{41}{10}, -\frac{19}{6}, -7 \right), \quad (2.19)$$

and

$$c_i^{\text{SM}} = \left(\frac{17}{20}, \frac{9}{4}, 8 \right), \quad c_i^{\prime\text{SM}} = \left(\frac{1}{4}, \frac{9}{4}, 8 \right), \quad c_i^{\prime\prime\text{SM}} = \left(\frac{9}{4}, \frac{9}{4}, 0 \right). \quad (2.20)$$

The $\overline{\text{MS}}$ gauge couplings are chosen to satisfy the boundary conditions

$$\begin{aligned}\alpha_1^{-1}(m_Z) &= 59.01 \ , \\ \alpha_2^{-1}(m_Z) &= 29.59 \ , \\ \alpha_3^{-1}(m_Z) &= 8.44 \ ,\end{aligned}\tag{2.21}$$

where $\alpha_i = g_i^2/4\pi$. These were computed using the values of $\alpha_{\text{EM}} = e^2/4\pi = 127.950$ and $\sin^2 \hat{\theta}_W = 0.23129$ renormalized at m_Z [1] as well as

$$e = g_Y \cos \hat{\theta}_W = g_2 \sin \hat{\theta}_W \quad \text{and} \quad g_1 = \sqrt{5/3} g_Y \ ,\tag{2.22}$$

where the latter equation converts the standard model hypercharge gauge coupling to SU(5) normalization [55]. The QCD coupling is given directly in Ref. [1].

At the flavor scale M_F , the Yukawa matrices are given by Eq. (2.13). For a given numerical choice of symmetry-breaking parameters and operator coefficients, the Yukawa matrices are run down to the scale m_Z and diagonalized. In addition to the nine fermion mass eigenvalues, three CKM mixing angles can be compared to experimental data. (In this work, we do not consider the CKM phase, which is not constrained by the flavor symmetry.) Equivalently, we take the predictions of the theory to consist of the nine fermion masses and the magnitudes of the three CKM elements, V_{us} , V_{ub} and V_{cb} .

To optimize the choice of parameters and operator coefficients for a given choice of flavor scale M_F , we follow the approach of Ref. [4] and minimize the function

$$\begin{aligned}\tilde{\chi}^2 &= \sum_{i=1}^9 \left(\frac{m_i^{\text{th}} - m_i^{\text{exp}}}{\Delta m_i^{\text{exp}}} \right)^2 + \left(\frac{|V_{us}^{\text{th}}| - |V_{us}^{\text{exp}}|}{\Delta V_{us}^{\text{exp}}} \right)^2 + \left(\frac{|V_{ub}^{\text{th}}| - |V_{ub}^{\text{exp}}|}{\Delta V_{ub}^{\text{exp}}} \right)^2 + \left(\frac{|V_{cb}^{\text{th}}| - |V_{cb}^{\text{exp}}|}{\Delta V_{cb}^{\text{exp}}} \right)^2 \\ &+ \sum_{i=1}^5 \left(\frac{\ln |u_i|}{\ln 3} \right)^2 + \sum_{i=1}^5 \left(\frac{\ln |d_i|}{\ln 3} \right)^2 + \sum_{i=1}^5 \left(\frac{\ln |\ell_i|}{\ln 3} \right)^2 \ .\end{aligned}\tag{2.23}$$

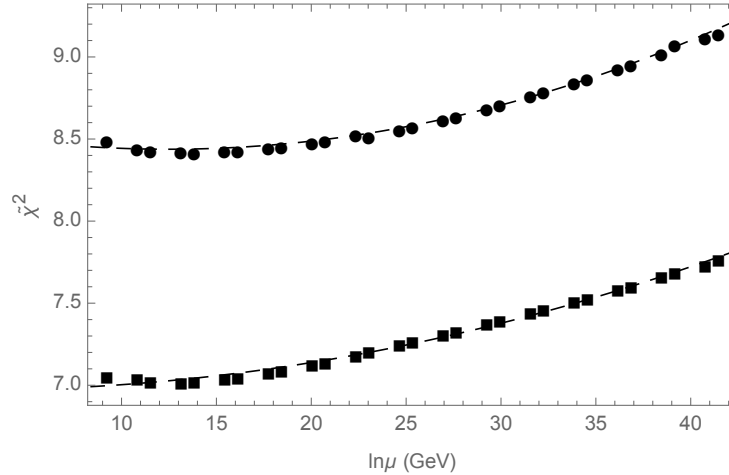


FIG. 2.1: Minimum $\tilde{\chi}^2$ values as a function of M_F , for two different model assumptions.

Here, the quantities with the superscript *th* refer to the predictions of the theory, obtained as we have described previously. The quantities with the superscript *exp* refer to the experimental data, taken from Ref. [1], and written as $X \pm \Delta X$, where the second term is the experimental uncertainty. Since we've omitted two-loop corrections and threshold effects, we take this uncertainty into account in the same way as Ref. [4]: we inflate experimental error bars to 1% of the central value if the experimental error is smaller than this. The terms involving ratios of logarithms in Eq. (2.23) ensure that the operator coefficients remain near unity [4].

We have called the function we minimize $\tilde{\chi}^2$ to make clear that it differs from the conventional χ^2 function one would define in a simple least-squares fit. The latter cannot be sensibly formulated for the purpose of our analysis. A conventional χ^2 function only involves differences between the theoretical predicted values and the experimental measurements. The conventional χ^2 function that would replace our Eq. (2.23) would thus involve the sum of 12 terms that are a function of 19 parameters. This means that the numbers of degrees of freedom is negative and the conventional χ^2 probability distribution is not

TABLE 2.1: Fit parameters and observables for $M_F = 10^6$ GeV with $\chi^2 = 7.021$. In this example, the operator corresponding to u_4 is absent from the theory. All masses are given in GeV. (Note that m_t is the \overline{MS} mass, not the pole mass.)

Best Fit Parameters		
$\epsilon = 0.182, \epsilon' = 0.005, \rho = 0.029, \xi = 0.014$		
$u_1 = 1.131$	$d_1 = 1.162$	$\ell_1 = 0.651$
$u_2 = 0.921$	$d_2 = -0.631$	$\ell_2 = -0.710$
$u_3 = -0.575$	$d_3 = 1.024$	$\ell_3 = -1.242$
$u_4 = 0$ (fixed)	$d_4 = 2.375$	$\ell_4 = -1.244$
$u_5 = 0.628$	$d_5 = -0.931$	$\ell_5 = -0.637$
Observable	Expt. Value [1]	Fit Value
m_u	$(2.3 \pm 0.6) \times 10^{-3}$	1.4×10^{-3}
m_c	1.275 ± 0.025	1.277
m_t	160 ± 4.5	160.1
m_d	$(4.8 \pm 0.4) \times 10^{-3}$	4.18×10^{-3}
m_s	$(9.5 \pm 0.5) \times 10^{-2}$	9.84×10^{-2}
m_b	4.18 ± 0.03	4.18
m_e	$(5.11 \pm 1\%) \times 10^{-4}$	5.11×10^{-4}
m_μ	$0.106 \pm 1\%$	0.106
m_τ	$1.78 \pm 1\%$	1.78
$ V_{us} $	$0.225 \pm 1\%$	0.226
$ V_{ub} $	$(3.55 \pm 0.15) \times 10^{-3}$	3.58×10^{-3}
$ V_{cb} $	$(4.14 \pm 0.12) \times 10^{-2}$	4.13×10^{-2}

defined. This reflects the fact that we could choose parameter values to set a conventional χ^2 function identically to zero (*i.e.*, there would be nothing to fit)³. Doing so, however, is not adequate since this does not prevent a parameter value from exceeding the limits that assure a valid effective field theory. For example, a choice of parameters that gives a very good match to all the experimental central values but includes an operator coefficient that

³Note that there is one way that one could do a conventional χ^2 fit, namely, if one arbitrarily fixes a subset of the model parameters. This approach, however, is not adequate: Imagine if one fixed 14 of the 19 model parameters, and fit the 12 predictions of the theory to the data in terms of the 5 free parameter values. There are over 11,000 different ways of choosing the set of free parameters in this example and no physical basis for choosing one set over another, nor for determining the precise values to which the fixed parameters should be set. We therefore follow an approach where all the parameters are allowed to float. Note that in the one case where do fix a parameter value, *i.e.*, $u_4 = 0$, there is a specific physics justification that follows from the model building considerations discussed in Sec. 3.4.

is, for example, 17.3, would be in wild conflict with the assumption that we have a valid effective field theory description. The $\tilde{\chi}^2$ function, on the other hand, includes additional terms that give weight to the theoretical constraint that the effective theory remain valid and consistent with naive dimensional analysis. Any alternative way of imposing such a theoretical constraint, which necessarily involves adding additional terms to the function that is minimized that are independent of the output predictions of the theory, would not be a conventional χ^2 function with the conventional statistical interpretation. Hence, we opt for a form that is both simple and consistent with what has been used in the past literature [4]. The quantity $\tilde{\chi}^2$ is useful in that it allows us to quantify the comparison of one of our fits to another. To interpret the meaning of a given value of $\tilde{\chi}^2$ in absolute terms, one then directly inspects the fit output, as we will discuss later. Since the u_i , d_i and ℓ_i are not treated as free parameters, we might expect qualitatively that a good fit will have a $\tilde{\chi}^2 \approx 8$, corresponding to 12 pieces of experimental data minus 4 unconstrained parameters (ϵ , ϵ' , ρ and ξ). We will see that this is consistent with our numerical results.

A plot of $\tilde{\chi}^2$ as a function of the flavor scale M_F is shown in Fig. 2.1. The two curves in this figure correspond to the cases where the coefficient u_4 is allowed to float, or is fixed to zero. (In the latter case, the sum over the u_i in the second line of Eq. (2.23) omits $i = 4$.) These cases are motivated by two variants of the Yukawa textures that may arise in explicit models, as we show in Sec. 3.4. Over the entire range of M_F we find good fits with $\tilde{\chi}^2 \approx 8$, but with clear and monotonic improvement in $\tilde{\chi}^2$ towards smaller values of M_F . In addition, the case where the operator corresponding to u_4 is absent from the theory (*i.e.*, where u_4 is fixed to zero), which we will see corresponds to more minimal model-building assumptions, provides a better description of the data than the case where it is present. We present two examples of our results in Tables 2.1 and 2.2, for $M_F = 10^6$ GeV and 10^{18} GeV, respectively, both in the case where $u_4 = 0$. The first choice corresponds to a flavor scale of the same order as the lower bounds from flavor-changing neutral current

TABLE 2.2: Fit parameters and observables for $M_F = 10^{18}$ GeV with $\chi^2 = 7.762$. In this example, the operator corresponding to u_4 is absent from the theory. All masses are given in GeV. (Note that m_t is the \overline{MS} mass, not the pole mass.)

Best Fit Parameters		
$\epsilon = 0.131, \epsilon' = 0.004, \rho = 0.02, \xi = 0.011$		
$u_1 = 1.005$	$d_1 = 1.005$	$\ell_1 = 0.847$
$u_2 = 1.01$	$d_2 = -0.64$	$\ell_2 = -0.633$
$u_3 = -0.458$	$d_3 = 1.024$	$\ell_3 = -1.193$
$u_4 = 0$ (fixed)	$d_4 = 2.397$	$\ell_4 = -1.199$
$u_5 = 0.369$	$d_5 = -0.676$	$\ell_5 = -0.847$
Observable	Expt. Value [1]	Fit Value
m_u	$(2.3 \pm 0.6) \times 10^{-3}$	1.4×10^{-3}
m_c	1.275 ± 0.025	1.277
m_t	160 ± 4.5	160.4
m_d	$(4.8 \pm 0.4) \times 10^{-3}$	4.2×10^{-3}
m_s	$(9.5 \pm 0.5) \times 10^{-2}$	9.8×10^{-2}
m_b	4.18 ± 0.03	4.18
m_e	$(5.11 \pm 1\%) \times 10^{-4}$	5.11×10^{-4}
m_μ	$0.106 \pm 1\%$	0.106
m_τ	$1.78 \pm 1\%$	1.78
$ V_{us} $	$0.225 \pm 1\%$	0.226
$ V_{ub} $	$(3.55 \pm 0.15) \times 10^{-3}$	3.58×10^{-3}
$ V_{cb} $	$(4.14 \pm 0.12) \times 10^{-2}$	4.13×10^{-2}

processes, as we discuss further in the next section, while the second is of the same order as the Planck scale. Interestingly, the latter demonstrates that the model is consistent with the possibility that there are only two important physical scales in nature, the weak and the Planck scales (with flavor associated with the latter) so that no additional hierarchies or fine-tuning need to be considered.

Note that Tables 2.1 and 2.2 correspond to the extreme values of $\tilde{\chi}^2$ on the lower curve of Fig. 2.1 and show directly that all the predictions of the theory are within one, or occasionally two, standard deviations of the experimental data, with model parameters consistent with naive dimensional analysis. One can then infer that every point on the

lower curve of Fig. 2.1 provides a reasonably good description of the data in comparison to these reference points, over the entire range of flavor scales studied, with a slight preference for lower values. Similar qualitative conclusions can be drawn about the upper curve in the same figure, though, for the sake of brevity, we omit the corresponding fit tables.

2.4 Direct lower bounds on the flavor scale

Our results in Fig 2.1 indicate that typical T' Yukawa textures provide a good description of charged fermion masses and CKM angles over a wide range of M_F , but with a preference for values closer to the TeV scale than to the Planck scale. The lowest possible values of M_F are separately constrained by flavor-changing-neutral-current (FCNC) processes that receive contributions from heavy flavor-sector fields. In this section, we provide some estimates of the lower bounds on M_F following from $K^0 - \bar{K}^0$, $D^0 - \bar{D}^0$, $B^0 - \bar{B}^0$ and $B_s^0 - \bar{B}_s^0$ mixing. In addition, we give the branching fractions predicted for the largest flavor-changing neutral meson decays, which also violate lepton flavor.

The new physics contributions to the FCNC processes of interest come from flavon exchange, or more precisely, the exchange of the physical fluctuations about the flavon vevs. We identify these as follows:

$$\phi = \begin{pmatrix} \varphi_1 \\ \epsilon M_F + \varphi_2 \end{pmatrix}, \quad S_{ab} = \begin{pmatrix} \tilde{S}_{11} & \tilde{S}_{12} \\ \tilde{S}_{12} & \epsilon M_F + \tilde{S}_{22} \end{pmatrix}, \quad A_{ab} = \begin{pmatrix} 0 & \epsilon' M_F + \tilde{A} \\ -\epsilon' M_F - \tilde{A} & 0 \end{pmatrix}, \quad (2.24)$$

where the φ_i , the \tilde{S}_{ij} and \tilde{A} are complex scalar fields. The couplings to standard model fermions originate from the same operators that gave us the Yukawa couplings. As an example, let us consider the origin of $\Delta S = 2$ operators, where S here refers to strangeness. We focus on the largest flavor-changing effects, ones that are present even in the absence

of a rotation from the gauge to mass eigenstate basis. Let Ψ be a three-component column vector with the elements d , s and b . Then the flavon-quark-anti-quark vertex in the down sector follows from

$$\mathcal{L} \supset -\frac{v}{\sqrt{2}}(\bar{\Psi}_L Y_D \Psi_R + \text{h.c.}) , \quad (2.25)$$

where we have set the standard model Higgs field to its vev $v/\sqrt{2}$, where $v = 246$ GeV, and where

$$Y_D = \left(\begin{array}{c|c} S_{ab}/M_F + A_{ab}/M_F & \phi/M_F \\ \hline \phi/M_F & 1 \end{array} \right) \xi , \quad (2.26)$$

with the flavons S , A and ϕ given by Eq. (2.24), and ξ is the dimensionless suppression factor defined earlier. (We provide an origin for ξ and ρ in the next section.) The flavon couplings involving fermions of the first two generations only are given by

$$d_1 \frac{v \xi}{\sqrt{2} M_F} (\bar{d}_L \tilde{A} s_R - \bar{s}_L \tilde{A} d_R) - d_2 \frac{v \xi}{\sqrt{2} M_F} (\bar{d}_L \tilde{S}_{12} s_R + \bar{s}_L \tilde{S}_{12} d_R) + \text{h.c.} . \quad (2.27)$$

Four-fermion operators are obtained by integrating out the heavy fields. It follows that the $\Delta S = 2$ operator that contributes to the $K^0 - \bar{K}^0$ mass splitting is

$$\mathcal{O}_{\Delta S=2} = - \left(\frac{d_1^2}{m_{\tilde{A}}^2} + \frac{d_2^2}{m_{\tilde{S}_{12}}^2} \right) \frac{v^2 \xi^2}{2 M_F^2} [\bar{d}_L s_R \bar{d}_R s_L], \quad (2.28)$$

where the d_i are the same order one coefficients defined in Eq. (2.13). As the flavon masses are not known exactly, we assume that they are of the same order as the symmetry-breaking scale associated with the given flavon; in the present example,

$$m_{\tilde{S}_{12}} \sim \epsilon M_F \quad \text{and} \quad m_{\tilde{A}} \sim \epsilon' M_F . \quad (2.29)$$

Moreover, we pick numerical values of ϵ , ϵ' , ρ and ξ that are characteristic of the values

found in our global fits for M_F below ~ 1000 TeV:

$$\epsilon \sim 0.1, \quad \xi \sim 0.03, \quad \rho \sim 0.02 \quad . \quad (2.30)$$

Mass Splitting	Operator	M_F Lower Bound
$K^0 - \overline{K^0}$	$-d_2^2 \frac{1}{m_{\tilde{S}_{12}}^2} \frac{v^2 \xi^2}{2M_F^2} \bar{d}_L s_R \bar{d}_R s_L$	85 TeV
$B^0 - \overline{B^0}$	$-d_3 d_4 \frac{1}{m_{\varphi_1}^2} \frac{v^2 \xi^2}{2M_F^2} \bar{d}_L b_R \bar{d}_R b_L$	22 TeV
$B_s^0 - \overline{B_s^0}$	$-d_3 d_4 \frac{1}{m_{\varphi_2}^2} \frac{v^2 \xi^2}{2M_F^2} \bar{b}_L s_R \bar{b}_R s_L$	14 TeV
$D^0 - \overline{D^0}$	$-u_2^2 \frac{1}{m_{\tilde{S}_{12}}^2} \frac{v^2 \rho^2}{2M_F^2} \bar{u}_L c_R \bar{u}_R c_L$	14 TeV

TABLE 2.3: Lower bounds on the flavor scale. See the text for definitions of our notation.

We set all order one coefficients equal to one. With these assumptions, the new physics contribution to the neutral pseudoscalar meson mass splittings, Δm , may be expressed as a function of the scale M_F . In general, given a $\Delta F = 2$ interaction of the form $c \mathcal{O}$, where c is the operator coefficient and F represents either strange (S), charm (C) or bottom (B), the mass splitting is given by

$$\Delta m = \frac{c}{m_{P^0}} |\langle P^0 | \mathcal{O} | \overline{P^0} \rangle| \quad , \quad (2.31)$$

where $P^0 (\overline{P^0})$ is the pseudoscalar meson (anti-meson) in question, and the states are

relativistically normalized. For an operator of the form

$$\mathcal{O} = \frac{1}{4}[\bar{h}^\alpha(1 - \gamma^5)\ell^\alpha][\bar{h}^\beta(1 + \gamma_5)\ell^\beta] , \quad (2.32)$$

where h, ℓ represent the heavy (light) quark flavors and α, β are color indices, the matrix element in Eq. (2.31) is given by [56]

$$\langle P^0 | \mathcal{O} | P^0 \rangle = \frac{1}{2} B_{P^0} \frac{m_{P^0}^4 f_{P^0}^2}{(m_h + m_\ell)^2}, \quad (2.33)$$

in the case where $P^0 = K^0$ or D^0 . Here, B_{P^0} is the bag parameter, m_{P^0} and f_{P^0} are the mass and decay constants of the meson and m_ℓ, m_h are the masses of the quarks that make up the meson. For $P^0 = B^0$ or B_s^0 , the matrix element is given by [57]

$$\langle P^0 | \mathcal{O} | P^0 \rangle = \frac{1}{2} B_{P^0} f_{P^0}^2 m_{P^0}^2 \left[\left(\frac{m_{P^0}}{m_h + m_\ell} \right)^2 + \frac{1}{6} \right] . \quad (2.34)$$

As computed on the lattice, the bag parameter in Eq. (2.33) is defined by the expression as shown [56], omitting the additional term proportional to $1/6$ that is retained in Eq. (2.34); in the case where $P^0 = K^0$ or D^0 , the effect of this term is negligible. All masses and mass splittings were obtained from the Review of Particle Properties [1], all decay constants were obtained from Ref. [58], the bag parameters for $\Delta S = 2$ and $\Delta C = 2$ were obtained from Ref. [56], and the bag parameters for $\Delta B = 2$ were obtained from Ref. [57]. To estimate the lower bound on M_F , we assume that the experimentally observed mass splittings are consistent with the standard model predictions and require that the new physics contributions not exceed the current 2σ experimental uncertainty. Such an approach is sufficient for an estimate given the theoretical uncertainties involved in determining the new physics contribution itself. Our results are shown in Table 2.3. As one might expect, we obtain the tightest bound from the $K^0 - \bar{K}^0$ mass splitting, which requires $M_F \gtrsim 85$

TeV.

Decays	BF (Ref. [1])	Operator	M_F Lower Bound	BF ($M_F = 85$ TeV)
$K_L^0 \rightarrow \bar{\mu}e$	$< 4.7 \times 10^{-12}$	$-d_2 \ell_2 \frac{1}{m_{\tilde{S}_{12}}^2} \frac{v^2 \xi^2}{2M_F^2} \bar{e}_L \mu_R \bar{s}_R d_L$	9.8 TeV	1.5×10^{-19}
$B^0 \rightarrow \bar{\tau}e$	$< 2.8 \times 10^{-5}$	$-d_4 \ell_3 \frac{1}{m_{\varphi_1}^2} \frac{v^2 \xi^2}{2M_F^2} \bar{e}_L \tau_R \bar{d}_R b_L$	0.62 TeV	2.3×10^{-22}
$B_s^0 \rightarrow \bar{\tau}\mu$	—	$-d_3 \ell_4 \frac{1}{m_{\varphi_2}^2} \frac{v^2 \xi^2}{2M_F^2} \bar{s}_L b_R \bar{\mu}_R \tau_L$	—	3.2×10^{-22}

TABLE 2.4: Lower bound on M_F for the largest flavor-changing decays. The predicted branching fraction for M_F set equal to the K^0 - \bar{K}^0 mixing bound is also shown.

Flavon exchange between quarks and leptons can also lead to flavor-changing neutral meson decays. We again focus on operators that are flavor-changing in the absence of a rotation of the fields from the gauge to mass eigenstate basis. The largest effects are shown in Table 2.4. The relevant operators are of the form $\mathcal{O}_{qde}^{ijkn} \equiv (\bar{\ell}_i e_j)(\bar{d}_k q_n)$, in the notation of Ref. [59]; in the same reference, bounds on the operator coefficients are conveniently summarized. We translate these into bounds on the scale M_F which, as can be seen from Table 2.4, are much weaker than those coming from the pseudoscalar meson mass splittings. Therefore, we also show the predicted branching fractions with M_F set equal to our lower bound from K^0 - \bar{K}^0 mixing. It is clear that the predicted branching fractions are far below the experimental bounds and unlikely to have observable consequences. Note that we have only considered CP conserving processes and it is generally known that bounds on CP violation in the neutral kaon system tends to give a better bound on the scale of new physics by about an order of magnitude compared to the CP-conserving FCNC bounds.

Given the smallness of these branching fractions, this fact does not change our qualitative conclusions, so we do not pursue that issue further.

2.5 Nonsupersymmetric models

In the renormalization group analysis of Sec. 2.3, the Yukawa matrices Y_i are defined by

$$\mathcal{L}_m = \frac{v}{\sqrt{2}} \overline{\psi}_L^i Y_i \psi_R^i + \text{h.c.} \quad , \quad (2.35)$$

where $i = U, D$ or E and generation indices are suppressed. In order to replicate the Yukawa textures of the supersymmetric models of Refs. [3, 4], we assign the right-handed fermions of the three generations to the $T' \times Z_3$ representations $\mathbf{2}^{0-} \oplus \mathbf{1}^{00}$. Hence, for example, we would assign the first two generations of the charge-2/3 quarks according to $(u_L^c, c_L^c) \sim (u_R, c_R) \sim \mathbf{2}^{0-}$, where the superscript ‘‘c’’ refers to charge conjugation; since $\overline{\psi} = i\psi^{cT} \gamma^0 \gamma^2$, this is equivalent to specifying the transformation properties of the Dirac adjoints $(\overline{u}_L, \overline{c}_L)$. We then identify the following transformation properties for the various blocks of the Y_i ,

$$Y_{U,D,E} \sim \begin{pmatrix} [\mathbf{3}^- \oplus \mathbf{1}^{0-}] & [\mathbf{2}^{0+}] \\ [\mathbf{2}^{0+}] & [\mathbf{1}^{00}] \end{pmatrix} \quad , \quad (2.36)$$

i.e., Eq. (2.13) (or Eq. (4.1) in Ref. [4]), which omits any additional symmetries that may be needed to explain the suppression factors ρ and ξ . As in the supersymmetric model, the transformation properties given in Eq. (2.36) determine the allowed flavon couplings. However, in the supersymmetric case, Eq. (2.36) dictates the form of terms in the superpotential, which is required to be a holomorphic function of the superfields. The absence of this constraint in the nonsupersymmetric case could lead, in principle, to additional flavon couplings that are not present in the supersymmetric theory. However,

we see that as far as the ϕ , S and A flavons are concerned, this is not the case: each has a nontrivial Z_3 charge, which prevents new flavon couplings at the same order that involve the complex conjugates of these fields.

In the supersymmetric theories of Refs. [3, 4], the additional suppression factors associated with the parameters ρ and ξ required the introduction of additional fields and symmetries. For example, in the simplest unified $T' \times Z_3$ model of Refs. [3, 4], SU(5) charge assignments of the flavon fields are responsible for forbidding the coupling of the A and S flavons in Y_U at lowest order in $1/M_F$. However, these couplings emerge via higher-order operators that involve a flavor-singlet, SU(5) adjoint field $\Sigma \sim \mathbf{24}$, just as in earlier models based on U(2) flavor symmetry [14]. The suppression associated with the parameter ξ , on the other hand, was assumed to arise via mixing in the Higgs sector, a reasonable possibility since supersymmetric models require more than one Higgs doublet.

Here we will also achieve the additional suppression factors by means of additional fields and symmetries. However, the additional symmetry will be much smaller than the product of supersymmetry and a grand unified gauge group. (The latter, of course, would not be appropriate for the non-supersymmetric case where the gauge couplings do not unify.) We will simply assume an additional Z_3 factor, so that the flavor group is $G_F^{new} = T' \times (Z_3)^2$. Defining one of the elements of the new Z_3 factor as $\omega = \exp(2i\pi/3)$, the only standard model fields that transform nontrivially under this symmetry are

$$H \rightarrow \omega H \quad \text{and} \quad t_R \rightarrow \omega t_R , \quad (2.37)$$

where H is the standard model Higgs field and t_R is the right-handed top quark. In the standard model, H couples to Y_D and Y_E , while $\sigma^2 H^*$ couples to Y_U . Hence, when the new Z_3 symmetry is unbroken, the assignments in Eq. (2.37) forbid Y_D and Y_E entirely, as well as the first two columns of Y_U . How one proceeds with the model building depends

on the desired relative sizes of ϵ , ϵ' , ρ and ξ . For example, for some choices of M_F , it is possible to find numerical results that are consistent with the simple possibility $\epsilon \sim \rho \sim \xi$, up to order one factors. In this case, we assume the symmetry-breaking pattern

$$T' \times (Z_3)^2 \xrightarrow{-\epsilon} Z_3^D \xrightarrow{-\epsilon'} \text{nothing} , \quad (2.38)$$

where the intermediate Z_3^D factor is exactly the same one as in the original theory, that transforms all first generation fields by a phase; in this case, the new Z_3 symmetry is broken at the first step in the symmetry-breaking chain. We introduce two new flavon fields

$$\rho_0 \rightarrow \omega^2 \rho_0 \quad \text{and} \quad \tilde{\phi} \rightarrow \omega \tilde{\phi} , \quad (2.39)$$

where $\tilde{\phi}$ transforms like $\phi \sim \mathbf{2}^{0+}$ under the original flavor group. With the assumed symmetry breaking pattern, the ρ_0 field and one component of the $\tilde{\phi}$ doublet can develop vevs of order ϵM_F . The Z_3 charges of these fields now allow us to rebuild our otherwise forbidden Yukawa matrices as follows:

(i.) For Y_D and Y_E , we may generate matrices proportional to the standard form if we replace H by $H \rho_0$; it follows that $\langle \rho_0 \rangle / M_F$ is identified with the suppression factor ξ , which we now predict to be of order ϵ , up to an order one factor. One might worry that we could obtain a lower-order contribution from operators that don't involve ρ_0 , but involve $\tilde{\phi}^*$ instead, which also transforms under the new Z_3 factor as $\tilde{\phi}^* \rightarrow \omega^2 \tilde{\phi}^*$. However, this does not occur since $\tilde{\phi}^* \sim \mathbf{2}^{0-}$ under the original flavor symmetry, which is not one of the representations that leads to a lowest order coupling. On the other hand, the product $\rho_0^* \tilde{\phi}$ does couple at the same order as $\rho_0 \phi$; however, this additional contribution does nothing to the form of the resulting Yukawa textures beyond a redefinition of the order one coefficients.

(ii.) For Y_U , the two-by-two block associated with the flavons A and S can now be recovered via operators involving $\rho_0^* A$ and $\rho_0^* S$. Hence, the parameter we called ρ previously is now predicted to be of the same order as ξ . In an analogous way, the 3-1 and 3-2 entries of Y_U can couple to the product $\rho_0^* \phi$, but this transforms in the same way as $\tilde{\phi}$, which may couple at lower-order. Hence the canonical Y_U texture with an additional suppression in only the upper-left two-by-two block is obtained. Note that we could simply omit $\tilde{\phi}$ from the theory and ignore the corresponding entries in Y_U ; this leads to an alternative texture in which $u_4 = 0$ in Eq. (2.13), neglecting corrections from higher-order operators. This was the alternative possibility considered in Sec. 2.3. It is worth noting that in the case where the $\tilde{\phi}$ is omitted from the theory, there is no longer a necessary connection between the scale of the additional Z_3 breaking and the scale of the T' doublet vev, ϵM_F . In this case, we could vary this additional scale independently so that ρ and ξ are still comparable, but intermediate in size between ϵ and ϵ' . This construction would be compatible with the numerical results in Tables 2.1 and 2.2.

In summary, we have provided an existence proof that the textures considered in our numerical analysis may arise in a relatively simple way in a non-supersymmetric framework.

2.6 Conclusions

In this chapter, we have reconsidered models of flavor based on the non-Abelian discrete flavor group T' that were proposed in Ref. [3, 4]. We have relaxed two assumptions made in these studies, that the models are supersymmetric and that the scale of the flavor sector is around the scale of supersymmetric grand unification. Our numerical study found that T' models without supersymmetry provide a viable description of charged fermion masses and CKM angles for a range of values of the flavor scale M_F . We find that

identification of M_F with the reduced Planck scale is a viable possibility, consistent with a simple picture in which no new physics appears between the weak and gravitational scales. However, we also find that our fits improve monotonically as M_F is lowered toward the lower bound dictated by the constraints from flavor-changing-neutral-current processes. In the case where M_F is as low as possible, we identified the largest flavor-changing neutral current effects that result from the exchange of heavy flavor-sector fields; these could provide indirect probes of the model. We then showed how the form of the Yukawa textures that we studied, which were the same as, or closely related to, those described in Ref. [3, 4], can nonetheless arise in a non-supersymmetric framework, where there is only a single Higgs doublet field and where the interactions do not originate from a superpotential, a holomorphic function of the fields. The models we described are arguably simpler than their supersymmetric counterparts; in the non-supersymmetric case, we needed only to extend the original flavor-group by a Z_3 factor to obtain the desired Yukawa textures shown in Eq. (2.13), while avoiding the well-known complications that come with a grand unified Higgs sector. Extending the present study to include the neutrino sector is more model dependent, but would be interesting for future work.

CHAPTER 3

Universal Landau Pole and Physics below the 100 TeV Scale ¹

In this chapter we reconsider the possibility that all standard model gauge couplings blow up at a common scale in the ultraviolet. The simplest implementation of this idea assumes supersymmetry and the addition of a single vector-like generation of matter fields around the TeV scale. We provide an up-to-date numerical study of this scenario and show that either the scale of the additional matter or the scale of the light superparticle masses falls below potentially relevant LHC bounds. We then consider minimal extensions of the extra matter sector that raise its scale above the reach of the LHC, to determine whether there are cases that might be probed at a 100 TeV collider. We also consider the possibility that the heavy matter sector involves new gauge groups constrained by the same ultraviolet boundary condition, which in some cases can provide an explanation for the multiplicity of heavy states. We comment on the relevance of this framework to theories with dark and visible sectors.

¹Work previously published in C. D. Carone, S. Chaurasia and J. C. Donahue, “Universal Landau pole and physics below the 100 TeV scale,” *Phys. Rev. D* **96**, no. 3, 035002 (2017), [arXiv:1705.09716 [hep-ph]].

3.1 Introduction

The idea that the three gauge couplings of the standard model may assume a common value at a high energy scale has motivated a vast literature on grand unified theories [15]. The particle content of the minimal supersymmetric standard model (MSSM) is consistent with such a unification, with a perturbative unified gauge coupling obtained around 2×10^{16} GeV. However, it was pointed out long ago [60, 61] that a different framework also leads to the correct predictions for the gauge couplings at observable energies, namely one in which the gauge couplings blow up at a common scale Λ in the ultraviolet (UV):

$$\alpha_1^{-1}(\Lambda) = \alpha_2^{-1}(\Lambda) = \alpha_3^{-1}(\Lambda) = 0 . \quad (3.1)$$

Since the SU(3) coupling is asymptotically free, this boundary condition can only be obtained via the introduction of extra matter [61, 62, 18, 63]. Supersymmetric models offer the simplest possibility, a single vector-like generation of mass m_V [61, 62, 18]. For a chosen value of m_V , one may fix the scale Λ by the requirement that the low-energy value of the fine structure constant α_{EM} is reproduced; the values of $\sin^2 \theta_W$ and α_3^{-1} are then predicted at any chosen renormalization scale μ , up to theoretical uncertainties. If a value of m_V can be found in which both $\sin^2 \theta_W(m_Z)$ and $\alpha_3^{-1}(m_Z)$ are consistent with the data, then a viable solution is obtained. This approach, followed in Ref. [18], found m_V around the TeV scale, assuming that m_V is also the scale of the light superparticle masses (which we call m_{susy} below).

A numerical renormalization group analysis cannot directly encode the boundary condition in Eq. (3.1) since the gauge couplings are in the non-perturbative regime, where the renormalization group equations (RGEs) cannot be trusted. In Ref. [18], the boundary condition studied was $\alpha_1(\Lambda) = \alpha_2(\Lambda) = \alpha_3(\Lambda) = 10$, values that are barely perturbative.

Since the couplings are rapidly increasing as the renormalization scale is increased, one makes the reasonable assumption that the value of Λ that satisfies this boundary condition is very close to the one given by Eq. (3.1). On the other hand, as the renormalization scale is decreased, the couplings become increasingly perturbative. Of particular importance is that the results are insensitive to the precise choice of boundary condition as long as each of the couplings is large [64]. It was shown in Ref. [18], that varying the $\alpha_i(\Lambda)$ by an order of magnitude in either direction has only a small effect on the final results. We will see this explicitly in our study of the one-vector-like-generation scenario in Sec. 3.2. The insensitivity of the predicted values of $\sin^2 \theta_W(m_Z)$ and $\alpha_3^{-1}(m_Z)$ to the choice of boundary conditions is due to the existence of an infrared fixed point in the renormalization group equation for the ratios of the gauge couplings [19]. Note that this insensitivity includes the case where the $\alpha_i(\Lambda)$ are taken to be large but not strictly identical at a common high scale.

The possibility that the gauge couplings may have large values in the UV is interesting from a variety of perspectives. Large couplings may arise in strongly coupled heterotic string theories, which often also provide the additional vector-like states necessary to drive the gauge couplings to large values [19]. On the other hand, a universal Landau pole, as defined by Eq. (3.1), may arise in models with composite gauge bosons: compositeness implies the vanishing of the gauge fields' wave-function renormalization factors at the compositeness scale, where the gauge fields become non-dynamical [65]. Redefining fields and couplings so that the gauge fields' kinetic terms are always kept in canonical form, one finds that the vanishing wave-function renormalization factors translate into the blow-up of the gauge couplings at the same scale. Thus, the framework we study may be consistent with a wider range of possible ultraviolet completions than a conventional grand unified theory (GUT) with a large unified gauge coupling, though it is not necessary to commit ourselves to any one of them in order to study the consequences at low energies.

An additional motivation relevant to the present work is that the assumption of a universal Landau pole leads to the expectation of new physics at a calculable energy scale, m_V , that is above the weak scale but potentially within the reach of future collider experiments¹. In Sec. 3.2, we show that the minimal scenario, involving one vector-like generation of additional matter, requires values of either m_V or m_{susy} that are below some of the current LHC bounds on vector-like quarks or colored superparticles, respectively. Although experimental bounds come with model-specific assumptions that are usually easy to evade, we pursue an alternative possibility. We show that there are small extensions of the new matter sector that successfully reproduce the correct values of the gauge couplings at m_Z while predicting values of m_V that are above the reach of the LHC, but below 100 TeV for some choices of m_{susy} . In some cases, m_V may be light enough for the vector-like states to be explored at a 100 TeV hadron collider, which makes study of this sector more interesting. Aside from the presence of the heavy matter fields, one possibility that we also discuss in the present work is that these fields may transform under an additional gauge group factor. The motivation is two-fold: (1) By placing the additional matter fields into irreducible representations of a new gauge group, we might provide an explanation for the multiplicity of states needed to achieve the desired UV boundary condition. In the case where the heavy matter remains vector-like, the new gauge group can be broken at a much lower scale. The resulting low-energy theory is that of a “dark” sector consisting of the new gauge and symmetry breaking fields; the heavy matter provides for communication between the dark and visible sectors, via a “portal” of higher-dimension operators that are induced when the heavy fields are integrated out. The gauge coupling of the dark gauge boson is predicted from a boundary condition analogous to Eq. (3.1) and the magnitude of the portal couplings are set by the value of m_V obtained in the RGE analysis. This

¹This, of course, assumes that the vector-like matter occurs at a single common scale. This assumption is relaxed in Ref. [63].

presents a simpler framework for constraining some of the otherwise free parameters of a dark sector than, for example, attempting to embed both dark and visible sectors in a conventional GUT. (2) The heavy matter may be chiral under the new gauge group. The structure of the new sector is then more analogous to the the electroweak sector of the MSSM, and the scale m_V is associated with one or more massive gauge bosons that may have observable consequences.

This chapter is organized as follows: In Sec. 3.2, we consider the consequences of a universal Landau pole in the minimal case where the MSSM is augmented by a single vector-like generation. The study presented in this section differs from the past literature not only in our use of up-to-date experimental errors for our input parameters, but also in that we allow the scales m_V and m_{susy} to vary independently. In addition, we consider an alternative choice for the vector-like matter that contributes the same amount to the beta functions at one loop, but differs from the one-generation scenario at two loops. In Sec. 3.3, we consider extensions of these minimal scenarios, in particular, including a small number of additional complete $SU(5)$ multiplets of vector-like matter. We focus on finding solutions in which m_V is less than 100 TeV, with a special interest in cases where the vector-like matter is light enough to be detected at a future hadron collider. In Sec. 3.4 we consider model building issues associated with the physics at the scale m_V , focusing on the implication of additional gauge groups. In Sec. 3.5, we summarize our conclusions.

3.2 One vector-like generation

In this section, we consider a minimal scenario studied in the past literature [61, 62, 18], the MSSM augmented by an additional vector-like generation of matter fields. We denote the scale of the vector-like matter m_V and we impose the same boundary conditions as in Ref. [18], namely $\alpha_1(\Lambda) = \alpha_2(\Lambda) = \alpha_3(\Lambda) = 10$ as an approximation to Eq. (3.1).

Taking m_V as an input, we determine Λ by the condition that the weak scale value of the fine structure constant $\alpha_{EM}(m_Z)$ is reproduced. With Λ fixed, we are now able to determine the gauge couplings at any lower scale, as a function of our choice for m_V . Above the scale m_{susy} , we use the two-loop supersymmetric RGEs for the gauge couplings. Below m_{susy} , we do the same using the two-loop nonsupersymmetric RGEs, aside from running between the top quark mass and m_Z which we treat as a threshold correction and include at one loop. We assume the presence of the second Higgs doublet required by supersymmetry above the scale m_{susy} . Expanding on the approach of Ref. [18], we do not assume that the scales m_V and m_{susy} are the same, though the relaxation of that requirement will only be important in Sec. 3.3.

As indicated in the introduction, the ratios of the gauge couplings are driven towards infrared fixed point values, so that predictions for $\sin^2 \theta_W$ and α_3^{-1} at m_Z are relatively insensitive to the choice of boundary conditions at the scale Λ . For example, allowing the $\alpha_i(\Lambda)$ to vary independently between 1 and 100, we find that their weak-scale values scatter within roughly 2% for $\alpha_1(m_Z)$ and $\alpha_2(m_Z)$ and 5% for $\alpha_3(m_Z)$. Given the same variation of boundary conditions, we take the resulting scatter in the values of $\sin^2 \theta_W(m_Z)$ and $\alpha_3^{-1}(m_Z)$ as a measure of the theoretical uncertainty in our output predictions. We include these estimates with our numerical results.

The RGEs that we use above the top mass have the form

$$\frac{dg_i}{dt} = \frac{g_i}{16\pi^2} \left[b_i g_i^2 + \frac{1}{16\pi^2} \left(\sum_{j=1}^3 b_{ij} g_i^2 g_j^2 - \sum_{j=U,D,E} a_{ij} g_i^2 \text{Tr}[Y_j Y_j^\dagger] \right) \right], \quad (3.2)$$

where $t = \ln \mu$ is the log of the renormalization scale, $\alpha_i = g_i^2/4\pi$, and the Y_i are Yukawa matrices. The beta function coefficients b_i and b_{ij} can be determined using general formulae [67, 68]. For example, in the case of one vector-like generation with $m_V = m_{susy}$, one

finds for $\mu > m_V$

$$b_i = \begin{pmatrix} \frac{53}{5} \\ 5 \\ 1 \end{pmatrix} \quad \text{and} \quad b_{ij} = \begin{pmatrix} \frac{977}{75} & \frac{39}{5} & \frac{88}{3} \\ \frac{13}{5} & 53 & 40 \\ \frac{11}{3} & 15 & \frac{178}{3} \end{pmatrix}, \quad (3.3)$$

while for $m_t < \mu < m_V$ we have the nonsupersymmetric beta functions

$$b_i^{NS} = \begin{pmatrix} \frac{41}{10} \\ \frac{19}{6} \\ -7 \end{pmatrix} \quad \text{and} \quad b_{ij}^{NS} = \begin{pmatrix} \frac{199}{50} & \frac{27}{10} & \frac{44}{5} \\ \frac{9}{10} & \frac{35}{6} & 12 \\ \frac{11}{10} & \frac{9}{2} & -26 \end{pmatrix}. \quad (3.4)$$

More general forms for the one- and two-loop beta functions that take into account the possibility of additional matter are presented in Sec. 3.3. Note that the gauge couplings for $\mu > m_{susy}$ are defined in the dimensional reduction ($\overline{\text{DR}}$) scheme, which preserves supersymmetry; the couplings are converted to the modified minimal subtraction scheme ($\overline{\text{MS}}$) at the matching scale $\mu = m_{susy}$ before they are run to lower energies. The gauge couplings in the two schemes are related by [69]

$$\frac{4\pi}{\alpha_i^{\overline{\text{MS}}}} = \frac{4\pi}{\alpha_i^{\overline{\text{DR}}}} + \frac{1}{3}(C_A)_i, \quad (3.5)$$

where $C_A = \{0, 2, 3\}$ for $i = 1, 2, 3$.

The coefficients for the terms that depend on the Yukawa couplings in Eq. (3.2) are given by

$$a_{ij} = \begin{pmatrix} \frac{26}{5} & \frac{14}{5} & \frac{18}{5} \\ 6 & 6 & 2 \\ 4 & 4 & 0 \end{pmatrix} \quad \text{and} \quad a_{ij}^{NS} = \begin{pmatrix} \frac{17}{10} & \frac{1}{2} & \frac{3}{2} \\ \frac{3}{2} & \frac{3}{2} & \frac{1}{2} \\ 2 & 2 & 0 \end{pmatrix}, \quad (3.6)$$

for $\mu > m_{susy}$ and $\mu < m_{susy}$, respectively. In practice, we only need to take the top quark Yukawa coupling y_t into account, since it is significantly larger than the other Yukawa couplings. Since y_t affects the running of the gauge couplings only through a two-loop term, we need only include its running at one-loop. For $\mu > m_{susy}$ we have [54]

$$\frac{dy_t}{dt} = \frac{y_t}{16\pi^2} \left(-\sum c_i g_i^2 + 6y_t^2 \right), \quad c_i = \left(\frac{13}{15}, 3, \frac{16}{3} \right), \quad (3.7)$$

while for $\mu < m_{susy}$ [54],

$$\frac{dy_t}{dt} = \frac{y_t}{16\pi^2} \left(-\sum c_i^{\text{SM}} g_i^2 + \frac{9}{2} y_t^2 \right), \quad c_i^{\text{SM}} = \left(\frac{17}{20}, \frac{9}{4}, 8 \right). \quad (3.8)$$

For definiteness, we assume $\tan \beta = 2$, and compute the weak scale value of y_t via $y_t(m_Z) = \frac{\sqrt{2} m_t}{v \sin \beta}$, using the $\overline{\text{MS}}$ value of the top quark mass, 160_{-4}^{+5} GeV [1], and $v = 246$ GeV. The value $y_t(\Lambda)$ is computed numerically so that we obtain the desired $y_t(m_Z)$ value for a given set of input parameters. While this approach is sufficient to determine the representative impact of including the top quark Yukawa coupling in our RGE analysis, it turns out to be overkill: in models where the gauge couplings blow up in the UV, the top quark Yukawa coupling is rapidly driven to zero in the same limit. Hence, its effect on the values of m_V and Λ determined in our numerical analysis turns out to be small, less than the estimates of theoretical uncertainty that we build into the analysis. Although we include it, ignoring y_t altogether does not affect our results qualitatively and can be a useful approach for speeding up numerical cross-checks.

For a given choice of m_V and m_{susy} , the blow-up scale Λ is chosen to yield the correct value of the fine structure constant at the weak scale,

$$\alpha_{\text{EM}}^{-1}(m_Z) = \frac{5}{3} \alpha_1^{-1}(m_Z) + \alpha_2^{-1}(m_Z), \quad (3.9)$$

where the factor of $5/3$ comes from the fact that we assume $SU(5)$ normalization [55] of the $U(1)$ gauge coupling, as in Ref. [18]. While this makes the analysis compatible with a conventional $SU(5)$ GUT at large coupling, this normalization can also arise directly in string theory without an $SU(5)$ GUT [66]. Other normalizations of the $U(1)$ factor are certainly possible, depending on the UV completion. However, we do not consider other possibilities here and adopt the normalization that has been assumed almost uniformly in the past literature. For our numerical study, we take the target central value of $\alpha_{\text{EM}}^{-1}(m_Z) = 127.95$ [1]. With Λ determined in this way, we compute $\alpha_3(m_Z)^{-1}$ and the Weinberg angle $\sin^2 \theta_W(m_Z)$, which is determined by $\alpha_1(m_Z)$ and $\alpha_2(m_Z)$:

$$\sin^2 \theta_W(m_Z) = \frac{3\alpha_1(m_Z)}{3\alpha_1(m_Z) + 5\alpha_2(m_Z)} . \quad (3.10)$$

We compare the output predictions of $\alpha_3(m_Z)^{-1}$ and $\sin^2 \theta_W(m_Z)$, including the theoretical uncertainty that we discussed earlier, to the experimentally measured values [1]

$$\sin^2 \theta_W = 0.23129 \pm 5 \times 10^{-5}, \quad \alpha_3^{-1}(m_Z) = 8.4674 \pm 0.0789 , \quad (3.11)$$

both given in the $\overline{\text{MS}}$ scheme. A previous study of the one vector-like generation scenario found viable solutions with $m_V = m_{\text{susy}} \approx 1$ TeV [18]. Since the time of that work, the experimental errors in $\sin^2 \theta_W(m_Z)$ and $\alpha_3^{-1}(m_Z)$ have decreased substantially. Nevertheless, as indicated in Table 3.1, we find $m_V = m_{\text{susy}} \approx 1.2$ TeV, assuming ± 2 standard deviation experimental error bands and using our protocol for determining theoretical error bands; those bands are both displayed in Fig. 3.1. To determine the theoretical error band, we find the maximum and minimum values of $\sin^2 \theta_W(m_Z)$ and $\alpha_3^{-1}(m_Z)$ that are obtained by varying the α_i independently between 1 and 100 at the blow-up scale. In particular, we find that $\sin^2 \theta_W(m_Z)$ is maximum when $\{\alpha_1(\Lambda), \alpha_2(\Lambda), \alpha_3(\Lambda)\} = \{100, 1, 100\}$ and minimum

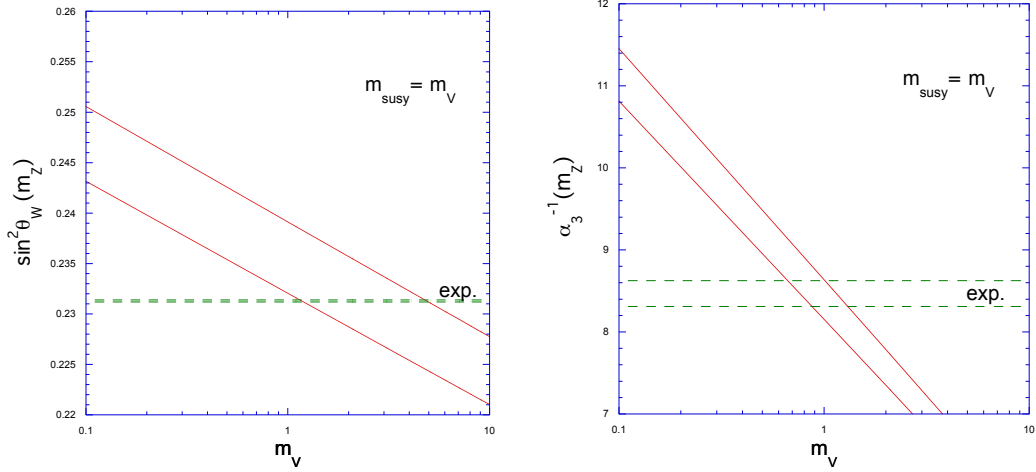


FIG. 3.1: The dependence of $\sin^2 \theta_W(m_Z)$ and $\alpha_3^{-1}(m_Z)$ on the mass of the vector-like generation, m_V , including theoretical uncertainties. In this example, the light superparticle mass scale m_{susy} is identified with m_V . The acceptable ranges of m_V in each of the plots have non-vanishing overlap for $1.15 \text{ TeV} < m_V < 1.31 \text{ TeV}$, indicating a viable solution.

when the boundary condition set is $\{1, 100, 1\}$; $\alpha_3^{-1}(m_Z)$ is maximized and minimized for the sets $\{100, 100, 1\}$ and $\{1, 1, 100\}$, respectively. We quote the variation in the output predictions as a percentage relative to the value obtained when the $\alpha_i(\Lambda) = 10$, for $i = 1 \dots 3$, in Table 3.1. For the values of m_V that yield viable predictions for $\sin^2 \theta_W(m_Z)$ and $\alpha_3^{-1}(m_Z)$, we find that the scale Λ is around $8 \times 10^{16} \text{ GeV}$.

Model	m_{SUSY} (TeV)	m_V range (TeV)	Λ range (GeV)	$\alpha_3^{-1}(m_Z)$ % error	$\sin^2 \theta_W(m_Z)$ % error
$(5, 2, 0, 0)$	m_V	1.15 – 1.31	$7.8 - 8.7 \times 10^{16}$	+3.7%, -2.1%	+1.5%, -1.5%
$(3, 2, 4, 0)$	m_V	0.66 – 1.16	$6.9 - 11 \times 10^{16}$	+2.8%, -1.5%	+1.4%, -1.2%

TABLE 3.1: Numerical results for m_V and Λ in the one-generation scenario, the $(5,2,0,0)$ model, and a model whose vector-like sector consists of four $\mathbf{5} + \bar{\mathbf{5}}$ pairs, the $(3,2,4,0)$ model. These models have the same one-loop beta functions, but differ at two-loop. Also shown are the theoretical error estimates as discussed in the text.

The value of m_{susy} for this solution can be compared to recent bounds on gluinos from the LHC, which now exceed 2 TeV (for example, see Ref. [70]). These bounds generally make assumptions about the supersymmetric particle spectrum (for example, light neutralinos) and one can always play the game of making model-specific adjustments to evade the assumptions of any given experimental exclusion limit. We will not pursue that

approach here. We instead consider the possibility that m_V and m_{susy} are not identical, so that m_{susy} can be raised unambiguously above the LHC reach. In this case, however, we obtain lower values of m_V , which in this model would place an entire vector-like generation below 1 TeV. As a point of comparison, current LHC bounds on a charge-2/3 vector-like quark that decays 100% of the time to bW is 1.295 TeV at the 95% CL [71]. The same comment regarding the limitations of experimental exclusion limits applies here as well; we will be content simply to point out that the one-generation model will become less plausible as time goes on given the increasing reach of LHC searches for superparticles and vector-like quarks.²

This result motivates the topic of the next section, extensions of this minimal sector that include sets of new particles that fill complete SU(5) multiplets. We find that these lead to larger values of m_V . In studies of perturbative gauge coupling unification, it is well known that adding additional matter in complete SU(5) multiplets preserves successful unification. In the present framework, we find viable solutions for m_V are also obtained when complete SU(5) multiplets are added. To study the effect on m_V and Λ , we consider adding the smallest SU(5) representations, with dimensions five and ten, allowing for multiple copies. We label models by four numbers (n_g, n_h, n_5, n_{10}) which represent the number of chiral generations, complex Higgs doublets, $\mathbf{5} + \bar{\mathbf{5}}$ pairs and $\mathbf{10} + \bar{\mathbf{10}}$ pairs.³ In this notation, the one-vector-like-generation scenario that we have discussed in this section will be called the $(5, 2, 0, 0)$ model henceforth. We note that a model with four $\mathbf{5} + \bar{\mathbf{5}}$ pairs added to the MSSM, the $(3, 2, 4, 0)$ model, has the same one-loop beta functions as the $(5, 2, 0, 0)$ model, and could be considered an equally minimal alternative. Results for the $(3, 2, 4, 0)$ model are also shown in Table 3.1, and are useful for illustrating the effect

²Unless, of course, some of these particles are discovered.

³It is interesting to note that in level-one string theories with Wilson line symmetry breaking, extra vector-like matter will naturally appear in $\mathbf{5} + \bar{\mathbf{5}}$ and $\mathbf{10} + \bar{\mathbf{10}}$ pairs, since these are representations found in the $\mathbf{27} + \bar{\mathbf{27}}$ of E_6 [19].

of different two-loop beta functions. The preferred range of m_V in the $(3, 2, 4, 0)$ model is slightly below that of the $(5, 2, 0, 0)$ model, again pointing to the need for alternative choices for the new matter sector to avoid potential phenomenological difficulties.

3.3 Next-to-minimal possibilities

In this section, we consider vector-like matter sectors that are consistent with values of the superparticle masses and m_V that are no smaller than 2 TeV. We look at next-to-minimal scenarios, *i.e.* ones with a small number of additional $\mathbf{5} + \bar{\mathbf{5}}$ and $\mathbf{10} + \bar{\mathbf{10}}$ pairs, for the reasons discussed at the end of the previous section. We have particular interest in solutions that may be plausible for exploration at a 100 TeV hadron collider. To proceed, we use the results for the one- and two-loop beta functions, derived from the general formulae in Refs. [67] and [68]. In the supersymmetric case, we find

$$b_i = \begin{pmatrix} 2 \\ 2 \\ 2 \end{pmatrix} n_g + \begin{pmatrix} \frac{3}{10} \\ \frac{1}{2} \\ 0 \end{pmatrix} n_h + \begin{pmatrix} 1 \\ 1 \\ 1 \end{pmatrix} n_5 + \begin{pmatrix} 3 \\ 3 \\ 3 \end{pmatrix} n_{10} + \begin{pmatrix} 0 \\ -6 \\ -9 \end{pmatrix}, \quad (3.12)$$

$$b_{ij} = \begin{pmatrix} \frac{38}{15} & \frac{6}{5} & \frac{88}{15} \\ \frac{2}{5} & 14 & 8 \\ \frac{11}{15} & 3 & \frac{68}{3} \end{pmatrix} n_g + \begin{pmatrix} \frac{9}{50} & \frac{9}{10} & 0 \\ \frac{3}{10} & \frac{7}{2} & 0 \\ 0 & 0 & 0 \end{pmatrix} n_h \\ + \begin{pmatrix} \frac{21}{45} & \frac{9}{5} & \frac{32}{15} \\ \frac{3}{5} & 7 & 0 \\ \frac{4}{15} & 0 & \frac{34}{3} \end{pmatrix} n_5 + \begin{pmatrix} \frac{23}{5} & \frac{3}{5} & \frac{48}{5} \\ \frac{1}{5} & 21 & 16 \\ \frac{6}{5} & 6 & 34 \end{pmatrix} n_{10} + \begin{pmatrix} 0 & 0 & 0 \\ 0 & -24 & 0 \\ 0 & 0 & -54 \end{pmatrix}, \quad (3.13)$$

while in the nonsupersymmetric case,

$$b_i^{NS} = \begin{pmatrix} \frac{4}{3} \\ \frac{4}{3} \\ \frac{4}{3} \end{pmatrix} n_g + \begin{pmatrix} \frac{1}{10} \\ \frac{1}{6} \\ 0 \end{pmatrix} n_h + \begin{pmatrix} \frac{2}{3} \\ \frac{2}{3} \\ \frac{2}{3} \end{pmatrix} n_5 + \begin{pmatrix} 2 \\ 2 \\ 2 \end{pmatrix} n_{10} + \begin{pmatrix} 0 \\ -\frac{22}{3} \\ -11 \end{pmatrix}, \quad (3.14)$$

$$b_{ij}^{NS} = \begin{pmatrix} \frac{19}{15} & \frac{3}{5} & \frac{44}{15} \\ \frac{1}{5} & \frac{49}{3} & 4 \\ \frac{11}{30} & \frac{3}{2} & \frac{76}{3} \end{pmatrix} n_g + \begin{pmatrix} \frac{9}{50} & \frac{9}{10} & 0 \\ \frac{3}{10} & \frac{13}{16} & 0 \\ 0 & 0 & 0 \end{pmatrix} n_h + \begin{pmatrix} \frac{7}{30} & \frac{9}{10} & \frac{16}{15} \\ \frac{3}{10} & \frac{49}{6} & 0 \\ \frac{2}{15} & 0 & \frac{38}{3} \end{pmatrix} n_5 \\ + \begin{pmatrix} \frac{23}{10} & \frac{3}{10} & \frac{24}{5} \\ \frac{1}{10} & \frac{49}{2} & 8 \\ \frac{3}{5} & 3 & 38 \end{pmatrix} n_{10} + \begin{pmatrix} 0 & 0 & 0 \\ 0 & -\frac{136}{3} & 0 \\ 0 & 0 & -102 \end{pmatrix}. \quad (3.15)$$

As indicated earlier, n_g , n_h , n_5 and n_{10} represent the number of chiral generations, Higgs doublets, $\mathbf{5} + \bar{\mathbf{5}}$ and $\mathbf{10} + \bar{\mathbf{10}}$ pairs, respectively. One can check that these formulae reduce to the expected results for the MSSM, where $n_g = 3$, $n_h = 2$, $n_5 = n_{10} = 0$ in Eqs. (3.12) and (3.13), and for the standard model, where $n_g = 3$, $n_h = 1$, $n_5 = n_{10} = 0$ in Eqs. (3.14) and (3.15).

Table 3.2 displays results analogous to those presented for the minimal scenario in Table 3.1, for a variety of heavy matter sectors, with $m_{susy} \leq m_V$. The cases considered fall into pairs that have the same one-loop beta functions; for example, adding one additional $\mathbf{5} + \bar{\mathbf{5}}$ pair to the one-vector-like generation scenario gives us the $(5, 2, 1, 0)$ model, which has the same b_i as a model with five $\mathbf{5} + \bar{\mathbf{5}}$ pairs, namely $(3, 2, 5, 0)$. The same can be said for the remaining two models, involving six $\mathbf{5} + \bar{\mathbf{5}}$ and two $\mathbf{10} + \bar{\mathbf{10}}$ pairs, respectively. Results are shown for values of m_{susy} ranging from 2 TeV to m_V . We see that solutions

Model	m_{SUSY} (TeV)	m_V range (TeV)	Λ range (GeV)	$\alpha_3^{-1}(m_Z)$ % error	$\sin^2 \theta_W(m_Z)$ % error
(5, 2, 1, 0)	2	95 – 260	$4.9 - 8.2 \times 10^{16}$	+4.2%, -2.8%	+1.5%, -1.4%
	m_V	13 – 28	$3.2 - 5.9 \times 10^{16}$	+4.0%, -2.7%	+1.5%, -1.4%
(3, 2, 5, 0)	2	65 – 217	$4.9 - 9.2 \times 10^{16}$	+3.4%, -2.2%	+1.4%, -1.2%
	10	17 – 32	$4.1 - 5.8 \times 10^{16}$	+3.3%, -2.2%	+1.4%, -1.2%
	m_V	13 – 17	$4.0 - 4.9 \times 10^{16}$	+3.3%, -2.2%	+1.4%, -1.2%
(3, 2, 6, 0)	2	$3.8 - 13 \times 10^3$	$4.3 - 8.6 \times 10^{16}$	+3.7%, -2.7%	+1.4%, -1.2%
	10	$1.2 - 2.6 \times 10^3$	$3.6 - 5.6 \times 10^{16}$	+3.7%, -2.7%	+1.4%, -1.2%
	30	522 – 794	$3.1 - 4.0 \times 10^{16}$	+3.6%, -2.7%	+1.4%, -1.2%
(3, 2, 0, 2)	2	$1.6 - 1.8 \times 10^4$	$7.1 - 7.6 \times 10^{16}$	+5.6%, -4.1%	+1.5%, -1.5%
	10	$3.0 - 5.3 \times 10^3$	$4.4 - 6.1 \times 10^{16}$	+5.4%, -3.9%	+1.5%, -1.5%
	100	277 – 961	$2.2 - 4.5 \times 10^{16}$	+5.1%, -3.8%	+1.5%, -1.5%
	m_V	166 – 370	$1.9 - 3.9 \times 10^{16}$	+5.0%, -3.7%	+1.5%, -1.5%

TABLE 3.2: Solutions for m_V and Λ , for a variety of next-to-minimal heavy matter sectors, for $m_{\text{susy}} \leq m_V$.

for m_V decrease as m_{susy} is increased. Holding m_{susy} fixed, heavy matter sectors that give larger contributions to the one-loop beta functions tend to have larger values of m_V . Larger collections of heavy matter do not provide additional solutions with $m_{\text{susy}} \leq m_V$ and $m_V < 100$ TeV.

Of the cases shown in Table 3.2, the lowest values of the vector-like matter scale, $m_V \approx 13$ TeV, are obtained in the (5, 2, 1, 0) and (3, 2, 5, 0) scenarios, for $m_V = m_{\text{susy}}$. While vector-like quarks with this mass are within the kinematic reach of a 100 TeV hadron collider, their detectability is a separate question. Assuming that a 100 TeV collider has a discovery reach that is greater than that of the LHC by a factor of 5 [72], and that the LHC's ultimate sensitivity to vector-like quarks is just below 2 TeV [73], one might roughly expect a discovery reach for vector-like quarks at a 100 TeV hadron collider just below ~ 10 TeV. This rough estimate is consistent with the 9 TeV reach projected in Ref. [74] for fermionic top quark partners, which are also color triplet fermions. These statements are very rough, and a detailed collider study would be required to determine whether the 13 TeV vector-like quarks in the (5, 2, 1, 0) and (3, 2, 5, 0) models would have observable consequences at a 100 TeV machine.

Fortunately, we find that if the superparticle mass scale is raised above the scale m_V , the reduction in m_V continues. For these cases, we take m_V to refer to the mass of the fermionic components of the vector-like states, while m_{susy} represents a common mass for the superpartners in both the ordinary and the vector-like sectors, in place of our earlier definition. This spectrum is consistent with allowed choices for the soft-supersymmetry-breaking parameters of the theory and simplifies the subsequent analysis. With this assumption, we only find the correct predictions for the gauge couplings at the weak scale in the $(3, 2, 0, 2)$ model. Although a higher m_{susy} indicates that supersymmetry is less effective at addressing the hierarchy problem, one could still argue that this case has its merits: (1) supersymmetry still ameliorates the hierarchy problem between m_{susy} and Λ , which are the scales with the widest separation in the models that we consider, and (2) supersymmetry may be expected if string theory is the UV completion, whether or not supersymmetry has anything to do with solving the hierarchy problem. From a purely phenomenological perspective, taking $m_{susy} > m_V$ brings the $(3, 2, 0, 2)$ heavy matter sector down into the range where it might be directly probed. In Table 3.3, we present numerical results for that case. As the superparticle mass scale increases from 250 TeV to 1500 TeV, the minimum allowed values of m_V decrease from 71 TeV to 3 TeV. It seems more likely in this case that the vector-like matter could be within the discovery reach of a 100 TeV hadron collider, while all the superpartners remain undetectable. It is interesting to note that it is easiest in the $(3, 2, 0, 2)$ model to incorporate an additional gauge group that acts on the heavy matter sector, a topic we turn to in the next section.

3.4 Model building issues

The results of the previous section indicate that there are values of m_V implied by Eq. (3.1) that are beyond the reach of the LHC, but may be within the reach of future

Model	m_{SUSY} (TeV)	m_V range (TeV)	Λ range (GeV)	$\alpha_3^{-1}(m_Z)$ % error	$\sin^2 \theta_W(m_Z)$ % error
(3, 2, 0, 2)	250	71 – 250	$1.7 - 2.8 \times 10^{16}$	+5.0%, -3.7%	+1.5%, -1.5%
	500	22 – 216	$1.5 - 3.6 \times 10^{16}$	+4.9%, -3.6%	+1.5%, -1.5%
	1000	7 – 64	$1.3 - 3.1 \times 10^{16}$	+4.8%, -3.5%	+1.5%, -1.5%
	1500	3 – 31	$1.2 - 2.8 \times 10^{16}$	+4.7%, -3.5%	+1.5%, -1.5%

TABLE 3.3: Solutions for m_V and Λ for $m_{\text{SUSY}} > m_V$. Here m_V refers to the fermionic components of the vector-like sector, while m_{SUSY} represents a common mass for the superparticles of the ordinary and vector-like sectors. Of the models in Table 3.2, only the (3, 2, 0, 2) case provides viable solutions.

collider experiments, particularly in the case where the superparticle mass scale exceeds the scale m_V . Aside from the extra matter fields, other physics associated with this sector might also be experimentally probed. In this section, we consider two motivations for including an extra gauge group that only affects the heavy fields:⁴ (1) The heavy fields may fall in irreducible representations of the new gauge group, explaining the multiplicity of new particles required to achieve the blow up of the couplings at the scale Λ , and (2) the new sector may be chiral under the new gauge groups, rendering it more analogous in structure to the matter sector of the MSSM. Although there are a large number of ways in which either possibility might arise, we consider one example here, based on the (3, 2, 0, 2) model discussed in the previous section.

Regarding the first motivation, we consider the possibility that the duplication of vector-like $\mathbf{10} + \overline{\mathbf{10}}$ pairs in the (3, 2, 0, 2) model is a result of their embedding into a two-dimensional representation of an additional gauge group, which is necessarily non-Abelian. The simplest possibility for the gauge group structure of the model is $G_{SM} \times \text{SU}(2)_X$, where G_{SM} represents the standard model gauge factors. As before, we indicate the standard model charge assignments implicitly and compactly by displaying the $\text{SU}(5)$ multiplets that the heavy matter fields would occupy in a conventional unified theory, even though that is not our assumption. Hence under $\text{SU}(5) \times \text{SU}(2)_X$, we now assume that the extra

⁴In the context of strong unification, extensions of the standard model gauge group have been considered for other purposes in Ref. [75].

matter is given by

$$\psi \sim (10, 2) \quad \text{and} \quad \bar{\psi} \sim (\overline{10}, 2) . \quad (3.16)$$

We also introduce two $SU(2)_X$ doublet Higgs fields that will be responsible for spontaneously breaking the new gauge group factor

$$\phi_1 \sim (1, 2) \quad \text{and} \quad \phi_2 \sim (1, 2) . \quad (3.17)$$

The matter fields in Eq. (3.16) and the new Higgs fields in Eq. (3.17) are separately vector-like, so that these fields may be made massive at any desired scale; it also follows that all chiral gauge anomalies are canceled. Note that the multiplicity of $SU(2)$ doublets in Eqs. (3.16) and (3.17) is even, which implies that the $SU(2)_X$ Witten anomaly is absent. Given these assignments, the one-loop beta function for the new gauge factor is positive, allowing for straightforward implementation of the UV boundary condition in Eq. (3.1).

One issue that needs to be addressed in a model like this one is the stability of the extra matter fields. Vector-like $\mathbf{5} + \bar{\mathbf{5}}$ and $\mathbf{10} + \overline{\mathbf{10}}$ pairs have the appropriate electroweak and color quantum numbers to participate in mass mixing with standard model matter fields. The amount of such mixing is arbitrary, and only a small amount is necessary so that the heavy states are rendered unstable, avoiding any cosmological complications. Assigning the matter fields of the heavy sector to multiplets of a new gauge group can have unwanted consequences if these states are rendered exactly stable (or extremely long lived). In the present model, this problem does not arise provided that the new gauge group is spontaneously broken, since mass mixing is generated via renormalizable couplings involving ψ , the ϕ_i , and the standard model fields identified with a $\mathbf{10}$. If embedding in an additional gauge group is used to account for the multiplicity of states in some of the other models that we have considered, the model must also provide for the decay of the

heavy states; the $(3, 2, 0, 2)$ models seem to naturally avoid this problem with smallest field content and the potentially simplest symmetry-breaking sector, which is one reason why we focus on this example here.

Note that the numerical results for the $(3, 2, 0, 2)$ model described in Sec. 3.3 must be adjusted to take into account the presence of the $SU(2)_X$ gauge group, whose coupling blows up at the same scale as the other gauge couplings and affects their renormalization group running. However, since the effect is only via two-loop terms, we don't expect a dramatic change in our qualitative conclusions. To support this statement, we consider the case where $m_{susy} = m_V$ and take into account the effect of the new gauge group by modifying the supersymmetric RGEs for running between the scales Λ and m_V . In this case, the supersymmetric beta functions become

$$b_i = \left(\begin{array}{cccc} \frac{63}{5} & 7 & 3 & 5 \end{array} \right) , \quad (3.18)$$

$$b_{ij} = \left(\begin{array}{cccc} \frac{429}{25} & \frac{33}{5} & \frac{184}{5} & 18 \\ \frac{11}{5} & 67 & 56 & 18 \\ \frac{23}{5} & 21 & 82 & 18 \\ 6 & 18 & 48 & 53 \end{array} \right) . \quad (3.19)$$

Repeating the analysis of Sec. 3.3, we find only a modest adjustment in the ranges for m_V and Λ , as shown in Table 3.4 below.

Model	m_{SUSY} (TeV)	m_V range (TeV)	Λ range (GeV)	$\alpha_3^{-1}(m_Z)$ % error	$\sin^2 \theta_W(m_Z)$ % error
$(3, 2, 0, 2)$	m_V	198 – 497	$1.6 - 3.6 \times 10^{16}$	+5.6%, -4.1%	+1.6%, -1.5%

TABLE 3.4: Results for the $(3, 2, 0, 2)$ scenario with $m_V = m_{susy}$ taking into account the effect of the $SU(2)_X$ gauge group.

It is interesting to note that $SU(2)_X$ breaking scale is not tied to the value of m_V in this model, which means it could in principal be much lower. For example, with $\langle \phi \rangle \sim 1$ GeV,

the resulting low-energy effective theory would be that of a non-Abelian dark sector with a one- or two-Higgs doublet symmetry-breaking sector. Communication between the visible and dark sectors would follow from operators generated when the m_V -scale physics is integrated out, suggesting that this sector may have other interesting consequences besides its effect on gauge coupling running. Whether phenomenologically interesting models of this type can be constructed remains an open question.

Finally, we note that a different motivation for an extra gauge factor is to render the m_V -scale physics chiral, so that the structure of the new matter sector is more similar to the rest of the MSSM. In the previous example, we could simply change the charge assignment of $\bar{\psi}$ to

$$\bar{\psi}_1 \sim (\bar{10}, 1) \quad \text{and} \quad \bar{\psi}_2 \sim (\bar{10}, 1) . \quad (3.20)$$

Now the mass terms for the extra matter are generated via Yukawa couplings involving ψ , $\bar{\psi}$ and the ϕ_i ; the vacuum expectation value $\langle \phi \rangle$ is now associated with the scale m_V determined in the RGE analysis. We make one additional modification to the theory, which is to add an additional pair of Higgs fields

$$\phi'_1 \sim (1, 2) \quad \text{and} \quad \phi'_2 \sim (1, 2) . \quad (3.21)$$

The modification in Eq. (3.20) leads to the vanishing of the one-loop beta function for $SU(2)_X$, while Eq. (3.21) restores the desired asymptotic non-freedom. Based on our earlier observations, it is clear that the numerical values for m_V and Λ in this model will be qualitatively similar to those of the other $(3, 2, 0, 2)$ models that we have considered, and we leave further numerical study for the interested reader.

3.5 Conclusions

In this chapter, we have revisited the possibility that the standard model gauge couplings reach a common Landau pole in the ultraviolet. This provides a predictive framework for relating the values of the gauge couplings at the weak scale, without the necessary assumption of conventional grand unification. To implement this framework, all the gauge couplings must be asymptotically non-free, which implies that new matter must be included in the theory. We have numerically explored the possibility that this new matter appears at two scales, a light superpartner mass scale m_{susy} , and the scale where additional heavier vector-like states appear, m_V . We have revisited a scenario considered in the past in which the minimal supersymmetric standard model is enlarged by a single vector-like generation and found that either m_{susy} or m_V falls below potentially relevant LHC lower bounds on colored MSSM superparticles or vector-like quarks. Although one cannot rule out the possibility that these states are present and have evaded detection for model-specific reasons, we are motivated to consider a safer possibility: we include a relatively small additional amount of extra heavy matter, which leads to solutions for m_V that are beyond the reach of the LHC, but potentially within the reach of a higher-energy hadron collider. For example, given a heavy sector consisting in total of five $\mathbf{5} + \bar{\mathbf{5}}$ pairs, we obtain successful gauge coupling predictions for $m_{susy} = m_V \approx 13$ TeV. For a heavy sector of two $\mathbf{10} + \bar{\mathbf{10}}$ pairs, we can achieve m_V as low as 3 TeV, if we allow higher values of $m_{susy} \approx 1500$ TeV. (In this case, m_V refers to the fermionic components of the vector-like sector, while m_{susy} represents a common mass for the superparticles of the ordinary and vector-like sectors.)

We also considered whether the size of the new matter sector could be related to its embedding into the irreducible representation of an additional non-Abelian gauge group. We presented the simplest model that was consistent with our numerical solutions, a

model with two $\mathbf{10} + \overline{\mathbf{10}}$ pairs, in which this duplication is due to their embedding in the fundamental representation of a new $SU(2)$ gauge group. In the case where the heavy matter sector is vector-like under the new $SU(2)$, the new gauge group can be broken at a much lower scale and the effective theory is that of a spontaneously broken non-Abelian dark sector. In the case where the heavy matter sector is chiral under the new $SU(2)$, m_V is associated with the symmetry breaking scale. In this case, new heavy gauge bosons would be among the spectrum of particles that might be sought at a future collider with a suitable reach.

CHAPTER 4

Curved Backgrounds in Emergent Gravity¹

Field theories that are generally covariant but nongravitational at tree level typically give rise to an emergent gravitational interaction whose strength depends on a physical regulator. In this chapter we consider emergent gravity models in which scalar fields assume the role of clock and rulers, addressing the problem of time in quantum gravity. We discuss the possibility of nontrivial dynamics for clock and ruler fields, and describe some of the consequences of those dynamics for the emergent gravitational theory.

¹Work previously published in S. Chaurasia, J. Erlich and Y. Zhou, “Curved Backgrounds in Emergent Gravity,” *Class. Quant. Grav.* **35**, no. 11, 115008 (2018), [arXiv:1710.07262 [hep-th]].

4.1 Introduction

The possibility that gravitation emerges from other interactions provides a promising paradigm for addressing the difficult conceptual questions that confront quantum gravity. These questions include the problem of time, namely that coordinate invariance implies a vanishing Hamiltonian and the consequent absence of dynamics of quantum states [76]; the question of predictivity in a theory with nonrenormalizable interactions such as gravitation; the question of what observables are physical in a diffeomorphism-invariant theory; and questions related to the vacuum, including why the Minkowski spacetime and its signature should be preferred to other spacetimes in a quantum theory in which spacetime geometries are integrated over.

The possibility of emergent long-range interactions in quantum field theory has been recognized for half a century.¹ Bjorken argued that four-fermi models with current-current interactions can give rise to emergent gauge interactions [22], and Eguchi later argued that the composite gauge field in such theories may render those theories renormalizable despite the presence of fundamental four-fermi interactions [23]. It did not take long for the idea of emergent interactions to be extended to gravitation, in a wonderfully short note by Sakharov [26]. Sakharov pointed out that the regularized effective action for the spacetime metric generically contains the Einstein-Hilbert term even if no such term is present at tree level, as long as general covariance is maintained by the regulator in the theory. This suggests that the dynamics of spacetime might emerge as an artifact of regulator-scale physics even if there is no such dynamics prior to quantization.²

Perhaps the most compelling argument for emergent gravity is its ubiquity: all that

¹In a classical context, Michael Faraday suspected a relationship between electromagnetism and gravitation, and in the 1840s searched experimentally for such an identification. He was unsuccessful [77].

²Sakharov had in mind that the spacetime metric was to be treated classically, in which case the induced gravity is semiclassical, with the vacuum expectation value of the energy-momentum tensor $T_{\mu\nu}$ being related to the spacetime metric by Einstein's equations (with cosmological constant, plus regulator-suppressed corrections).

is needed is a generally covariant description of the interactions of a field theory and a covariant regulator that resolves infinities in perturbation theory, both of which are likely to be required of quantum gravity, in any case. Much work has been done in an attempt to turn Sakharov's observation into a compelling description of quantum gravity [78, 79, 80, 81], but certain difficulties remain. More recently, alternative paradigms that also appear to lead to emergent gravitational interactions have gained favor, such as the AdS/CFT correspondence [82], entropic gravity [83], and emergent spacetime via networks of entangled states [84, 85]. However, the present work concerns the old-fashioned approach to the subject as motivated by Sakharov's induced gravity.

The problem of nonrenormalizability of the gravitational interaction persists in emergent gravity, unless the quantum theory is asymptotically safe by virtue of an ultraviolet fixed point [86]. However, with the presumption of a physical regulator, the lack of predictivity of the theory is augmented by the more fundamental ontological question of what is to be demanded of the theory at short distances. Regulators in quantum field theory have the habit of violating some cherished principle or another, such as unitarity or boundedness of the Hamiltonian from below. In the present work we are agnostic about the physical regulator and its consequences for the interpretation of the theory at short-distances, and we require only that the theory provide a definite rule for calculating correlation functions of appropriate observables at all physical scales. For the purpose of illustration we will use dimensional regularization, fixing the spacetime dimension D by holding $\epsilon = D - 4$ small but fixed.

The problem of time demands that physical degrees of freedom playing the roles of clock and rulers be identified in any generally covariant theory. This allows dynamics to be interpreted in terms of correlations, or entanglement [87], between physical degrees of freedom and the clock and rulers. For example, certain scalar fields $X^J(x^\mu)$ can play the role of the physical clock and rulers by a gauge-fixing condition analogous to the

static-gauge condition in string theory, under the presumption that field configurations dominating the functional integral can be put into that gauge. Here x^μ are the spacetime parameters integrated over in the action, and the indices J and μ both take values in $\{0, \dots, D - 1\}$. The gauge choice is $X^J = c x^\mu \delta_\mu^J$ for some constant c that will be specified for convenience later. In the models considered here, this choice for the fields X^J satisfy the classical equations of motion with all other fields sitting at the minimum of the potential, and there is a natural perturbative expansion about this classical background.

In this chapter we generalize a particular toy model of emergent gravity that was recently studied in Ref. [27]. The model contains only scalar fields, and D of the fields play the role of clock and rulers in D dimensions. The model was shown to include a massless composite graviton in its spectrum which couples at leading order to the energy-momentum tensor of the physical (non-gauge-fixed) fields as in Einstein gravity. The model is generally covariant from the outset, has a vanishing energy-momentum tensor (including the contributions of the clock and ruler fields), and thereby evades the Weinberg-Witten no-go theorem which prohibits the existence of massless spin-2 particles in a broad class of Lorentz-invariant theories [88]. Diffeomorphism invariance is expected to lead to gravitational self-interactions beyond leading order consistent with general relativity up to Planck-suppressed corrections, and evidence for this by direct computation was recently provided in Ref. [89]. Here we generalize the theory to the case in which the clock and ruler fields have a nontrivial field-space metric, and we demonstrate that, at leading order in a perturbative expansion, scattering is as in Einstein gravity in a spacetime background identified with the field-space metric.

4.2 Emergent Gravity with Curved Backgrounds

The theory that we study includes N scalar fields ϕ^a , $a \in \{1, \dots, N\}$, in addition to the D scalar fields X^J that play the role of clocks and rulers. We assume the potential depends only on ϕ^a but not the clock and ruler fields. The theory is defined so as to be diffeomorphism invariant, and at the classical level the theory is independent of any geometric structure imposed on the spacetime other than differentiability. In particular, the action is independent of spacetime metric on the coordinates x^μ , and correspondingly the theory has an identically vanishing energy-momentum tensor. The action for the theory is,

$$S = \int d^D x \left(\frac{\frac{D}{2} - 1}{V(\phi^a)} \right)^{\frac{D}{2} - 1} \sqrt{\left| \det \left(\sum_{a=1}^N \partial_\mu \phi^a \partial_\nu \phi^a + \sum_{I,J=0}^{D-1} \partial_\mu X^I \partial_\nu X^J G_{IJ}(X^K) \right) \right|}. \quad (4.1)$$

Aside from the dependence of the action on a potential $V(\phi^a)$, this theory is in the class of induced gravity theories based on the Nambu-Goto-like membrane action, as analyzed recently in Ref. [90].

The theory described by Eq. (4.1) is nonlinear, but it is reminiscent of the Nambu-Goto action for the string and we can motivate it by introducing an auxiliary spacetime metric which is fixed by a constraint of vanishing energy-momentum tensor. The Polyakov-like description of the theory is given by the action,

$$S = \int d^D x \sqrt{|g|} \left[\frac{1}{2} g^{\mu\nu} \left(\sum_{a=1}^N \partial_\mu \phi^a \partial_\nu \phi^a + \sum_{I,J=0}^{D-1} \partial_\mu X^I \partial_\nu X^J G_{IJ}(X^K) \right) - V(\phi^a) \right]. \quad (4.2)$$

The quantum theory is defined by functional integral quantization over the scalar fields and $g_{\mu\nu}(x)$, subject to the constraint $T_{\mu\nu} = 0$. The constraint can be thought of as arising from integrating out the auxiliary-field metric $g_{\mu\nu}$, although in that case a Jacobian func-

tional determinant would also arise from the functional integration, which would appear to modify the theory nonperturbatively. (An analogy to this in the context of a model of emergent gauge interactions was pointed out in Ref. [91].) Nonetheless, as long as the action, constraints and regulator are covariant, an emergent gravitational interaction can be expected as in Sakharov's induced gravity.

The partition function for the theory is,

$$Z = \int_{T_{\mu\nu}=0} \mathcal{D}g_{\mu\nu} \mathcal{D}\phi^a \mathcal{D}X^I e^{iS(\phi^a, X^I, g_{\mu\nu})}, \quad (4.3)$$

where the symmetric energy-momentum tensor is defined in the usual way,

$$T_{\mu\nu}(x) = \frac{2}{\sqrt{|g|}} \frac{\delta S}{\delta g^{\mu\nu}(x)} \quad (4.4)$$

$$= \sum_{a=1}^N \partial_\mu \phi^a \partial_\nu \phi^a + \sum_{I,J=0}^{D-1} \partial_\mu X^I \partial_\nu X^J G_{IJ} - g_{\mu\nu} \mathcal{L}, \quad (4.5)$$

where the Lagrangian \mathcal{L} is defined by the action in Eq. (4.2), $S \equiv \int d^D x \sqrt{|g|} \mathcal{L}$. Eq. (4.5) is solved by

$$g_{\mu\nu} = \frac{D/2 - 1}{V(\phi^a)} \left(\sum_{a=1}^N \partial_\mu \phi^a \partial_\nu \phi^a + \sum_{I,J=0}^{D-1} \partial_\mu X^I \partial_\nu X^J G_{IJ} \right), \quad (4.6)$$

which together with Eq. (4.2) gives the membrane-like action Eq. (4.1). Note that $g_{\mu\nu}$ of Eq. (4.6) is auxiliary and does not have dynamics other than that due to its dependence on the fields ϕ^a and X^I . Also note that, despite the similarity of the actions Eq. (4.1) and Eq. (4.2) to the Nambu-Goto and Polyakov actions of string theory, the factor of $D/2 - 1$ in Eq. (4.6) hints that the case $D = 2$ is special. In $D = 2$, a conformal factor rescaling the metric of Eq. (4.6) factors out of the equations of motion and allows for the transition from the Polyakov form to the Nambu-Goto form of the string action.

We assume that the potential $V(\phi)$ has the form $V(\phi) = V_0 + \Delta V(\phi)$, with the

minimum of the potential V_0 much larger than any other scales in the theory with the possible exception of a scale associated with the physical regulator. For simplicity we also assume in our analysis that the field-space metric $G_{IJ}(X^K) \equiv \eta_{IJ} + \tilde{H}_{IJ}(X^K)$, with Minkowski (mostly-minus) metric η_{IJ} , admits a perturbative expansion in \tilde{H}_{IJ} and its derivatives.

The theory described by Eq. (4.1) is invariant under coordinate reparametrizations, $X^I(x) \rightarrow X^I(x'(x))$ and $\phi^a(x) \rightarrow \phi^a(x'(x))$; and under field redefinitions the field-space metric G_{IJ} transforms like a metric: If $X^I(x)$ is replaced with $X'^I(X^J(x))$ and $G_{IJ}(X)$ is replaced with $G'_{IJ}(X')$,

$$\begin{aligned} \partial_\mu X^I \partial_\nu X^J G_{IJ}(X) &\rightarrow \partial_\mu X'^I \partial_\nu X'^J G'_{IJ}(X') \\ &= \partial_\mu X^K \partial_\nu X^L \frac{\partial X'^I}{\partial X^K} \frac{\partial X'^J}{\partial X^L} G'_{IJ}(X'(X)) \\ &= \partial_\mu X^I \partial_\nu X^J G_{IJ}(X), \end{aligned} \quad (4.7)$$

where the last line follows if

$$G'_{IJ}(X) = \frac{\partial X^K}{\partial X'^I} \frac{\partial X^L}{\partial X'^J} G_{KL}(X'(X)). \quad (4.8)$$

Note that a field redefinition cannot take a curved-space G_{IJ} to a flat-space one, so the theory with generic field-space metric is genuinely inequivalent to the flat-field-space version of the theory studied previously.

In order to provide physical meaning to the spacetime background in which dynamics take place, we identify X^I with the corresponding spacetime coordinates (up to a constant factor), analogous to a static gauge condition in string theory:

$$X^I = \sqrt{\frac{V_0}{D/2 - 1}} x^\mu \delta_\mu^I, \quad I = 0, \dots, D - 1, \quad (4.9)$$

Then the field X^0 can be interpreted as an internal clock [87], while the fields $X^i, i = 1, \dots, D-1$ are interpreted as rulers. In this case the Fadeev-Popov determinant is

$$\begin{aligned} \det \left(\frac{\delta X^{I,\alpha}(y)}{\delta \alpha^\mu(y')} \right) &= \det \left(\sqrt{\frac{V_0}{\frac{D}{2}-1}} \frac{\delta(y^\mu + \alpha^\mu(y))}{\delta \alpha^\mu(y')} \delta_\mu^I \right) \\ &= \det \left(\sqrt{\frac{V_0}{\frac{D}{2}-1}} \delta_\mu^I \delta^{(D)}(y-y') \right), \end{aligned} \quad (4.10)$$

which is trivial and consequently there are no Fadeev-Popov ghosts resulting from gauge fixing X^I .

The classical equations of motion for ϕ^a and X^I following from the action Eq. (4.2) are

$$\frac{1}{\sqrt{-g}} \partial_\mu (\sqrt{-g} g^{\mu\nu} \partial_\nu \phi^a) = -\frac{\partial V}{\partial \phi^a}, \quad (4.11)$$

$$\partial_\mu (\sqrt{-g} g^{\mu\nu} G_{IJ} \partial_\nu X^J) = \frac{1}{2} \sqrt{-g} g^{\mu\nu} \partial_\mu X^J \partial_\nu X^K \frac{\partial}{\partial X^I} G_{JK}. \quad (4.12)$$

If we set $\phi^a = \phi_{\min}^a$ where ϕ_{\min}^a minimizes V such that $V(\phi_{\min}^a) = V_0$, then the equation of motion for ϕ^a is trivially satisfied. Meanwhile, with the gauge-fixed background X^I as in Eq. (4.9), the spacetime metric at $\phi^a = \phi_{\min}^a$ is

$$g_{\mu\nu} = \frac{\frac{D}{2}-1}{V_0} \frac{(\sqrt{V_0} \delta_\mu^I) (\sqrt{V_0} \delta_\nu^J) G_{IJ}}{\frac{D}{2}-1} = G_{\mu\nu}(x^I), \quad (4.13)$$

so the spacetime background in which the fields ϕ^a propagate is now identified with the field-space metric for the clock and ruler fields. Furthermore, the equations of motion for the clock and ruler fields, Eq. (4.12), are also satisfied by the static gauge condition, as is readily checked using the identity,

$$\frac{1}{\sqrt{|g|}} \frac{\partial \sqrt{|g|}}{\partial x^\alpha} = \frac{1}{2} g^{\mu\nu} \frac{\partial g_{\mu\nu}}{\partial x^\alpha}. \quad (4.14)$$

Hence, the static-gauge configuration with fields ϕ^a uniform at the minimum of the potential, and with $g_{\mu\nu}(x) = G_{\mu\nu}(x)$, solve the equations of motion and provide a classical background about which the dynamics for the fields ϕ^a can now be analyzed.

We now show that the background G_{IJ} modifies the emergent gravitational interaction by coupling to the matter fields as in Einstein gravity, at linear order in the expansion about the Minkowski metric. Thus we write the background G_{IJ} as,

$$G_{\mu\nu} = g_{\mu\nu}^{(B)} = \eta_{\mu\nu} + \tilde{H}_{\mu\nu}, \quad (4.15)$$

where $\tilde{H}_{\mu\nu}$ determines the background spacetime but is assumed to be small compared to $\eta_{\mu\nu}$. Consequently the gauge-fixed action takes the form,

$$S = \int d^D x \frac{V_0}{D/2 - 1} \left(\frac{V_0}{V_0 + \Delta V(\phi^a)} \right)^{D/2-1} \sqrt{\left| \det \left(\eta_{\mu\nu} + \tilde{H}_{\mu\nu} + \tilde{h}_{\mu\nu} \right) \right|}, \quad (4.16)$$

where

$$\tilde{h}_{\mu\nu} \equiv \frac{D/2 - 1}{V_0} \left(\sum_{a=1}^N \partial_\mu \phi^a \partial_\nu \phi^a \right), \quad (4.17)$$

and $g_{\mu\nu}$ depends on the field configuration via,

$$g_{\mu\nu} = \frac{V_0}{V(\phi)} \left(\eta_{\mu\nu} + \tilde{H}_{\mu\nu} + \tilde{h}_{\mu\nu} \right). \quad (4.18)$$

In order to analyze the theory perturbatively, we expand Eq. (4.16) in powers of $1/V_0$ and \tilde{H} . We take $\tilde{h}_{\mu\nu}$ and $\tilde{H}_{\mu\nu}$ to be of the same order. We also assume for simplicity that N , the number of fields ϕ^a , is large, and keep only leading terms in a $1/N$ expansion. Expanding the determinant via the identity $\det M = \exp(\text{tr} \ln M)$, the action can be

written as

$$\begin{aligned}
S &= \int d^D x \frac{V_0}{D/2-1} \left(1 + \frac{\Delta V(\phi^a)}{V_0}\right)^{1-D/2} \left[1 + \frac{1}{2}(\tilde{h} + \tilde{H}) \right. \\
&\quad \left. - \frac{1}{4}(\tilde{h}_{\mu\nu} + \tilde{H}_{\mu\nu})(\tilde{h}^{\mu\nu} + \tilde{H}^{\mu\nu}) + \frac{1}{8}(\tilde{h} + \tilde{H})^2 + \dots\right] \\
&= \int d^D x \left(\frac{V_0}{D/2-1} - \Delta V(\phi^a) + \frac{D}{4} \frac{(\Delta V(\phi^a))^2}{V_0} + \dots\right) \times \left[1 + \frac{1}{2}(\tilde{h} + \tilde{H}) \right. \\
&\quad \left. - \frac{1}{4}(\tilde{h}_{\mu\nu}\tilde{h}^{\mu\nu} + \tilde{H}_{\mu\nu}\tilde{H}^{\mu\nu} + 2\tilde{h}_{\mu\nu}\tilde{H}^{\mu\nu}) + \frac{1}{8}(\tilde{h}^2 + \tilde{H}^2 + 2\tilde{h}\tilde{H}) + \dots\right], \tag{4.19}
\end{aligned}$$

where index contractions are done with the Minkowski metric and $\tilde{h} = \eta_{\mu\nu}\tilde{h}^{\mu\nu}$ (likewise $\tilde{H} = \eta_{\mu\nu}\tilde{H}^{\mu\nu}$). Keeping terms up to first order in \tilde{H} and $1/V_0$, and using Eq. (4.17), we arrive at the action

$$\begin{aligned}
S &= \int d^D x \left\{ \frac{V_0}{D/2-1} + \frac{1}{2} \sum_{a=1}^N \partial_\mu \phi^a \partial^\mu \phi^a - \Delta V(\phi^a) + \frac{1}{2} \frac{V_0}{D/2-1} \tilde{H} \right. \\
&\quad \left. - \frac{D/2-1}{4V_0} \left[\sum_{a=1}^N \partial_\mu \phi^a \partial_\nu \phi^a \sum_{b=1}^N \partial^\mu \phi^b \partial^\nu \phi^b - \frac{1}{2} \left(\sum_{a=1}^N \partial_\mu \phi^a \partial^\mu \phi^a \right)^2 \right] \right. \\
&\quad \left. - \frac{D/2-1}{2} \frac{\Delta V(\phi^a)}{V_0} \sum_{a=1}^N \partial_\mu \phi^a \partial^\mu \phi^a + \frac{D}{4} \frac{(\Delta V(\phi^a))^2}{V_0} \right. \\
&\quad \left. - \frac{1}{2} \tilde{H}^{\mu\nu} \sum_{a=1}^N \partial_\mu \phi^a \partial_\nu \phi^a + \frac{1}{4} \eta_{\mu\nu} \tilde{H}^{\mu\nu} \sum_{a=1}^N \partial_\alpha \phi^a \partial^\alpha \phi^a - \frac{1}{2} \Delta V(\phi^a) \eta_{\mu\nu} \tilde{H}^{\mu\nu} \right. \\
&\quad \left. + \mathcal{O}\left(\tilde{H}^2, \frac{1}{V_0^2}\right) \right\}. \tag{4.20}
\end{aligned}$$

The first three lines in Eq. (4.20) are equivalent to the action analyzed in Ref. [27] up to the addition of a ϕ -independent contribution to the action.

The interactions between ϕ^a and $\tilde{H}^{\mu\nu}$ are new, and will shortly be shown to give rise to scattering off of the background spacetime in accordance with general relativity. For a

free theory with $O(N)$ -symmetric potential

$$\Delta V(\phi^a) = \sum_{a=1}^N \frac{m^2}{2} \phi^a \phi^a, \quad (4.21)$$

the first line of Eq. (4.20) contains the free part of the action. The energy-momentum tensor for free fields ϕ^a is

$$\mathcal{T}_{\mu\nu} = \sum_{a=1}^N \left[\partial_\mu \phi^a \partial_\nu \phi^a - \eta_{\mu\nu} \left(\frac{1}{2} \partial^\alpha \phi^a \partial_\alpha \phi^a - \frac{1}{2} m^2 \phi^a \phi^a \right) \right], \quad (4.22)$$

and the interacting terms excluding $\tilde{H}^{\mu\nu}$ can be written,

$$\mathcal{L}_{\tilde{h}} = -\frac{1}{4V_0} \mathcal{T}_{\mu\nu} \mathcal{T}_{\alpha\beta} \left(\left(\frac{D}{2} - 1 \right) \eta^{\nu\alpha} \eta^{\mu\beta} - \frac{1}{2} \eta^{\mu\nu} \eta^{\alpha\beta} \right). \quad (4.23)$$

In Ref. [27], it was shown that these interactions give rise to a massless spin-two graviton state that mediates the gravitational interaction in two-into-two scattering of ϕ bosons.

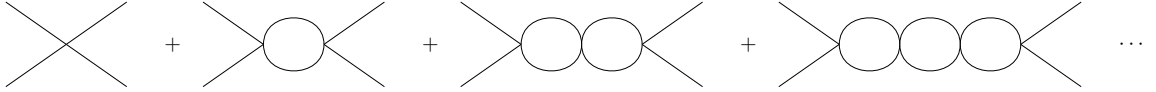
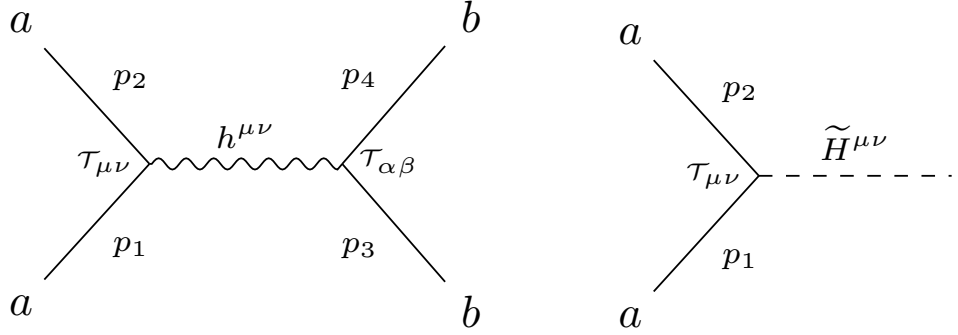


FIG. 4.1: Leading large- N diagrams that give rise to the emergent gravitational interaction.



(a) The graviton pole that emerges from two-into-two scattering of ϕ bosons.

(b) Scattering of ϕ bosons off of $\tilde{H}^{\mu\nu}$.

FIG. 4.2: Feynman diagrams for our current theory.

The diagrams in Fig. 4.1 are responsible for the emergent gravitational interaction, which can be equivalently described by exchange of a composite graviton as in Fig. 4.2(a). Hence, the emergent gravity persists in this model, at least at the perturbative level to which we are working.

At the same order in perturbation theory, we can interpret the interactions with the background metric $\tilde{H}^{\mu\nu}$ as arising from a background source. Notice the contribution from $\tilde{H}^{\mu\nu}$ in the last line of Eq. (4.20) takes the form

$$\mathcal{L}_{\tilde{H}} = -\frac{1}{2}\tilde{H}^{\mu\nu} \sum_{a=1}^N \left[\partial_\mu \phi^a \partial_\nu \phi^a - \eta_{\mu\nu} \left(\frac{1}{2} \partial^\alpha \phi^a \partial_\alpha \phi^a - \frac{1}{2} m^2 \phi^a \phi^a \right) \right] = -\frac{1}{2}\tilde{H}^{\mu\nu} \mathcal{T}_{\mu\nu}, \quad (4.24)$$

which confirms the agreement of the theory with the linearized coupling of matter to the background metric in general relativity, and results in the interactions shown in Fig. 4.2(b). From Eq. (4.24), we can read off the momentum space Feynman rule for interactions involving $\tilde{H}^{\mu\nu}$, with p_1 ingoing and p_2, q outgoing:

$$\left(\tilde{H} - \mathcal{T} \right) \text{ vertex} = -\frac{i}{2} E_{\mu\nu}(p_1, p_2) \tilde{H}^{\mu\nu}(q) \delta^D(p_1 - p_2 - q) \quad (4.25)$$

for inwardly (outwardly) directed external momenta p_1 (p_2), and where

$$E_{\mu\nu}(p_1, p_2) \equiv (p_1^\mu p_2^\nu + p_1^\nu p_2^\mu) + \eta^{\mu\nu} (-p_1 \cdot p_2 + m^2) \quad (4.26)$$

is determined by Eq. (4.22), summing over the ways in which the fields can annihilate (or create) incoming (or outgoing) scalar bosons. The interactions involving $\tilde{H}^{\mu\nu}$ don't contribute to scattering but instead create an instability in $G_{\mu\nu}$, rendering $\mathcal{T}_{\mu\nu} \neq 0$. Hence there is a background field (call this $\mathcal{T}^{(B)}_{\mu\nu}$) that appears as a source for $\tilde{H}^{\mu\nu}$ in the Einstein-Hilbert action.

We note that interactions at higher-order in $1/V_0$ can contribute at the same order as the diagrams that we have considered if they include tadpoles which are also proportional to V_0 . However, as in Ref. [27], we can add a counterterm c_2 to V_0 which cancels tadpoles from insertions of $m^2 \overline{\phi^a \phi^a}$ in interactions, and we can shift the gauge by a parameter c_1 in order to cancel tadpoles from insertions of $\overline{\partial_\mu \phi^a \partial_\nu \phi^a}$ in interactions:

$$\begin{aligned} X^I &= x^I \sqrt{\frac{V_0}{D/2 - 1} - c_1}, \\ \Delta V &= \frac{1}{2} m^2 \overline{\phi^a \phi^a} - c_2, \end{aligned} \quad (4.27)$$

There are no other tadpoles in this theory, so all relevant diagrams have been accounted for at leading order in $1/N$ and $1/V_0$. All additional diagrams from couplings of higher order in $1/V_0$ are consistently neglected at leading order.

The linearized coupling of the composite field $h_{\mu\nu}$ to matter is given by

$$\mathcal{L}_{hT} = -\frac{1}{2} h^{\mu\nu} \mathcal{T}_{\mu\nu}, \quad (4.28)$$

where $h^{\mu\nu}$ is the composite operator representing the fluctuation about the Minkowski metric,

$$h^{\mu\nu} = \frac{1}{V_0} P^{\mu\nu}{}_{\lambda\kappa} \mathcal{T}^{\lambda\kappa} + \mathcal{O}(1/V_0^2) = \frac{1}{V_0} \sum_{a=1}^N \left[(D/2 - 1) \partial^\mu \phi^a \partial^\nu \phi^a - \frac{1}{2} \eta^{\mu\nu} m^2 \phi^a \phi^a \right], \quad (4.29)$$

$$P^{\mu\nu}{}_{\lambda\kappa} \equiv \frac{1}{2} [(D/2 - 1) (\delta_\lambda^\mu \delta_\kappa^\nu + \delta_\kappa^\mu \delta_\lambda^\nu) - \eta^{\mu\nu} \eta_{\lambda\kappa}].$$

Now that there is a source creating a background in which $T_{\mu\nu}$ fluctuates, we find that

$$\mathcal{L}_{int} = -\frac{1}{2} (h^{\mu\nu} + \tilde{H}^{\mu\nu}) \mathcal{T}_{\mu\nu} \quad (4.30)$$

at the linearized level.

Thus we have interactions in which the matter fields can scatter off themselves, corresponding to the exchange of a massless composite graviton $h^{\mu\nu}$, or they can scatter off the background spacetime defined by $\tilde{H}^{\mu\nu}$. We can interpret the scattering off of the background spacetime as due to the existence of a background energy-momentum tensor. Here we can draw an analogy to electromagnetism. Consider a scenario in which there is a current creating a background electromagnetic field; then incoming charged particles feel the effects of the field as they scatter off of one another. But we can recast this scenario into an equivalent one in which the incoming charged particles scatter off the current which generates the background electromagnetic field, thereby rendering the source dynamical.

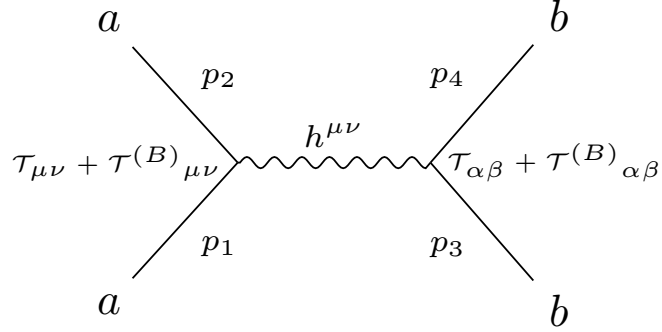


FIG. 4.3: In this redefined theory, the matter field $\mathcal{T}_{\mu\nu}$ can scatter off of itself and the background field $\mathcal{T}^{(B)}_{\mu\nu}$. The scattering of $\mathcal{T}^{(B)}_{\mu\nu}$ off of itself is unphysical, thus should not be considered.

Likewise we can consider a process in which the scalar bosons scatter off of one another and off of the source that generates $\tilde{H}^{\mu\nu}$, so that the graviton couples to the matter and background source, as shown in Fig. 4.3. As a result the interacting Lagrangian reads

$$\mathcal{L}'_{int} = -\frac{1}{2}h^{\mu\nu} (\mathcal{T}_{\mu\nu} + \mathcal{T}^{(B)}_{\mu\nu}(x)). \quad (4.31)$$

We can extract $\mathcal{T}^{(B)}_{\mu\nu}$ from the linearized equation of motion for $\tilde{H}^{\mu\nu}$:

$$D_{\mu\nu\lambda\kappa}\tilde{H}^{\lambda\kappa}(x) = -\mathcal{T}^{(B)}_{\mu\nu}(x). \quad (4.32)$$

Here D is the linearized equation of motion operator describing the dynamics of the composite graviton,

$$D_{\mu\nu\lambda\kappa}\tilde{H}^{\lambda\kappa}(x) = \frac{D-2}{M_P^{2-D}} \left(\square \tilde{H}^{\mu\nu} + \partial^\mu \partial^\nu \tilde{H} - \eta^{\mu\nu} \square \tilde{H} \right. \\ \left. + \eta^{\mu\nu} \partial_\lambda \partial_\kappa \tilde{H}^{\lambda\kappa} - \eta^{\nu\lambda} \partial_\lambda \partial_\kappa \tilde{H}^{\mu\kappa} - \eta^{\nu\lambda} \partial^\mu \partial^\kappa \tilde{H}_{\lambda\kappa} \right), \quad (4.33)$$

where M_P characterizes the strength of the interaction. It is the reduced Planck mass deduced by comparing the scattering amplitude due to the effective 1-graviton exchange

with general relativity, and was calculated in Ref. [27] to have the value³,

$$M_P = m \left[\frac{N\Gamma(1 - D/2)}{6(4\pi)^{D/2}} \right]^{1/(D-2)}. \quad (4.34)$$

If we instead want to recover the background spacetime from the background energy-momentum tensor, we need to invert the equation of motion operator, which requires fixing the coordinate ambiguity. For example, by a field redefinition of the fields X^I as in Eq. (4.8), we can choose the background $\tilde{H}^{\mu\nu}$ to be in the de Donder gauge, $\partial^\nu \tilde{H}_{\mu\nu} = \frac{1}{2} \partial_\mu \tilde{H}$. The linearized Einstein equation in de Donder gauge is,

$$D_{\mu\nu\lambda\kappa} \tilde{H}^{\lambda\kappa}(x) = \frac{D-2}{M_P^{2-D}} \left(\square \tilde{H}^{\mu\nu} - \frac{1}{2} \eta^{\mu\nu} \square \tilde{H} \right). \quad (4.35)$$

Since this expression is invertible, we can calculate schematically,

$$\tilde{H}^{\mu\nu} = - (D^{-1})^{\mu\nu\lambda\kappa} \mathcal{T}^{(B)}_{\lambda\kappa}. \quad (4.36)$$

Upon a Fourier transformation to momentum space,

$$\tilde{H}^{\mu\nu}(q) = - (D^{-1})^{\mu\nu\lambda\kappa}(q) E^{(B)}_{\lambda\kappa}(p_3, p_4), \quad (4.37)$$

for incoming (outgoing) momenta p_3 (p_4 , $q = p_3 - p_4$).

We can compare in more detail the theories defined by Lagrangians Eq. (4.30) and Eq. (4.31). Seeing that both \mathcal{L}_{int} and \mathcal{L}'_{int} contain a factor of $h^{\mu\nu} \mathcal{T}_{\mu\nu}$, the scattering amplitude of scalar particles off one another remains the same at this order, so we only need to consider interactions involving the source and the background it creates. The

³We thank Chris Carone and Diana Vaman for correcting a minus sign in this expression from the first version of Ref. [27].

scattering amplitude for Fig. 4.2(b) is

$$\mathcal{M}_{MB} = -\frac{i}{2} E_{\mu\nu}(p_1, p_2) \tilde{H}^{\mu\nu}(q), \quad (4.38)$$

while the scattering amplitude for Fig. 4.3 is

$$\begin{aligned} \mathcal{M}'_{MB} &= -\frac{i}{2} E_{\mu\nu}(p_1, p_2) (-i) (D^{-1})^{\mu\nu\alpha\beta}(q) 2 \times \left(-\frac{i}{2} E^{(B)}_{\alpha\beta}(p_3, p_4) \right) \\ &= -\frac{i}{2} E_{\mu\nu}(p_1, p_2) 2 \times \left(\frac{1}{2} \tilde{H}^{\mu\nu}(q) \right) \\ &= -\frac{i}{2} E_{\mu\nu}(p_1, p_2) \tilde{H}^{\mu\nu}(q), \end{aligned} \quad (4.39)$$

Evidently $\mathcal{M}_{MB} = \mathcal{M}'_{MB}$; thus we can infer that the amplitude of the matter fields scattering off of the background source is the same as if it was scattering off of the background metric. Indeed then \mathcal{L}_{int} gives rise to the same physics as \mathcal{L}'_{int} at the linearized level.

4.3 Discussion and Conclusions

We have analyzed scattering amplitudes in a model of emergent gravity with general field-space metric for scalar fields that play the role of clock and rulers after gauge-fixing. The classical equations of motion admit a background solution in which the emergent spacetime metric is equal to the field-space metric. The quantum theory then admits a perturbative expansion about this background, so that the theory describes an emergent quantum gravity about the prescribed spacetime background. In the case that the field-space metric is nearly flat, we demonstrated that scattering off of the background spacetime is as in general relativity, as is 2-into-2 scattering through the exchange of a composite spin-2 graviton.

We note that even if the regulator scale is taken to infinity (for example $\epsilon \rightarrow 0$ in

dimensional regularization), so that the effective $M_{\text{Pl}} \rightarrow \infty$, matter will still scatter off of the gauge-fixed clock and ruler fields in such a way that the field-space metric plays the role of the background spacetime.

It was important in our analysis that the dynamics of the clock and ruler fields was due only to the field-space kinetic term. If the potential had depended on the fields X^I then the classical backgrounds for the clock and rulers would generally not admit the static-gauge condition $X^I \propto x^\mu \delta_\mu^I$. For example, oscillating configurations of a massive clock field would be bounded in magnitude and could not be transformed by a coordinate transformation to an unbounded solution like the static-gauge configuration. The possibility of configurations that do not admit the static gauge condition also raises another issue. By assuming the static gauge we are only integrating over a subset of field configurations. These are configurations close to the classical background, so we suspect that these solutions dominate perturbative contributions to correlation functions. However, the contribution of other configurations, which are nonperturbative in the present approach, deserve further investigation.

Although our analysis has been to leading order in a perturbative expansion, and we have demonstrated that the theory generates the gravitational interactions of general relativity at lowest order, diffeomorphism invariance of the theory is expected to lead to the expected nonlinear gravitational interactions, as well. Calculation of the leading graviton self-interactions in this theory (with flat field-space metric) was done in Ref. [89], and was shown to agree with the predictions of general relativity. We also note that the field-space metric for the clock and ruler fields determines the global symmetries of the spacetime background. For example, with a flat field-space metric the theory maintains a global Lorentz invariance that acts on the clock and ruler fields. The lesson is that in this approach global spacetime symmetries act on spacetime fields, while diffeomorphism invariance acts on the coordinate-dependence of both the spacetime fields and the physical

fields.

There are several ways to generalize the class of theories described here in order to incorporate realistic matter and gauge interactions. The approach that we advocate is to begin with a covariant description of the Standard Model coupled to gravity, include the clock and ruler fields possibly with a nontrivial field-space metric but otherwise massless and free, and then demand $T_{\mu\nu} = 0$ as was done in the scalar toy model presented here. This defines a theory that should resemble the Standard Model at long distances compared to the regulator scale, coupled to emergent gravity by analogy with the discussion presented here. One remaining challenge is to define a physical regulator that would allow for a well-defined description of the physics at distances shorter than the regulator scale, or else provide an explanation for why such short distances are not meaningful.

Finally, we note that because the linearized couplings of the matter fields to both the composite graviton state and to the background spacetime metric are through the energy-momentum tensor, an extension of the theory to include scalars with different masses is guaranteed to contain universal gravitational couplings.

CHAPTER 5

Dark sector portal with vector-like leptons and flavor sequestering¹

In this chapter we consider models with fermionic dark matter that transforms under a non-Abelian dark gauge group. Exotic, vector-like leptons that also transform under the dark gauge group can mix with standard model leptons after spontaneous symmetry breaking and serve as a portal between the dark and visible sectors. We show in an explicit, renormalizable model based on a dark $SU(2)$ gauge group how this can lead to adequate dark matter annihilation to a standard model lepton flavor so that the correct relic density is obtained. We identify a discrete symmetry that allows mass mixing between the vector-like fermions and a single standard model lepton flavor. This flavor sequestering avoids unwanted lepton-flavor-violating effects, substantially relaxing constraints on the mass scale of the vector-like states. We discuss aspects of the phenomenology of the model, including direct detection of the dark matter.

¹Work previously published in C. D. Carone, S. Chaurasia and T. V. B. Claringbold, “Dark sector portal with vectorlike leptons and flavor sequestering,” *Phys. Rev. D* **99**, no. 1, 015009 (2019) [arXiv:1807.05288 [hep-ph]].

5.1 Introduction

Although the literature on dark matter models is vast and diverse, the organizational structure of many of these models is similar. The visible sector includes all the fields normally associated with the minimal standard model; the dark sector consists of a collection of fields that communicate very weakly with the visible sector; the messenger or portal sector consists of those fields that allow for a weak coupling between the visible and dark sectors. In this chapter, we are interested in a possible portal for dark matter models, specifically ones in which fermionic dark matter is charged under a dark gauge group. Our model will include vector-like fermions that are also in nontrivial representations of the dark gauge group but can mix with standard model fermions when the gauge symmetries of the theory are spontaneously broken. We identify a mechanism, based on symmetries, that we call “flavor sequestering” which allows this mixing to be non-negligible, while simultaneously suppressing unwanted flavor-changing processes. This mechanism is new to the literature; it can provide for vector-like fermion portal sectors that are lighter and more accessible experimentally than would otherwise be possible. For the purposes of illustration, we choose to study a theory with a non-Abelian dark gauge group, where an additional portal involving kinetic mixing of some dark gauge boson components with hypercharge is naturally suppressed. In models like the one we propose, where there are vector-like states charged both under the dark and hypercharge gauge groups, the kinetic mixing parameter in an Abelian theory would typically run below the Planck scale, leading to low-energy values that are not necessarily small; this makes a non-Abelian dark sector the natural setting for formulating our proposal. Scenarios in which multiple portals are relevant (for example, a vector-like fermion portal, a Higgs-portal, a higher-dimension-operator portal, *etc.*) are of course possible and more complicated; in the present work, however, we focus on the case where the vector-like fermion portal is dominant. Examples of non-Abelian

dark matter models can be found in Refs. [40, 41, 42, 43, 44, 45, 46], [92, 93, 94] and [95]; we will not focus on models like those in Refs. [92, 93, 94] where a dark gauge boson is itself the dark matter. Our model is also very different from the models of Refs. [95] which involve unbroken non-Abelian dark gauge groups, either chosen to assure composite dark matter candidates in the cases where there is confinement, or dark radiation in the case where the dark gauge coupling is too small for confinement to be cosmologically relevant. In our proposal, mixing between the vector-like and standard model fermions will only be present when the non-Abelian dark gauge group is spontaneously broken.

Given these assumptions, we would like the vector-like fermion portal in our model to allow the dark gauge bosons to develop a small coupling to the visible sector, adequate enough to facilitate the annihilation of the dark matter for a successful thermal freeze-out, without running afoul of direct detection bounds. This can be arranged if the effective coupling between the dark and visible sectors does not appear at the same order in the dark matter annihilation and dark-matter-nucleon elastic scattering cross sections. To achieve this, we choose the quantum numbers of the vector-like states to allow mixing only with standard model leptons. The induced coupling of the dark gauge bosons would allow dark matter annihilation to leptons via tree-level diagrams, while diagrams involving quarks would be higher-order. One might wonder whether coupling the dark gauge bosons to standard model leptons directly might be a more economical alternative. However, proceeding in this way leads to significant model building complications. For example, if one tries to couple the dark gauge bosons to the standard model leptons directly, then the dark gauge bosons are potentially no longer “dark,” unless their gauge coupling is taken to be very small. However, this choice suppresses the coupling of the dark gauge bosons to both the dark and visible sectors, making it ineffective as a channel for dark matter annihilation. Moreover, such direct couplings lead generically to chiral anomalies, which must be cancelled by additional states that are charged under both the dark and

standard model gauge groups. There is no guarantee that the simplest Higgs field content of the dark and visible sectors will have the correct quantum numbers to provide Yukawa couplings for these additional states, so that additional Higgs representations may be required. Another potential problem is that charging standard model leptons under the new non-Abelian group may either restrict the form of the standard model lepton Yukawa matrices in unwanted ways, or forbid them entirely, unless a Higgs field charged under both the dark and standard model gauge groups is introduced. While the proliferation of fields implied by these considerations does not rise to the level of a no-go theorem, it does make the approach described a lot less appealing.

To avoid these complications, we assume that the non-Abelian dark gauge boson may couple to a vector-like state χ that can mix with standard model leptons after the gauge symmetries of the theory (both dark and visible) are spontaneously broken. We will refer to the χ states as heavy, vector-like leptons. If the dark gauge boson's coupling to dark matter is g_D , which may be substantial, then the induced coupling to the standard model lepton in the mass eigenstate basis will be proportional to θg_D where θ is a small mixing angle. Since the gauge boson couples directly to a vector-like state, anomalies are cancelled, and a mass term $-M_\chi \bar{\chi} \chi$ can be written down at tree-level. A case of particular phenomenological interest is where the vector-like sector is as light as possible. In this case, the mixing angle θ can be large enough so that the desired dark matter relic density is obtained entirely via dark matter annihilation to a standard model lepton-anti-lepton pair. This scenario would not be possible in a similar model without flavor sequestering, so we focus on this region of parameter space as the proof of principle that our flavor-sequestering idea can be incorporated in viable models. The range of M_χ is then determined by the requirement that the the mixing angle θ is large enough to produce the desired value of the dark matter relic density. In this chapter, we will present an explicit and renormalizable model that illustrates this proposal. Our focus differs from that of

Refs. [40, 41, 42, 43, 44, 45, 46], where the origin of higher-dimension operators connecting the dark and visible sectors was either unspecified, or assumed to arise from a sector whose flavor structure and phenomenology was not explicitly investigated.

The idea that a dark sector could communicate to the visible sector in any appreciable way through mixing between vector-like leptons and their standard model counterparts would seem to conflict with the stringent lower bounds on the mass scale of heavy vector-like leptons that appear in the literature, which exceed 100 TeV [47]. Such stringent bounds, however, come from consideration of lepton-flavor-violating processes that emerge when the vector-like states mix with all three standard model lepton flavors. One expects such mixing to be present generically, and this would doom the approach that we have just outlined. In this chapter, we show how a more favorable outcome can be achieved via discrete symmetries that allow us to suppress the unwanted mass mixing arbitrarily. In our model, vector-like leptons mix only with a single flavor of the standard model leptons, which in turn does not mix substantially with the remaining two flavors, thus avoiding problems with lepton flavor violation. We will show that the discrete symmetry used to achieve this flavor sequestering does not adversely affect the remaining flavor structure of the charged leptons or neutrino mass matrices. Phenomenological considerations place constraints on the mass spectrum of the flavor-sequestered vector-like lepton states that can be tested in direct collider searches.

This chapter is organized as follows. In the next section, we define the simplest model that illustrates a portal involving vector-like leptons and flavor sequestering. In Sec. 3, we show how the flavor structure of the theory can be achieved using a discrete symmetry, so that exclusive mixing with one standard model lepton generation is obtained and lepton-flavor-violating effects avoided. In Sec. 4 we demonstrate the viability of our example model by identifying the region of parameter space in which the correct dark matter relic density is obtained through annihilation to a standard model lepton-anti-lepton pair. We

also consider the constraints from dark matter-nucleon elastic scattering, which follows from the suppressed kinetic mixing that is induced after the non-Abelian gauge group is spontaneously broken. In the final section, we summarize our conclusions.

5.2 The Model

We consider the simplest non-Abelian dark gauge group, $SU(2)_D$. As stated earlier, we denote the heavy, vector-like leptons χ , and assume the quantum numbers

$$\chi_L \sim \chi_R \sim (\mathbf{2}, \mathbf{1}, \mathbf{1}, -1) , \quad (5.1)$$

where we indicate the representations of $SU(2)_D \times SU(3)_C \times SU(2)_W \times U(1)_Y$, in that order. In other words, these states are $SU(2)_D$ doublets, but have the same electroweak charges as right-handed leptons. We further assume the simplest assignment for the dark matter, *i.e.*, that it is a doublet under $SU(2)_D$. However, to avoid a Witten anomaly [96] there must be an even number of $SU(2)$ fermion doublets, so we take

$$\psi_L \sim \psi_R \sim (\mathbf{2}, \mathbf{1}, \mathbf{1}, 0) . \quad (5.2)$$

Since the ψ fields are charged only under $SU(2)_D$, we can construct Dirac or Majorana mass terms, or both. We will assume Dirac mass terms, for simplicity, though it is easy to make this the only possibility by imposing additional discrete symmetries. For example, an unbroken Z_3 symmetry can forbid Majorana masses for ψ , and also serve as the symmetry which stabilizes the dark matter, which we identify henceforth as the lightest component of the ψ doublet.

We assume that the dark gauge symmetry is spontaneously broken by two $SU(2)_D$

Higgs field representations,

$$H_D \sim (\mathbf{2}, \mathbf{1}, \mathbf{1}, 0) \quad \text{and} \quad H_T \sim (\mathbf{3}, \mathbf{1}, \mathbf{1}, 0) \quad . \quad (5.3)$$

We show at the end of this section that the Higgs potential has local minima consistent with the pattern of vacuum expectation values (vevs):

$$\langle H_D \rangle = \begin{pmatrix} v_{D1} \\ v_{D2} \end{pmatrix} \quad \text{and} \quad \langle H_T \rangle = \begin{pmatrix} v_T/2 & 0 \\ 0 & -v_T/2 \end{pmatrix} \quad . \quad (5.4)$$

If we decompose $H_T = H_T^a (\sigma^a/2)$, where the σ^a are Pauli matrices, then the H_T vev above corresponds to $\langle H_T^3 \rangle = v_T$ and $\langle H_T^a \rangle = 0$ for $a = 1, 2$. In fact, an arbitrary vev for H_T can always be rotated into the H_T^3 direction by an $SU(2)_D$ transformation. With this choice, vevs in both components of H_D are expected, and one of those can be made real by a further $SU(2)_D$ phase rotation. The fact that the remaining H_D vev in Eq. (5.4) is assumed real will be shown to be consistent with the minimization of a potential later.

We can now say something more concrete about the mass spectrum of the model. The relevant Lagrangian terms are $\mathcal{L} \supset \mathcal{L}_\psi + \mathcal{L}_{\chi e}$, where

$$\mathcal{L}_\psi = -M_\psi \bar{\psi}_L \psi_R + \lambda_s \bar{\psi}_L H_T \psi_R + \text{h.c.} \quad , \quad (5.5)$$

and

$$\mathcal{L}_{\chi e} = -M_\chi \bar{\chi}_L \chi_R + \lambda'_s \bar{\chi}_L H_T \chi_R - y_1 \bar{\chi}_L H_D e_R - y_2 \bar{\chi}_L \tilde{H}_D e_R - y_e \bar{L}_L H e_R + \text{h.c.} \quad , \quad (5.6)$$

where $\tilde{H}_D \equiv i\sigma^2 H_D^*$, and the final term is the usual standard model Yukawa coupling for a single lepton flavor. Eq. (5.6) assumes the existence of a symmetry that leads to exclusive

mixing between any one standard model, right-handed charged lepton flavor (called e_R above) and the vector-like χ fields. We show how this flavor sequestering can be arranged by a discrete symmetry in Sec. 5.3. The first terms in Eqs. (5.5) and (5.6) provide a common mass for each component of the given doublet, while the second terms lead to mass splittings proportional to the vev v_T . The third and fourth terms in Eq. (5.6) allow mixing between the standard model lepton e_R and the χ fields, since the coupling to the dark doublet Higgs field H_D allows for the formation of an $SU(2)_D$ singlet. The final term leads to an e mass when the standard model Higgs field develops a vacuum expectation value $\langle H \rangle = (0, v/\sqrt{2})$, with $v = 246$ GeV. Defining the column vector $\Upsilon \equiv (e, \chi^{(1)}, \chi^{(2)})^T$, which displays the two components of the χ doublet, we may write the mass matrix that is produced after spontaneous symmetry breaking by

$$\mathcal{L}_{mass}^{\chi e} = -\bar{\Upsilon}_L M \Upsilon_R + \text{h.c.} \quad , \quad (5.7)$$

where

$$M = \begin{pmatrix} \frac{h_e v}{\sqrt{2}} & 0 & 0 \\ \frac{(y_1 v_{1D} + y_2 v_{2D})}{\sqrt{2}} & M_\chi - \frac{\lambda'_s v_T}{2} & 0 \\ \frac{(y_1 v_{2D} - y_2 v_{1D})}{\sqrt{2}} & 0 & M_\chi + \frac{\lambda'_s v_T}{2} \end{pmatrix} \equiv \begin{pmatrix} m_0 & 0 & 0 \\ m_1 & M_1 & 0 \\ m_2 & 0 & M_2 \end{pmatrix} \quad , \quad (5.8)$$

where the second form is a convenient parametrization. This matrix can be diagonalized by a bi-unitary transformation, $M = U_L M^{diag} U_R^\dagger$. While this diagonalization can be done numerically, there are certain limits that are relevant to us in which simple results can be obtained. In particular, when $M_1, M_2 \gg m_1, m_2 \gg m_0$, we find that the largest mixing

angles, which occur in U_R , are given by

$$U_R = \begin{pmatrix} 1 - \frac{1}{2} \left(\frac{m_1^2}{M_1^2} + \frac{m_2^2}{M_2^2} \right) & m_1/M_1 & m_2/M_2 \\ -m_1/M_1 & 1 - \frac{1}{2} \frac{m_1^2}{M_1^2} & -\frac{M_1}{M_2} \frac{m_1 m_2}{M_1^2 - M_2^2} \\ -m_2/M_2 & \frac{M_2}{M_1} \frac{m_1 m_2}{M_1^2 - M_2^2} & 1 - \frac{1}{2} \frac{m_2^2}{M_2^2} \end{pmatrix} + \dots, \quad (5.9)$$

where the \dots represent terms that are cubic order or higher in m_i/M_j . For this case, we can now find the leading coupling of the dark gauge fields $A_{D\mu}^a$ to the mass eigenstate fields. In the gauge basis, the coupling to Υ_R can be written

$$\mathcal{L} = i\bar{\Upsilon}_R \gamma^\mu (\partial_\mu - ig_D A_{D\mu}^a \mathcal{T}^a) \Upsilon_R + \dots, \quad (5.10)$$

where

$$\mathcal{T}^a = \left(\begin{array}{c|c} 0 & 0 \\ \hline 0 & T^a \end{array} \right), \quad (5.11)$$

and $T^a = \sigma^a/2$, $a = 1, \dots, 3$, are the generators of SU(2). The zero in the 1-1 element reflects the fact that the standard model lepton is not charged under the dark gauge group. In the mass eigenstate basis, the couplings of the a^{th} dark gauge boson are therefore proportional to $U_R^\dagger \mathcal{T}^a U_R$. In the same approximation as Eq. (5.9), these matrices are given by

$$U_R^\dagger \mathcal{T}^a U_R = \left[\begin{pmatrix} \frac{m_1 m_2}{M_1 M_2} & -\frac{m_2}{2 M_2} & -\frac{m_1}{2 M_1} \\ -\frac{m_2}{2 M_2} & 0 & \frac{1}{2} \\ -\frac{m_1}{2 M_1} & \frac{1}{2} & 0 \end{pmatrix}, \begin{pmatrix} 0 & -\frac{i m_2}{2 M_2} & \frac{i m_1}{2 M_1} \\ \frac{i m_2}{2 M_2} & 0 & -\frac{i}{2} \\ -\frac{i m_1}{2 M_1} & \frac{i}{2} & 0 \end{pmatrix}, \begin{pmatrix} \frac{m_1^2}{2 M_1^2} - \frac{m_2^2}{2 M_2^2} & -\frac{m_1}{2 M_1} & \frac{m_2}{2 M_2} \\ -\frac{m_1}{2 M_1} & \frac{1}{2} & 0 \\ \frac{m_2}{2 M_2} & 0 & -\frac{1}{2} \end{pmatrix} \right], \quad (5.12)$$

where we only show results to linear order in m_i/M_j , with the exception of the 1-1 entries, because of their relevance to our subsequent discussion. For example, for the lightest dark gauge boson, A_D^3 , the coupling to $e^+ e^-$ is given by

$$g_D \bar{\Upsilon}_R \gamma^\mu A_{D\mu}^3 (U_R^\dagger \mathcal{T}^3 U_R) \Upsilon_R = \frac{g_D}{2} \left(\frac{m_1^2}{M_1^2} - \frac{m_2^2}{M_2^2} \right) \bar{e}_R \gamma^\mu A_{D\mu}^3 e_R + \dots \quad (5.13)$$

which provides the A_D^3 gauge boson with a decay channel (since we assume its mass is greater than $2 m_e$) and allows for dark matter annihilation to a charged standard model lepton-anti-lepton pair. For later convenience, we define

$$\theta^2 \equiv g_D \left(\frac{m_1^2}{M_1^2} - \frac{m_2^2}{M_2^2} \right). \quad (5.14)$$

We illustrate the qualitative idea in Fig. 5.1 that the dark matter annihilation to a charged standard model lepton-anti-lepton pair emerges from mixing that affects two of the external legs.

We note that in the case where m_0 is comparable to m_1 and m_2 we find via numerical diagonalization that our expression U_R in Eq. (5.9) still provides an accurate approximation. Moreover, we can prove that m_0 appears only as a higher-order correction to

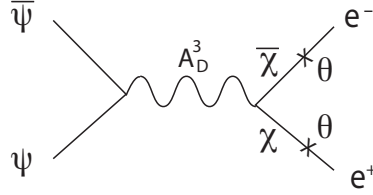


FIG. 5.1: Qualitative picture of dark matter annihilation to a charged lepton-anti-lepton pair, as discussed in the text. The insertions labelled by θ represent mass mixing.

θ , as defined in Eq. (5.14), the quantity that is most relevant to our phenomenological discussion later. The argument is as follows: if m_1 or m_2 were to vanish, then U_R must become the identity. This implies that any corrections to the 1-2, 1-3, 2-1 and 3-1 entries of U_R that are proportional to m_0 must come at no lower order than $m_0 m_{1,2}/M_{1,2}^2$. This potential contribution is nonetheless higher-order than the values shown for these entries in Eq. (5.9). It is also the case that the 1-1 entry of $U_R^\dagger \mathcal{T}^3 U_R$, from which θ is extracted, depends only on these four entries. Hence, the value of θ , which controls the induced coupling of A_D^3 to the chosen standard model lepton flavor, remains unaffected at leading order.

Eq. (5.12) indicates that all states other than the lightest ψ mass eigenstate have available decay channels that ultimately lead to standard model particles. Since the free parameter space of our model is substantial, for definiteness we assume henceforth the following about the spectrum:

- Due to the triplet vev, $\psi^{(1)}$ and $A_D^{(3)}$ are the lightest states of the dark sector, while $\psi^{(2)}$, $A_D^{(1)}$ and $A_D^{(2)}$ are substantially heavier. We will consider the case where the lighter dark sector states are in the $\mathcal{O}(1) - \mathcal{O}(100)$ GeV range, with the restriction that $m_{\psi^{(1)}} \leq m_{A_D^{(3)}}$, so that the dominant dark matter annihilation channel proceeds through the vector-like lepton portal (see Sec. 5.4).
- We assume that the vector-like leptons χ have masses above $M_Z/2$, so that the Z width

is unaffected. Note that more substantial collider bounds apply when vector-like leptons are either in weak doublets, or are long-lived [1], neither of which applies in the present case.

With these assumptions, let us first sketch out the decay modes when the standard model lepton flavor involved is the electron: the coupling matrices $U_R^\dagger \mathcal{T}^a U_R$, for $a = 1$ and $a = 3$ allow decays of A_D^1 and A_D^3 directly to $e^+ e^-$; the same is not true for $a = 2$, but the A_D^2 boson does couple to the two different ψ mass eigenstates, which we will call $\psi^{(1)}$ (the lighter, dark matter component) and $\psi^{(2)}$ (the heavier). The eigenstate $\psi^{(2)}$ can decay to dark matter $\psi^{(1)}$ plus $e^+ e^-$ via A_D^1 exchange. Hence A_D^2 can decay to two dark matter particles and an $e^+ e^-$ pair, whether or not $\psi^{(1)}$ is on shell. Due to the $\chi A_D^3 e$ couplings in $U_R^\dagger \mathcal{T}^3 U_R$, both χ mass eigenstates can decay to a same-sign e plus an $e^+ e^-$ pair via A_D^3 exchange. Finally, the exotic Higgs fields H_D and H_T couple to fermion pairs via their Yukawa couplings. Since we have already established that those fermions couple ultimately to either e 's or $\psi^{(1)}$'s, our claim is established. Note that if the standard model fermion is either μ or τ , nothing above is changed if $M_{A_D^3} > 2m_\mu$ or $2m_\tau$; otherwise, decays to lighter charged leptons plus neutrinos can still occur with the μ 's or τ 's off shell.

Since the χ and e_R have identical electroweak quantum numbers, there is no effect on the coupling of the Z boson to e_R in the mass eigenstate basis. However, χ and e_L couple differently to the electroweak gauge bosons, and diagonalization of Eq. (5.8) also involves a left-handed rotation matrix U_L which differs from the identity. Fortunately, the left-handed mixing angles are much smaller than those in Eq. (5.9) so that this does not present any phenomenological difficulties. For example, the fractional shift in the standard model $Z e_L e_L$ vertex is of $\mathcal{O}(\frac{m_0 m_1}{M_1^2} \frac{m_0 m_2}{M_2^2})$, which is negligible given the spectrum we assume in Sec. 5.4. We also may take the mostly χ mass eigenstates to be heavy enough so that rare Z decays to χe are kinematically forbidden.

Finally, let us return to the issue of the spontaneous breaking of the dark gauge symmetry. In the effective theory well below the electroweak scale, the most general renormalizable potential involving the dark Higgs fields is given by

$$\begin{aligned}
V(H_D, H_T) = & -m_D^2 H_D^\dagger H_D - m_T^2 \text{tr}(H_T H_T) + \lambda_1 (H_D^\dagger H_D)^2 + \lambda_2 [\text{tr}(H_T H_T)]^2 \\
& + \lambda_3 H_D^\dagger H_T H_T H_D + \mu_1 H_D^\dagger H_T H_D + \left(\mu_2 H_D^\dagger H_T \tilde{H}_D + \text{h.c.} \right),
\end{aligned} \tag{5.15}$$

where we have used the fact that $H_T^\dagger = H_T$. We assume the potential does not violate CP, so that all the couplings are real. Further, we require at least one of $(-m_D^2, -m_T^2)$ to be negative so that the H_D and H_T fields may develop non-zero vevs. It should be noted that there are other terms involving the Higgs fields that could be added to the potential, such as $\tilde{H}_D^\dagger \tilde{H}_D$, $\text{tr}(H_T^4)$, $\tilde{H}_D^\dagger H_T \tilde{H}_D$, $H_D^\dagger H_D \text{tr}(H_T H_T)$, but these are not linearly independent of the terms included in Eq. (5.15) and so have been omitted.

The Higgs doublet assumes the standard real-field parametrization,

$$H_D = \frac{1}{\sqrt{2}} \begin{pmatrix} \phi_1 + i\phi_2 \\ \phi_3 + i\phi_4 \end{pmatrix}, \tag{5.16}$$

while the Higgs triplet can be represented by a 2×2 matrix of real fields H_1, H_2 and H_3 ,

$$H_T = H^a \frac{\sigma^a}{2} = \frac{1}{2} \begin{pmatrix} H_3 & H_1 - iH_2 \\ H_1 + iH_2 & -H_3 \end{pmatrix}. \tag{5.17}$$

The normalization assures canonical kinetic terms. We proceed to show that there exists a stable, local minimum of the potential for the pattern of vacuum expectation values described in Eq. (5.4). One approach to studying the potential is to fix all the parameters and search for minima, using standard steepest descent algorithms. However the downside to this approach is that one may then have to repeatedly discard local minima that do

not provide the pattern of vevs desired for the model. So instead, we will fix the vevs and work backwards, showing that an extremum exists that is also a local minimum for a fixed set of parameters.

The extremization of Eq. (5.15) with the fields set to the vevs shown in Eq. (5.4) provides the following nontrivial, linearly independent constraints:

$$\begin{aligned}
 -m_D^2 v_{D1} + \lambda_1 v_{D1}^3 + \lambda_1 v_{D1} v_{D2}^2 + \mu_2 v_{D2} v_T + \frac{1}{4} v_{D1} v_T (\lambda_3 v_T + 2\mu_1) &= 0 \\
 \frac{1}{2} (-\mu_2 v_{D1}^2 + \mu_1 v_{D1} v_{D2} + \mu_2 v_{D2}^2) &= 0 \\
 -m_T^2 v_T + \frac{1}{4} \lambda_3 v_T (v_{D1}^2 + v_{D2}^2) + \frac{1}{4} \mu_1 (v_{D1}^2 - v_{D2}^2) + \mu_2 v_{D1} v_{D2} + \lambda_2 v_T^3 &= 0.
 \end{aligned} \tag{5.18}$$

For the purpose of numerical evaluation we work here in units where $\mu_1 = 1$. For fixed choices of the vevs and the couplings $\lambda_{1,2,3}$, we may then determine m_D , m_T and μ_2 . To determine whether the extremum is a minimum, maximum or saddle point, we need to examine the eigenvalues of the mass squared matrix (the second derivative matrix with all fields set to their vevs and with the solutions for m_D , m_T and μ_2 corresponding to the extremum). Since $SU(2)_D$ is spontaneously broken to nothing, we expect three Goldstone bosons, one for each broken $SU(2)$ generator, according to Goldstone's theorem. Thus we would expect three of the eigenvalues to be zero, corresponding to the massless degrees of freedom that are "eaten" by the dark gauge bosons. The remaining eigenvalues must be positive for the extremum to be a local minimum. For example, let us set $v_T = v_{D1} = v_{D2}/2 = \lambda_{1,2,3} = \mu_1$ (here we require $v_{D1} \neq v_{D2}$ for a solution to exist). Then we find $m_D^2 = 53/12$, $m_T^2 = 1/6$ and $\mu_2 = -2/3$. The corresponding mass squared eigenvalues are $\{0, 0, 0, 3.75, 3.75, 4, 10\}$, in units of μ_1^2 , thus confirming that we are at a local minimum of the potential. This provides an existence proof that local minima exist in which the pattern of vevs shown in Eq. (5.4) is obtained. It is not difficult to find similar solutions for other choices of v_{D1} , v_{D2} and v_T .

The $SU(2)_D$ breaking vevs affect the χ - e mass spectrum via Eq. (5.8); the triplet vev also splits the ψ mass eigenstates

$$m_{\psi^{(1)}} = M_\psi - \frac{1}{2}\lambda_s v_T, \quad m_{\psi^{(2)}} = M_\psi + \frac{1}{2}\lambda_s v_T \quad (5.19)$$

for $\psi_{L,R} = (\psi^{(1)}, \psi^{(2)})_{L,R}^T$. The gauge field spectrum is obtained from the kinetic terms for H_D and H_T ,

$$\mathcal{L}_{kin}(H_D, H_T) = (D_\mu H_D)^\dagger (D^\mu H_D) + \text{tr} [(D_\mu H_T)^\dagger (D^\mu H_T)], \quad (5.20)$$

where $D_\mu H_D = \partial_\mu H_D - ig_D A_{D\mu}^a \frac{\sigma^a}{2} H_D$ and $D_\mu H_T = \partial_\mu H_T - ig_D \frac{\sigma^a}{2} A_{D\mu}^a H_T + ig_D A_{D\mu}^a H_T \frac{\sigma^a}{2}$. Following symmetry breaking the gauge bosons develop masses

$$m_{A_D^1}^2 = m_{A_D^2}^2 = \frac{g_D^2}{4}(v_{D1}^2 + v_{D2}^2 + 4v_T^2), \quad m_{A_D^3}^2 = \frac{g_D^2}{4}(v_{D1}^2 + v_{D2}^2). \quad (5.21)$$

In splitting the ψ and A_D multiplet masses, the triplet vev leads to a simple low-energy effective theory consisting of the dark matter $\psi^{(1)}$ (we assume $\lambda_s > 0$) and the mediator A_D^3 , which has small induced couplings to a right-handed standard model lepton flavor. This effective theory is relevant below the masses of the heavy vector-like leptons, $\psi^{(2)}$ and the $A_D^{1,2}$ bosons, which we will associate with a common scale, for simplicity. In addition, we will see that the triplet vev leads to induced couplings of the dark matter to quarks via kinetic mixing, which will lead to avenues for direct detection. We discuss the phenomenology of this scenario in Sec. 5.4.

5.3 Flavor sequestering

In this section, we show that it is possible to allow for non-negligible mixing between one flavor of the standard model leptons and the heavier, vector-like leptons, while suppressing the mixing with the other standard-model flavors, so that bounds on lepton-flavor-violating processes become irrelevant. In the discussion below, we refer to that one flavor as the electron e , though the approach described applies equally well if the chosen flavor were μ or τ . Let us consider the structure of the standard model Yukawa matrices first, and then introduce couplings to the vector-like states.

We represent the three generation of standard model lepton doublets by L_{iL} and the right-handed charged leptons by E_{iR} , for $i = 1, \dots, 3$. We imagine that the Yukawa couplings are determined by a flavor symmetry of the form $Z_N \times G_F$. Our interest is in the effect of the Z_N factor, while we do not commit to any specific G_F . We aim to show that the restrictions that follow from the Z_N symmetry are sufficient to suppress the flavor mixing effects that we would like to avoid, while remaining compatible with a variety of possible flavor models that may determine the remaining, detailed structure of the Yukawa matrices.

We represent an element of Z_N by ω^j , for $j = 1, \dots, N$, where $\omega^N \equiv 1$. We assign the following transformation properties to the L and E fields, representing them here as column vectors:

$$L_L \rightarrow \Omega L_L \quad \text{and} \quad E_R \rightarrow \Omega E_R , \quad (5.22)$$

where

$$\Omega = \begin{pmatrix} 1 & 0 & 0 \\ 0 & \omega^{-n} & 0 \\ 0 & 0 & \omega^n \end{pmatrix} . \quad (5.23)$$

Note that $\omega^{-n} \equiv \omega^{N-n}$. Assuming that the standard model Higgs doublet is unaffected

by the Z_N symmetry, the transformation properties of the charged-lepton Yukawa matrix entries that lead to invariant couplings are summarized by

$$Y_E \sim \left(\begin{array}{c|cc} 1 & \omega^n & \omega^{-n} \\ \hline \omega^{-n} & 1 & \omega^{-2n} \\ \omega^n & \omega^{2n} & 1 \end{array} \right), \quad (5.24)$$

where the transformation property of, for example, the 1-2 entry is understood to be $Y_E^{12} \rightarrow \omega^n Y_E^{12}$, and so on. We will choose $N = 2n$ so that the entire two-by-two block on the lower right is unconstrained by the Z_N symmetry, the least restrictive possibility that meets our needs¹. The amount by which the electron mass eigenstate is affected by the second and third generation fields, however, is entirely controlled by the size of n , once Z_N breaking fields are introduced, as we discuss later.

A symmetry affecting the left-handed charged leptons also affects the left-handed neutrinos, so we must verify that neutrino phenomenology is not adversely affected. For example, if we had imposed a Z_2 symmetry, with $n = 1$, and required it to remain exactly unbroken, we can also completely eliminate mixing between the first generation charged leptons and those of the second and third generations. However, if we then introduce three generations of right-handed neutrinos N_i , for $i = 1, \dots, 3$, one can show that there are no Z_2 charge assignments for the N fields that leads to the correct neutrino mass squared differences and mixing angles, assuming the light mass eigenstates follow from the see-saw mechanism. However, more favorable results may be obtained when the Z_N symmetry is spontaneously broken. Here, we assume the same transformation for all three right-handed

¹This choice is also compatible with G_F having a non-Abelian component in which two flavors of standard model leptons transform as a doublet. However, it is sufficient (and simplest) for present purposes to imagine that G_F has only Abelian factors.

neutrino fields:

$$N_R \rightarrow \omega^p N_R \ , \quad (5.25)$$

where p is an integer. Defining the Dirac neutrino mass via $\mathcal{L} \supset \bar{L}_L \tilde{H} Y_{LR} N_R + \text{h.c.}$, the transformation properties of the Yukawa coupling is given by

$$Y_{LR} \sim \left(\begin{array}{c|cc} \omega^{-p} & \omega^{-p} & \omega^{-p} \\ \hline \omega^{-n-p} & \omega^{-n-p} & \omega^{-n-p} \\ \omega^{n-p} & \omega^{n-p} & \omega^{n-p} \end{array} \right) . \quad (5.26)$$

For the choice $n = 2p$, or equivalently $N = 2n = 4p$, we may use the fact that $\omega^{-n-p} \equiv \omega^p$ and $\omega^{n-p} \equiv \omega^p$ to write

$$Y_{LR} \sim \left(\begin{array}{c|cc} \omega^{-p} & \omega^{-p} & \omega^{-p} \\ \hline \omega^p & \omega^p & \omega^p \\ \omega^p & \omega^p & \omega^p \end{array} \right) . \quad (5.27)$$

The significance of this form is clear if we assume that there is a flavon field ρ with the Z_N transformation property

$$\rho \rightarrow \omega \rho \ , \quad (5.28)$$

and a vacuum expectation value such that $\langle \rho \rangle / M \equiv \epsilon$ is a small parameter. Here M is the flavor scale, which is the ultraviolet cut off of the effective theory. Then all the entries of Y_{LR} are non-vanishing, and proportional to either $(\rho/M)^p$ or to $(\rho^*/M)^p$. Hence, we may write

$$Y_{LR} = \epsilon^p \tilde{Y}_{LR} \ , \quad (5.29)$$

where \tilde{Y}_{LR} is a three-by-three matrix that is thus far arbitrary. Following a similar argument, we define the right-handed neutrino Majorana mass matrix by the Lagrangian term

$\overline{N}_R^c M_{RR} N_R$, and see immediately that

$$M_{RR} \rightarrow \omega^{-2p} M_{RR} . \quad (5.30)$$

Again, this is consistent with the transformation property of $(\rho^*/M)^{2p}$, so we may write

$$M_{RR} = \epsilon^{2p} \widetilde{M}_{RR} , \quad (5.31)$$

where \widetilde{M}_{RR} is a three-by-three Majorana mass matrix that is also arbitrary thus far. With \widetilde{Y}_{LR} and \widetilde{M}_{RR} arbitrary, it is possible to obtain any desired neutrino phenomenology, which demonstrates that the Z_N symmetry does not lead to unwanted phenomenological restrictions. Theories that predict the detailed structure of \widetilde{Y}_{LR} and \widetilde{M}_{RR} by the breaking of an additional symmetry G_F are compatible with this framework. Note that the overall powers of ϵ in Eqs. (5.29) and (5.31) scale out of the see-saw formula which determines the Majorana mass matrix for the three light neutrino mass eigenstates

$$M_{LL} = M_{LR} M_{RR}^{-1} M_{LR}^T, \quad (5.32)$$

where $M_{LR} = (v/\sqrt{2}) Y_{LR}$. The effect of the Z_N symmetry on the form of the charged lepton Yukawa matrix is to impose the form

$$Y_E \sim \left(\begin{array}{c|cc} y_{11} & \epsilon^n \tilde{y}_{12} & \epsilon^n \tilde{y}_{13} \\ \hline \epsilon^n \tilde{y}_{21} & y_{22} & y_{23} \\ \epsilon^n \tilde{y}_{31} & y_{32} & y_{33} \end{array} \right) . \quad (5.33)$$

For ϵ sufficiently small, or n sufficiently large, or both, we can make Y_E as close to block diagonal as we like.

Now we include the vector-like state χ with the same electroweak quantum numbers as a right-handed electron, but charged also under a dark gauge group. Yukawa couplings involving $\bar{\chi}_L e_R$ and a dark Higgs field are unaffected by the Z_N symmetry, while those involving $\bar{\chi}_L \mu_R$ or $\bar{\chi}_L \tau_R$ transform by $\omega^{\pm n}$. These potential sources of unwanted mixing that may emerge after the dark gauge symmetry is spontaneously broken are therefore highly suppressed by the same factors of ϵ^n that appear in the unwanted entries in Y_E . We conclude that it is possible to make the χ , e , μ , τ mass matrix as block diagonal as desired, by suitable choice of ϵ^n , such that χ mixes substantially only with e , or any one desired lepton flavor, by a similar construction².

The question of which lepton flavor is selected to mix with the heavier, vector-like states impacts the phenomenology of the dark gauge bosons. For example, if the mixing only involves the τ lepton, then bounds on the A_D^a from searches for s -channel resonances in low-energy e^+e^- collisions, or from indirect processes like the electron or muon $g-2$ would be irrelevant. The phenomenology in the case where the mixing involves either a first or second generation lepton would lead to more meaningful constraints, but one that would depend on other assumptions about the spectrum, for example if A_D^3 decays visibly or invisibly, which depends on the dark matter mass. In the following section, we will assume the least constrained possibility, that the χ 's mix with the τ . This has the appealing aesthetic feature that the flavor symmetry distinguishes the third generation from the other two, an idea that has appeared in many other contexts in the literature on the flavor structure of the standard model, see for example Refs. [3, 4].

²We also note that this result is not linked in any fundamental way to our initial choice to study a non-Abelian dark gauge group. The present approach would be equally effective if the χ mass mixing terms were generated after the spontaneous breaking of a dark Abelian gauge symmetry. However, as noted earlier, Abelian theories would generically have kinetic mixing with hypercharge at tree-level and one-loop running of the mixing parameter below the Planck scale induced by the presence of the vector-like lepton states. The flavor sequestering mechanism could be applied in Abelian dark sector models provided that an additional mechanism is specified that adequately suppresses these kinetic mixing effects.

5.4 Phenomenology

To confirm the viability of our flavor-sequestered model, we wish to show that it can achieve the correct dark matter relic density. We will not do a complete study of the model's parameter space, but focus on a region that is unique to the flavor-sequestered scenario, namely where the vector-like states are light enough so that sufficient dark matter annihilation is achieved to standard model lepton-anti-lepton pairs, even in the absence of other annihilation channels. We then comment on direct detection via the suppressed kinetic mixing effects that emerge when the gauge symmetries are broken.

5.4.1 Relic Density

The scattering amplitude for s -channel dark matter annihilation into standard model particles depicted in Fig. 5.1, with e replaced by τ , is given by

$$\mathcal{M}(\psi^{(1)}\overline{\psi^{(1)}} \rightarrow \tau^+\tau^-) = \frac{ig_D^2\theta^2}{4(q^2 - m_{A_D^3}^2 + im_{A_D^3}\Gamma^D)} \bar{v}(p')\gamma^\mu u(p) \bar{u}(k)\gamma_\mu v(k') \quad (5.34)$$

where p (p') is the momentum of the incoming dark matter fermion (anti-fermion), k (k') is the momentum of the outgoing τ^- (τ^+) and $q = p + p'$ is the momentum flowing through the A_D^3 propagator. As discussed in Sec. 5.2, the lightest gauge boson A_D^3 couples to the vector-like states $\chi^{(1)}$ and $\chi^{(2)}$, which then mix with a standard model lepton flavor (chosen here as τ) after spontaneous symmetry breaking. This results in a factor of θ^2 , defined in Eq. (5.14), in the scattering amplitude.

Our numerical results for dark matter annihilation depend on assumptions about the dark particle mass spectrum and couplings. We assume the picture described earlier, where the lightest states consist of $\psi^{(1)}$ and A_D^3 , and decays of A_D^3 to any of the heavier exotic states are not kinematically allowed. For the mass range studied in this section,

A_D^3 can decay to $\tau^+\tau^-$, and possibly also $\psi^{(1)}\overline{\psi^{(1)}}$, depending on the dark matter mass. Consequently, the total decay width of the dark gauge boson appearing in the propagator is given by

$$\Gamma^D = \Gamma(A_D^3 \rightarrow \tau^+\tau^-) + \Theta(m_{A_D^3} - 2m_{\psi^{(1)}}) \Gamma(A_D^3 \rightarrow \psi^{(1)}\overline{\psi^{(1)}}) \quad (5.35)$$

where Θ is a step function, *i.e.*, $\Theta(x) = 1$ if $x \geq 0$ and $\Theta(x) = 0$ if $x < 0$, and

$$\Gamma(A_D^3 \rightarrow \tau^+\tau^-) = \frac{1}{48\pi} g_D^2 m_{A_D^3} \theta^4 \left(1 + \frac{2m_\tau^2}{m_{A_D^3}^2}\right) \left(1 - \frac{4m_\tau^2}{m_{A_D^3}^2}\right)^{1/2}, \quad (5.36)$$

$$\Gamma(A_D^3 \rightarrow \psi^{(1)}\overline{\psi^{(1)}}) = \frac{1}{48\pi} g_D^2 m_{A_D^3} \left(1 + \frac{2m_{\psi^{(1)}}^2}{m_{A_D^3}^2}\right) \left(1 - \frac{4m_{\psi^{(1)}}^2}{m_{A_D^3}^2}\right)^{1/2}. \quad (5.37)$$

Since the mean dark matter velocity is typically around 220 km/s [1], we work in the non-relativistic limit where $E_{\psi^{(1)}} \approx m_{\psi^{(1)}}$. We then find the thermally averaged annihilation cross section times velocity

$$\langle\sigma_{AV}\rangle = \frac{g_D^4 \theta^4}{32\pi} \frac{2m_{\psi^{(1)}}^2 + m_\tau^2}{(4m_{\psi^{(1)}}^2 - m_{A_D^3}^2)^2 + m_{A_D^3}^2 \Gamma_D^2} \left(1 - \frac{m_\tau^2}{m_{\psi^{(1)}}^2}\right)^{1/2}. \quad (5.38)$$

Using this we calculate the freeze-out temperature T_F and the dark matter relic density by standard methods [34]. Dark matter freeze out occurs when the interaction probability per unit time $\Gamma_{\psi^{(1)}}$, equals the expansion rate of the universe, H , *i.e.*,

$$\frac{\Gamma_{\psi^{(1)}}}{H} \Big|_{T=T_F} = \frac{n_{EQ}^{\psi^{(1)}} \langle\sigma_{AV}\rangle}{H} \Big|_{T=T_F} \simeq 1. \quad (5.39)$$

Here $n_{EQ}^{\psi(1)}$ is the equilibrium number density of the dark matter particle, given by

$$n_{EQ}^{\psi(1)} = 2 \left(\frac{m_{\psi(1)} T}{2\pi} \right)^{3/2} e^{-m_{\psi(1)}/T}. \quad (5.40)$$

Freeze-out occurs during the radiation-dominated epoch in which case

$$H = 1.66 g_*^{1/2} T^2 / M_{pl}, \quad (5.41)$$

where $M_{pl} = 1.22 \times 10^{19}$ GeV is the Planck mass and $g_*(T)$ the number of relativistic degrees of freedom at temperature T ,

$$g_*(T) = \sum_{i=bosons} g_i \left(\frac{T_i}{T} \right)^4 + \frac{7}{8} \sum_{i=fermions} g_i \left(\frac{T_i}{T} \right)^4. \quad (5.42)$$

Finally the dark matter relic density is given by

$$\Omega_D h^2 = \frac{2 \cdot (1.07 \times 10^9 \text{ GeV}^{-1}) x_F}{\sqrt{g_*(T_F)} M_{Pl} \langle \sigma_A v \rangle}. \quad (5.43)$$

We define $x_F \equiv m_{\psi(1)}/T_F$ where T_F is obtained by solving Eq. (5.39). The factor of 2 is included because we are accounting for the density of dark matter particles and antiparticles. We require Eq. (5.43) to reproduce the WMAP result 0.1186 ± 0.0020 [1] within two standard deviations.

To display our results, we fix $m_{A_D^3}$ and θ and find the regions of the g_D - $m_{\psi(1)}$ plane in which the desired dark matter relic density is obtained. We assume that the mixing angle remains small ($\theta < 1$) but not so small that a satisfactory dark matter annihilation cross section cannot be obtained. So that the dark gauge coupling remains perturbative, we assume $\alpha_D/(4\pi) < 1/3$ or equivalently $g_D < 4\pi/\sqrt{3} \sim 7.25$; one-loop corrections become comparable to tree-level amplitudes when $\alpha/(4\pi) \approx 1$, so one-third of this value is a rea-

reasonable upper limit on the dark coupling constant. For the purposes of determining g_* , we assume all exotic mass eigenstates other than $\psi^{(1)}$ and A_D^3 , are at $m_Z = 91.1876$ GeV. With this choice, the Z boson cannot decay into $\chi\bar{\chi}$ or $\chi\tau$, which could lead to an unacceptable broadening of the precisely measured Z boson width [1].

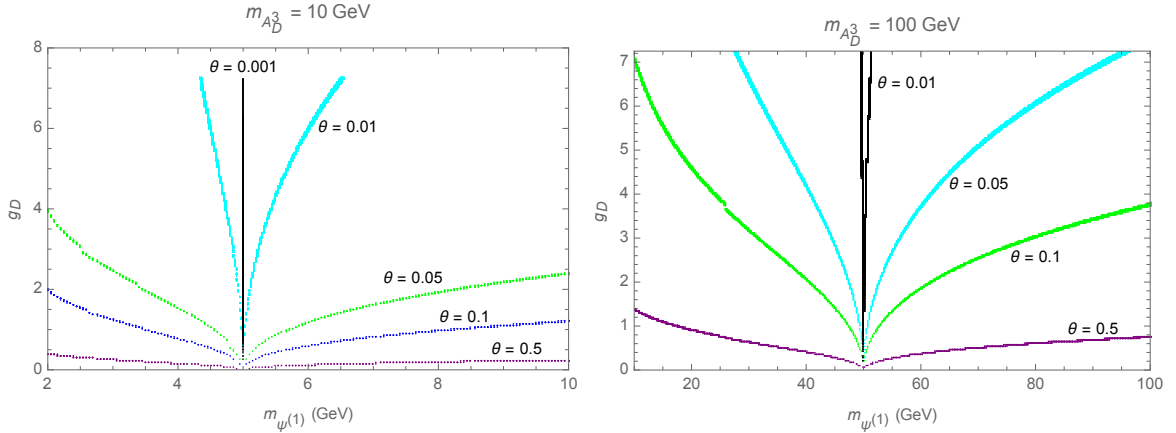


FIG. 5.2: Regions of the g_D - $m_{\psi^{(1)}}$ plane in which the dark matter relic density is within two standard deviations of the WMAP result 0.1186 ± 0.0020 [1], for fixed choices of $m_{A_D^3}$ and θ . The allowed bands are not perfectly smooth due to their dependence on g_* , which is not a continuous function. The point of minimum g_D corresponds to resonance annihilation, where $m_{\psi^{(1)}} = m_{A_D^3}/2$. Note that as θ decreases the range of $m_{\psi^{(1)}}$ in which g_D remains perturbative moves towards the resonance region.

Fig. 5.2 shows the regions of the g_D - $m_{\psi^{(1)}}$ plane in which the dark matter relic density is within two standard deviations of the WMAP result 0.1186 ± 0.0020 [1], for fixed choices of $m_{A_D^3}$ and θ . We have intentionally centered the plots around the point of resonance annihilation $m_{\psi^{(1)}} = m_{A_D^3}/2$ where the cross section is largest. For small values of g_D at fixed θ , some tuning is required to achieve a large enough annihilation cross section. However, Fig. 5.2 indicates that we can have larger, perturbative values of g_D without requiring that we sit unnaturally close to the resonance. As θ is made progressively smaller, however, more tuning is required. This is indicated by the narrowing range in $m_{\psi^{(1)}}$ for each solution in which g_D is also perturbative.

Of course, the values of θ that are indicated in Fig 5.2 are related to choices for the

masses and coupling in the model, such that $\theta^2 = g_D \left(\frac{m_1^2}{M_1^2} - \frac{m_2^2}{M_2^2} \right)$, where the m_i and M_i were defined in Eq. (5.8). It is not hard to verify that the values of θ shown in Fig. 5.2 can be achieved given the assumptions that went into the making of the plots. For example, in the $m_{A_D^3} = 10$ GeV plot, consider the point where $g_D \approx 1$ and $m_{\psi^{(1)}} \approx 8.5$ GeV, on the $\theta = 0.1$ band. Given our earlier assumption in computing g_* that the heavier exotic states are at m_Z , one can check that this is consistent with, for example, $v_{D1} = v_{D2} \approx 14$ GeV, $v_T \approx 49$ GeV, $\lambda_s \approx 0.85$, and $y_1 = y_2 \approx 0.06$, where the Yukawa couplings y_i were defined in Eq. (5.6). Similar statements can be made about other points on the allowed bands³.

5.4.2 Direct Detection

The interactions that we have discussed to this point have involved leptons exclusively, but couplings to quarks that are generated at the loop level also have significant consequences. In this section, we consider direct detection of the dark matter in the model via dark-matter-nucleon elastic scattering. The couplings to quarks arise after the $SU(2)_D$ symmetry is spontaneously broken, since kinetic mixing between A_D^3 and hypercharge is then allowed, via an effective dimension-5 operator

$$\mathcal{L}_{eff} = X \text{tr} (\langle H_T \rangle T^a A_{D\mu\nu}^a) Y^{\mu\nu} , \quad (5.44)$$

where we have set the triplet Higgs to its vev, as per Eq. (5.4). Here, X is a constant with

³The scenario that we have considered assumes that communication between dark and visible sectors occurs primarily through the portal that we have proposed, involving mixing with vector-like leptons. It is of course possible to have scenarios in which communication is also significant through Higgs portal couplings or other mediators. The present model could therefore represent a subset of the parameters space of a more complicated model with other dark matter annihilation channels. There are also different parameter regions in the model as we have defined it where other annihilation channels become relevant, for example $\psi^{(1)}\overline{\psi^{(1)}} \rightarrow A_D^3 A_D^3$, when $m_{A_D^3} \leq m_{\psi^{(1)}}$. The results presented in this section demonstrate the effectiveness of the portal we have proposed in a region of parameter space where it provides the dominant contribution to the dark matter annihilation cross section due to mixing effects that would not be possible in models without flavor sequestering. This does not imply that other viable regions of parameter space

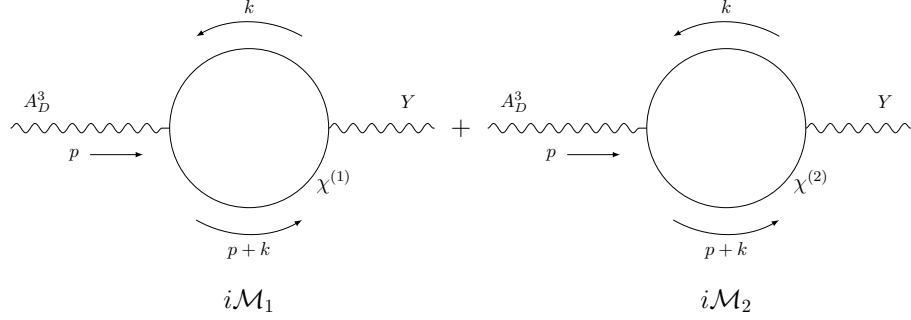


FIG. 5.3: Self energies leading to kinetic mixing between the third dark gauge boson $A_D^{(3)}$ and hypercharge Y after $SU(2)_D$ is spontaneously broken.

units of GeV^{-1} which is found by integrating out the “heavy” physics, *i.e.*, the χ fields, the only fields that are charged both under $SU(2)_D$ and hypercharge $U(1)_Y$. To proceed, we study the self-energy shown in Fig. 5.3, where $\chi^{(1)}$ and $\chi^{(2)}$ here represent the heavy mass eigenstates, whose mass eigenvalues are given approximately by $m_{\chi^{(1)}} = M_\chi - \delta$ and $m_{\chi^{(2)}} = M_\chi + \delta$ where $\delta \equiv \lambda'_s v_T/2$. (For the purposes of this estimate, we ignore mass mixing with the standard model lepton, which is a subleading correction.) The first diagram is given by

$$i\mathcal{M}_1 = -\frac{g_D g_Y}{2} \int \frac{d^4 k}{(2\pi)^4} \frac{\text{tr} [\gamma^\mu (\not{k} + m_{\chi^{(1)}}) \gamma^\nu (\not{k} + \not{p} + m_{\chi^{(1)}})]}{[k^2 - m_{\chi^{(1)}}^2 + i\epsilon][(k+p)^2 - m_{\chi^{(1)}}^2 + i\epsilon]} . \quad (5.45)$$

After carrying out this loop integral using dimensional regularization in $D = 4 - \epsilon$ dimensions, the amplitude is

$$i\mathcal{M}_1 = -\frac{g_D g_Y}{8\pi^2} \int_0^1 dx x(1-x) \left(\frac{4}{\epsilon} - 2\gamma + 2 \log(4\pi) - 2 \log(\Delta_1) \right) i(g^{\mu\nu} p^2 - p^\mu p^\nu) , \quad (5.46)$$

where $\Delta_1 = m_{\chi^{(1)}}^2 - x(1-x)p^2$. Since A_D^3 couples to the χ proportional to $\sigma^3/2$, the amplitude $i\mathcal{M}_2$ shown in Fig. 5.3 will differ from $i\mathcal{M}_1$ by a overall minus sign and the replacement of the $\chi^{(1)}$ by the $\chi^{(2)}$ mass. Hence, Δ_1 is replaced by $\Delta_2 = m_{\chi^{(2)}}^2 - x(1-x)p^2$.

are impossible.

Then, when these two amplitudes are added together, all terms in the remaining Feynman parameter integral cancel, except for the terms that depend on the fermion masses:

$$i\mathcal{M}_1 + i\mathcal{M}_2 = i(g^{\mu\nu}p^2 - p^\mu p^\nu) \frac{g_D g_Y}{4\pi^2} \int_0^1 dx x(1-x) \log\left(\frac{\Delta_1}{\Delta_2}\right) . \quad (5.47)$$

Assuming the mass splitting δ is small compared to the χ masses (which will turn out to be the case) the integrand can be expanded in δ . The leading order term can be found using $x(1-x) \log(\Delta_1/\Delta_2) \approx -\frac{4mx(1-x)}{m^2 - x(1-x)p^2} \delta$. Moreover, we can also expand the result in powers of momentum, which can later be compared to a derivative expansion in the low-energy effective theory. We find

$$i\mathcal{M}_1 + i\mathcal{M}_2 = -i \frac{g_D g_Y \delta}{6\pi^2 M_\chi} (g^{\mu\nu}p^2 - p^\mu p^\nu) + \dots , \quad (5.48)$$

where the \dots represents terms involving higher powers of δ and p^2/M_χ^2 . The result in Eq. (5.48) must be matched to a similar amplitude in the low-energy effective theory in which the χ fields have been integrated out. We identify this as the tree-level amplitude associated with the Eq. (5.44), treated as a two-point vertex,

$$i\mathcal{A} = iX v_T (p^2 g^{\mu\nu} - p^\mu p^\nu) , \quad (5.49)$$

from which we conclude

$$X = -\frac{g_D g_Y \delta}{6\pi^2 M_\chi v_T} . \quad (5.50)$$

Using Eqs. (5.44) and (5.50), we can now calculate the cross section for dark matter scattering off of nucleons. We will be working in the limit of low momentum transfer $q \sim \mathcal{O}(100)$ MeV ($\ll M_\chi$), where the effective description is accurate and where scattering

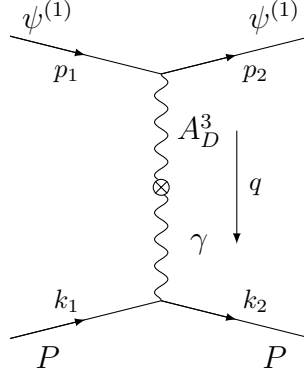


FIG. 5.4: The Feynman diagram for the scattering of the dark matter particles, $\psi^{(1)}$, off of protons, P , through kinetic mixing of the dark matter boson A_D^3 and the photon, γ .

through the Z boson is suppressed by $q^2/m_Z^2 \sim 10^{-6}$ compared to the photon. Hence, we will consider kinetic mixing involving the photon only from here on. First, we consider the dark matter, $\psi^{(1)}$, scattering off of a quark, q_f , as in the diagram in Fig. 5.4, with the protons replaced by a quark of flavor f . This can be described by the effective dimension-six operator

$$\mathcal{L}_{eff,q} = C_f \overline{\psi^{(1)}} \gamma^\mu \psi^{(1)} \overline{q_f} \gamma_\mu q_f . \quad (5.51)$$

In the full theory, this quark-dark matter scattering amplitude is

$$i\mathcal{M}_f = iXv_T Q_f \frac{g_D}{2} e \frac{1}{(q^2 - m_{A_D^3}^2 + i\epsilon)(q^2 + i\epsilon)} \overline{\psi^{(1)}} \gamma^\mu \psi^{(1)} \overline{q_f} \gamma_\mu q_f \quad (5.52)$$

or, in the limit of $q^2 \ll m_{A_D^3}^2$,

$$i\mathcal{M}_f = -i \frac{Xv_T Q_f g_D}{m_{A_D^3}^2} e \overline{\psi^{(1)}} \gamma^\mu \psi^{(1)} \overline{q_f} \gamma_\mu q_f . \quad (5.53)$$

From this, we conclude the coefficient C_f for quarks is

$$C_f = -\frac{g_d e X v_T Q_f}{2m_{A_D^3}^2} = \frac{g_D^2 e^2 \delta Q_f}{12\pi^2 M_\chi m_{A_D^3}^2} . \quad (5.54)$$

Of interest, however, is the effective interactions involving nucleons rather than quarks, which can be written

$$\mathcal{L}_{eff,N} = C_n \overline{\psi^{(1)}} \gamma^\mu \psi^{(1)} \bar{n} \gamma_\mu n + C_p \overline{\psi^{(1)}} \gamma^\mu \psi^{(1)} \bar{p} \gamma_\mu p . \quad (5.55)$$

Using the fact that the quark vector currents are conserved, so that the spatial integral of the zeroth component is a quark number operator, one can match matrix elements of Eq. (5.51) between nucleon states with the same for Eq. (5.55), from which one concludes $C_n = C_u + 2C_d$ and $C_p = 2C_u + C_d$, for the neutron and proton, respectively. (There are no form factors as there would be for scalar quark operators.) Since the flavor dependence of the C_f comes only from the electric charge, the coefficient C_n and thus the scattering amplitude for $\psi^{(1)}$ off of neutrons are both zero. Therefore, the only relevant scattering is with the proton, for which

$$C_p = 2C_u + C_d = \frac{g_D^2 e^2 \delta}{12\pi^2 M_\chi m_{A_D}^2} . \quad (5.56)$$

Taking into account that the dark matter is non-relativistic and that momentum transfers are small, a straightforward calculation of the scattering cross section yields

$$\langle \sigma_{\psi^{(1)}p \rightarrow \psi^{(1)}p} \rangle = \frac{g_D^4 e^4 m_p^2 m_{\psi^{(1)}}^2}{576\pi^5 (m_p + m_{\psi^{(1)}})^2 m_{A_D}^4} \left(\frac{2\delta}{M_\chi} \right)^2 , \quad (5.57)$$

where we have separated out the dependence on $2\delta/M_\chi$, the fractional mass splitting of the vector-like leptons. Since this splitting is a free parameter in our model, we can use the experimental bounds on the dark-matter-nucleon elastic scattering cross section to say something about the vector-like lepton spectrum.

Using experimental bounds on the cross section from XENON1T [97] and CDM-

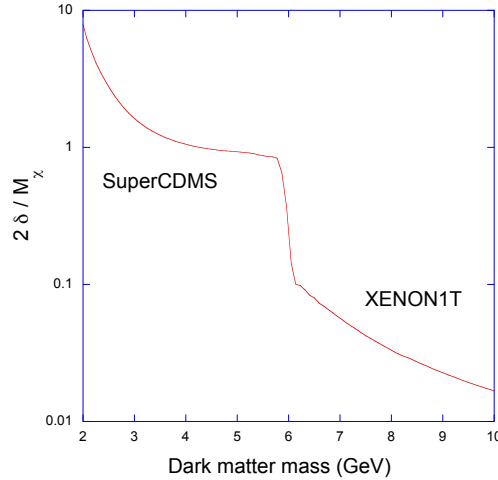


FIG. 5.5: Upper bound on the fractional mass splitting of the $\chi^{(1)}$ and $\chi^{(2)}$ fermions as a function of the mass of the dark matter particle, $\psi^{(1)}$, assuming $g_D = 0.3$ and $m_{A_D^3} = 10$ GeV. The discontinuity in the curve reflects that the bounds on the dark-matter-nucleon elastic scattering cross section originate from the CDMSlite experiment [98] below $m_{\psi^{(1)}} \approx 6$ GeV, where the otherwise tighter bounds from the XENON1T experiment [97] do not exist. The results shown are reliable in the region where $2\delta/M_\chi$ is a perturbative expansion parameter less than 1.

Slite [98], we show bounds on the $\chi^{(1)}$ - $\chi^{(2)}$ mass splitting for dark matter masses between 2 GeV and 10 GeV. The results of this calculation are shown in Fig. 5.5, where a dark coupling of $g_D = 0.3$ and a dark boson mass of $m_{A_D^3} = 10$ GeV have been used. For dark matter masses below approximately 6 GeV, the cross section bounds from CDMSlite are used, since no data from XENON1T is available in this region. Although there is CDMSlite data for dark matter masses above 6 GeV, these bounds are superseded by the stricter ones from XENON1T. For the range of $\psi^{(1)}$ masses in Fig. 5.5 that are affected by the XENON1T bounds, the masses of the charged fermions $\chi^{(1)}$ and $\chi^{(2)}$ are degenerate at the 1-10% level at minimum. This feature could be observed in collider searches for the vector-like leptons and possibly correlated with a dark matter direct detection signal.

5.5 Conclusions

We have presented a framework based on flavor symmetries that allows for a light portal sector of vector-like leptons connecting a dark sector to the standard model. To illustrate our approach, we considered an explicit, renormalizable non-Abelian dark SU(2) model which contains two vector-like fermion doublets. One of them, ψ , includes a dark matter candidate; the other doublet, χ , has the same electroweak quantum numbers as a right-handed electron, so that communication with the visible sector can occur via mass mixing. The ψ and χ fields communicate with each other via the dark gauge group, so that the dark matter may annihilate to standard model leptons. The dark SU(2) symmetry is spontaneously broken via a Higgs sector involving doublet and triplet fields. The doublet vacuum expectation value (vev) leads to mixing between the χ and standard model lepton fields, while the triplet vev splits the mass spectrum leaving a simple lower-energy theory consisting of the dark matter (the lightest ψ mass eigenstate) and the mediator (the third component of the SU(2) gauge multiplet). We identify a discrete flavor symmetry that allows mixing between the vector-like leptons χ and a single standard model lepton flavor exclusively; the remaining standard model lepton flavors may mix only with each other. This flavor sequestering eliminates lepton-flavor-violating effects, relaxing bounds on the vector-like lepton mass scale. As a consequence, mixing between the chosen lepton flavor and the χ can be large enough so that the correct relic density can be obtained exclusively via dark matter annihilation to lepton-anti-lepton pairs, for perturbative values of the dark gauge coupling. This is true even if no other significant annihilation channels are available.

The structure of our model avoids complications that would ensue if we tried to couple the dark gauge bosons directly to standard model fields, such as the necessity of including extraneous fermions to cancel chiral anomalies, or special Higgs representations to allow for acceptable standard model Yukawa couplings. Unlike some of the non-Abelian dark

matter models appearing in the literature, the portal we present is renormalizable and completely specified, including the discrete flavor symmetries that control the pattern of mixing between exotic and standard model fermions states. The portal we define for communication between the dark and visible sectors can be lighter than in models without the flavor sequestering we have proposed and presents a well defined framework for answering phenomenological questions. In this chapter, we showed that there are regions of the dark gauge coupling - dark matter mass plane where the correct relic density is obtained, and where current direct detection bounds are satisfied. The latter consideration also allowed us to conclude that the two heavy lepton mass eigenstates (roughly the two components of the χ doublet) are notably degenerate in mass (to keep kinetic mixing effects small), a feature that could be tested in collider searches for these states. This observation, together with the distinct lepton flavor structure of the χ decays, suggests that the collider signatures of the portal that we have proposed are worthy of future detailed investigation.

CHAPTER 6

Conclusions

In this thesis we strived to solve various issues either not explained by or included in the Standard Model by extending its particle content and symmetries. In Chapter 1, we solved the flavor problem via a model based on the double tetrahedral group, a discrete subgroup of $SU(2)$. We showed how such models can arise simply in a nonsupersymmetric framework, and found that our theory provides a viable description of charged fermion masses and CKM angles for a range of values of the flavor scale M_F , with a preference for values around the TeV scale. Nonetheless identification of M_F with the reduced Planck scale remains a valid possibility, consistent with a simple picture in which there is no new physics between the weak and gravitational scales. Indirect probes of the model are provided by further constraining the lowest M_F by flavor-changing-neutral-current processes that receive contributions from the physical components of the flavon fields. Here we only considered the charged Yukawa sector, so it would be interesting to incorporate the neutrino sector as an extension of the study.

Whereas we sought to explain the origin of the hierarchies in the fermion mass spectrum in Chapter 2, in Chapter 3 we sought to explain the origins of the Standard Model

gauge couplings. As an alternative to conventional unification, we assumed the existence of a universal Landau pole in which the gauge couplings blow up at a common scale in the ultraviolet. Since all the gauge couplings must be asymptotically non-free to achieve a Landau pole, we added extra matter to the theory. We considered two scales, the scale of supersymmetry breaking m_{susy} and the scale where the additional vector-like states appeared m_V . We revisited the minimal scenario, in which the minimal supersymmetric standard model is augmented by a single vector-like generation of matter fields, but found this to be in some tension with current LHC bounds. Thus we studied extensions of the minimal scenario, which leads to values of m_V that are beyond the reach of the LHC, but potentially within the reach of a 100 TeV hadron collider.

In Chapter 3 we considered unification of the electromagnetic, weak and strong forces, but we turn our focus to the fourth fundamental force in Chapter 4: gravity. We visited a model where gravitational interactions emerged via a constraint of vanishing energy-momentum tensor in a scalar field theory. We generalized this model to accommodate a general field space metric for scalar fields that play the role of clock and rulers by a gauge-fixing condition analogous to the static-gauge condition in string theory. The classical equations of motion admit a background solution, and the quantum theory then admits a perturbative expansion about this background. We wrote the curved-space metric as an expansion about the Minkowski metric and demonstrated that scattering off of the background spacetime is as in general relativity. Our study opens several avenues of exploration, including investigation of the contribution of configurations beyond the static-gauge one, extension of the theory to include scalars with different masses, and definition of a physical regulator that would allow for a well-defined description of the physics at distances shorter than the regulator scale, or else provide an explanation for why such short distances are not meaningful.

Lastly we addressed the issue of dark matter in Chapter 5, with a model containing

a light vector-like fermion portal connecting a dark sector to the standard model. The vector-like lepton is charged under the dark gauge group but has the same electroweak quantum numbers as a right-handed electron, so that communication with the visible sector can occur via mass mixing. To avoid the lepton-flavor-violating processes that emerge when the vector-like leptons mix with all three standard model flavors, we identify a mechanism, based on discrete symmetries, that we have called “flavor sequestering.” This allows for mixing between the vector-like leptons and a single standard model lepton flavor exclusively. We proved that there are regions of the dark gauge coupling - dark matter mass plane where the correct relic density is obtained, and where current direct detection bounds are satisfied. We found that the heavy lepton mass eigenstates are notably degenerate in mass, a feature that could be observed in collider searches for the vector-like leptons and possibly correlated with a dark matter direct detection signal.

BIBLIOGRAPHY

- [1] M. Tanabashi *et al.* [Particle Data Group], “Review of Particle Physics,” *Phys. Rev. D* **98**, 030001 (2018).
- [2] P. Ramond, R. G. Roberts and G. G. Ross, “Stitching the Yukawa quilt,” *Nucl. Phys. B* **406**, 19 (1993) [hep-ph/9303320].
- [3] A. Aranda, C. D. Carone and R. F. Lebed, “U(2) flavor physics without U(2) symmetry,” *Phys. Lett. B* **474**, 170 (2000) [hep-ph/9910392].
- [4] A. Aranda, C. D. Carone and R. F. Lebed, “Maximal neutrino mixing from a minimal flavor symmetry,” *Phys. Rev. D* **62**, 016009 (2000) [hep-ph/0002044].
- [5] Y. Nir and N. Seiberg, “Should squarks be degenerate?,” *Phys. Lett. B* **309**, 337 (1993) [hep-ph/9304307];
- [6] M. Leurer, Y. Nir and N. Seiberg, “Mass matrix models: The Sequel,” *Nucl. Phys. B* **420**, 468 (1994) [hep-ph/9310320];
- [7] D.B. Kaplan and M. Schmaltz, “Flavor unification and discrete non-Abelian symmetries,” *Phys. Rev. D* **49**, 3741 (1994);
- [8] M. Dine, R. G. Leigh and A. Kagan, “Flavor symmetries and the problem of squark degeneracy,” *Phys. Rev. D* **48**, 4269 (1993) [hep-ph/9304299];
- [9] L.J. Hall and H. Murayama, “Geometric Model of the Generations,” *Phys. Rev. Lett.* **75**, 3985 (1995);

- [10] C.D. Carone, L.J. Hall, and H. Murayama, “ $(S_3)^3$ flavor symmetry and $p \rightarrow K^0 e^+$,” Phys. Rev. D **53**, 6282 (1996);
- [11] P. H. Frampton and O. C. W. Kong, “Horizontal symmetry for quark and squark masses in supersymmetric SU(5),” Phys. Rev. Lett. **77**, 1699 (1996) [hep-ph/9603372].
- [12] R. Barbieri, G. R. Dvali and L. J. Hall, “Predictions from a U(2) flavor symmetry in supersymmetric theories,” Phys. Lett. B **377**, 76 (1996) [hep-ph/9512388].
- [13] R. Barbieri, L. J. Hall and A. Romanino, “Consequences of a U(2) flavor symmetry,” Phys. Lett. B **401**, 47 (1997) [hep-ph/9702315].
- [14] R. Barbieri, L. J. Hall, S. Raby and A. Romanino, “Unified theories with U(2) flavor symmetry,” Nucl. Phys. B **493**, 3 (1997) [hep-ph/9610449].
- [15] P. Langacker, “Grand Unified Theories and Proton Decay,” Phys. Rept. **72**, 185 (1981).
- [16] G. G. Ross, “Grand Unified Theories,” Reading, Usa: Benjamin/cummings (1984) 497 P. (Frontiers In Physics, 60)
- [17] K. Abe *et al.* [Super-Kamiokande Collaboration], “Search for proton decay via $p \rightarrow e^+ \pi^0$ and $p \rightarrow \mu^+ \pi^0$ in 0.31??megatonyears exposure of the Super-Kamiokande water Cherenkov detector,” Phys. Rev. D **95**, no. 1, 012004 (2017) [arXiv:1610.03597 [hep-ex]].
- [18] T. Moroi, H. Murayama and T. Yanagida, “The Weinberg angle without grand unification,” Phys. Rev. D **48**, R2995 (1993) [hep-ph/9306268].
- [19] D. Ghilencea, M. Lanzagorta and G. G. Ross, “Strong unification,” Phys. Lett. B **415**, 253 (1997). [hep-ph/9707462].

- [20] S. Deser, “Infinities in quantum gravities,” *Annalen Phys.* **9**, 299 (2000) [gr-qc/9911073].
- [21] L. J. Dixon, “Ultraviolet Behavior of $\mathcal{N} = 8$ Supergravity,” *Subnucl. Ser.* **47**, 1 (2011) [arXiv:1005.2703 [hep-th]].
- [22] J. D. Bjorken, “A Dynamical origin for the electromagnetic field,” *Annals Phys.* **24**, 174 (1963).
- [23] T. Eguchi, “A New Approach to Collective Phenomena in Superconductivity Models,” *Phys. Rev. D* **14**, 2755 (1976).
- [24] D. Amati and M. Testa, “Quark imprisonment as the origin of strong interactions,” *Phys. Lett.* **48B**, 227 (1974).
- [25] G. Rajasekaran and V. Srinivasan, “Generation of Gluons from Quark Confinement,” *Pramana* **10**, 33 (1978).
- [26] A. D. Sakharov, “Vacuum quantum fluctuations in curved space and the theory of gravitation,” *Sov. Phys. Dokl.* **12**, 1040 (1968) [*Dokl. Akad. Nauk Ser. Fiz.* **177**, 70 (1967)] [*Sov. Phys. Usp.* **34**, 394 (1991)] [*Gen. Rel. Grav.* **32**, 365 (2000)].
- [27] C. D. Carone, J. Erlich and D. Vaman, “Emergent Gravity from Vanishing Energy-Momentum Tensor,” *JHEP* **1703**, 134 (2017) [arXiv:1610.08521 [hep-th]].
- [28] M. Lisanti, “Lectures on Dark Matter Physics,” arXiv:1603.03797 [hep-ph].
- [29] D. S. Akerib *et al.* [LUX Collaboration], *Phys. Rev. Lett.* **118**, no. 2, 021303 (2017) doi:10.1103/PhysRevLett.118.021303 [arXiv:1608.07648 [astro-ph.CO]].

- [30] E. Aprile *et al.* [XENON Collaboration], “First Dark Matter Search Results from the XENON1T Experiment,” *Phys. Rev. Lett.* **119**, no. 18, 181301 (2017) [arXiv:1705.06655 [astro-ph.CO]].
- [31] R. Agnese *et al.* [SuperCDMS Collaboration], “Results from the Super Cryogenic Dark Matter Search Experiment at Soudan,” *Phys. Rev. Lett.* **120**, no. 6, 061802 (2018) [arXiv:1708.08869 [hep-ex]].
- [32] O. Adriani *et al.* [PAMELA Collaboration], “Cosmic-Ray Positron Energy Spectrum Measured by PAMELA,” *Phys. Rev. Lett.* **111**, 081102 (2013) [arXiv:1308.0133 [astro-ph.HE]].
- [33] M. G. Aartsen *et al.* [IceCube Collaboration], “Search for neutrinos from decaying dark matter with IceCube,” *Eur. Phys. J. C* **78**, no. 10, 831 (2018) [arXiv:1804.03848 [astro-ph.HE]].
- [34] E. W. Kolb and M. S. Turner, “The Early Universe,” *Front. Phys.* **69**, 1 (1990).
- [35] N. Arkani-Hamed, D. P. Finkbeiner, T. R. Slatyer and N. Weiner, “A Theory of Dark Matter,” *Phys. Rev. D* **79**, 015014 (2009) [arXiv:0810.0713 [hep-ph]].
- [36] R. Foot and S. Vagnozzi, “Dissipative hidden sector dark matter,” *Phys. Rev. D* **91**, 023512 (2015) [arXiv:1409.7174 [hep-ph]].
- [37] P. Foldenauer, “Let there be Light Dark Matter: The gauged $U(1)_{L_\mu-L_\tau}$ case,” arXiv:1808.03647 [hep-ph].
- [38] G. Blanger, J. Da Silva and H. M. Tran, “Dark matter in $U(1)$ extensions of the MSSM with gauge kinetic mixing,” *Phys. Rev. D* **95**, no. 11, 115017 (2017) [arXiv:1703.03275 [hep-ph]].

- [39] M. Dutra, M. Lindner, S. Profumo, F. S. Queiroz, W. Rodejohann and C. Siqueira, “MeV Dark Matter Complementarity and the Dark Photon Portal,” *JCAP* **1803**, 037 (2018) [arXiv:1801.05447 [hep-ph]].
- [40] J. Choquette and J. M. Cline, “Minimal non-Abelian model of atomic dark matter,” *Phys. Rev. D* **92**, no. 11, 115011 (2015) [arXiv:1509.05764 [hep-ph]].
- [41] K. Cheung, W. C. Huang and Y. L. S. Tsai, “Non-abelian Dark Matter Solutions for Galactic Gamma-ray Excess and Perseus 3.5 keV X-ray Line,” *JCAP* **1505**, no. 05, 053 (2015) [arXiv:1411.2619 [hep-ph]].
- [42] J. M. Cline and A. R. Frey, “Nonabelian dark matter models for 3.5 keV X-rays,” *JCAP* **1410**, 013 (2014) [arXiv:1408.0233 [hep-ph]].
- [43] J. M. Cline, A. R. Frey and F. Chen, “Metastable dark matter mechanisms for INTEGRAL 511 keV γ rays and DAMA/CoGeNT events,” *Phys. Rev. D* **83**, 083511 (2011) [arXiv:1008.1784 [hep-ph]].
- [44] C. D. Carone, J. Erlich and R. Primulando, “Decaying Dark Matter from Dark Instantons,” *Phys. Rev. D* **82**, 055028 (2010) [arXiv:1008.0642 [hep-ph]].
- [45] F. Chen, J. M. Cline and A. R. Frey, “Nonabelian dark matter: Models and constraints,” *Phys. Rev. D* **80**, 083516 (2009) [arXiv:0907.4746 [hep-ph]].
- [46] H. Zhang, C. S. Li, Q. H. Cao and Z. Li, “A Dark Matter Model with Non-Abelian Gauge Symmetry,” *Phys. Rev. D* **82**, 075003 (2010) [arXiv:0910.2831 [hep-ph]].
- [47] K. Ishiwata and M. B. Wise, “Phenomenology of heavy vectorlike leptons,” *Phys. Rev. D* **88**, no. 5, 055009 (2013) [arXiv:1307.1112 [hep-ph]].

- [48] I. Girardi, A. Meroni, S. T. Petcov and M. Spinrath, “Generalised geometrical CP violation in a T' lepton flavour model,” JHEP **1402**, 050 (2014) [arXiv:1312.1966 [hep-ph]]; M. C. Chen, J. Huang, K. T. Mahanthappa and A. M. Wijangco, “Large θ_{13} in a SUSY $SU(5)\times T'$ Model,” JHEP **1310**, 112 (2013) [arXiv:1307.7711 [hep-ph]]; P. H. Frampton, C. M. Ho and T. W. Kephart, “Heterotic discrete flavor model,” Phys. Rev. D **89**, no. 2, 027701 (2014) [arXiv:1305.4402 [hep-ph]]; Y. H. Ahn, “Leptons and Quarks from a Discrete Flavor Symmetry,” Phys. Rev. D **87**, no. 11, 113011 (2013) [arXiv:1303.4863 [hep-ph]]; A. Meroni, E. Molinaro and S. T. Petcov, “Revisiting Leptogenesis in a SUSY $SU(5)\times T'$ Model of Flavour,” Phys. Lett. B **710**, 435 (2012) [arXiv:1203.4435 [hep-ph]]; D. A. Eby and P. H. Frampton, “Nonzero θ_{13} signals nonmaximal atmospheric neutrino mixing,” Phys. Rev. D **86**, 117304 (2012) [arXiv:1112.2675 [hep-ph]]; D. A. Eby and P. H. Frampton, “Dark Matter from Binary Tetrahedral Flavor Symmetry,” Phys. Lett. B **713**, 249 (2012) [arXiv:1111.4938 [hep-ph]]; D. A. Eby, P. H. Frampton, X. G. He and T. W. Kephart, “Quartification with T' Flavor,” Phys. Rev. D **84**, 037302 (2011) [arXiv:1103.5737 [hep-ph]]; M. C. Chen, K. T. Mahanthappa and F. Yu, “A Viable Randall-Sundrum Model for Quarks and Leptons with T' Family Symmetry,” Phys. Rev. D **81**, 036004 (2010) [arXiv:0907.3963 [hep-ph]]; M. C. Chen and K. T. Mahanthappa, “Group Theoretical Origin of CP Violation,” Phys. Lett. B **681**, 444 (2009) [arXiv:0904.1721 [hep-ph]]; P. H. Frampton, T. W. Kephart and S. Matsuzaki, “Simplified Renormalizable T' Model for Tribimaximal Mixing and Cabibbo Angle,” Phys. Rev. D **78**, 073004 (2008) [arXiv:0807.4713 [hep-ph]]; C. Luhn, “Discrete Anomalies of Binary Groups,” Phys. Lett. B **670**, 390 (2009) [arXiv:0807.1749 [hep-ph]]; G. J. Ding, “Fermion Mass Hierarchies and Flavor Mixing from T' Symmetry,” Phys. Rev. D **78**, 036011 (2008) [arXiv:0803.2278 [hep-ph]]; S. Sen, “Quark masses in supersymmetric $SU(3)_C\times SU(3)_W\times U(1)_X$ model with discrete T' flavor symmetry,” Phys. Rev. D

- 76**, 115020 (2007) [arXiv:0710.2734 [hep-ph]]; A. Aranda, “Neutrino mixing from the double tetrahedral group T' ,” Phys. Rev. D **76**, 111301 (2007) [arXiv:0707.3661 [hep-ph]]; P. H. Frampton and T. W. Kephart, “Flavor Symmetry for Quarks and Leptons,” JHEP **0709**, 110 (2007) [arXiv:0706.1186 [hep-ph]]; M. C. Chen and K. T. Ma-hanthappa, “CKM and Tri-bimaximal MNS Matrices in a $SU(5) \times {}^{(d)}T$ Model,” Phys. Lett. B **652**, 34 (2007) [arXiv:0705.0714 [hep-ph]]; F. Feruglio, C. Hagedorn, Y. Lin and L. Merlo, “Tri-bimaximal Neutrino Mixing and Quark Masses from a Discrete Flavour Symmetry,” Nucl. Phys. B **775**, 120 (2007) Erratum: [Nucl. Phys. B **836**, 127 (2010)] [hep-ph/0702194]; P. H. Frampton and T. W. Kephart, “Simple non-Abelian finite flavor groups and fermion masses,” Int. J. Mod. Phys. A **10**, 4689 (1995) [hep-ph/9409330].
- [49] M. Ibe, S. Matsumoto and T. T. Yanagida, “Flat Higgs Potential from Planck Scale Supersymmetry Breaking,” Phys. Lett. B **732**, 214 (2014) [arXiv:1312.7108 [hep-ph]].
- [50] S. Abel, K. R. Dienes and E. Mavroudi, “Towards a nonsupersymmetric string phenomenology,” Phys. Rev. D **91**, no. 12, 126014 (2015) [arXiv:1502.03087 [hep-th]].
- [51] P. W. Graham, D. E. Kaplan and S. Rajendran, “Cosmological Relaxation of the Electroweak Scale,” Phys. Rev. Lett. **115**, no. 22, 221801 (2015) [arXiv:1504.07551 [hep-ph]].
- [52] S. Dubovsky, V. Gorbenko and M. Mirbabayi, “Natural Tuning: Towards A Proof of Concept,” JHEP **1309**, 045 (2013) [arXiv:1305.6939 [hep-th]].
- [53] H. Georgi and C. Jarlskog, Phys. Lett. **86B**, 297 (1979).
- [54] V. Barger, M.S. Berger, and P. Ohmann, “Supersymmetric grand unified theories: Two-loop evolution of gauge and Yukawa couplings,” Phys. Rev. D **47**, 3 (1993).

- [55] M. E. Peskin, “Beyond the standard model,” In *Carry-le-Rouet 1996, High-energy physics* 49-142 [hep-ph/9705479].
- [56] N. Carrasco *et al.* [ETM Collaboration], “ $S = 2$ and $C = 2$ bag parameters in the standard model and beyond from $N_f=2+1+1$ twisted-mass lattice QCD,” Phys. Rev. D **92**, no. 3, 034516 (2015) [arXiv:1505.06639 [hep-lat]].
- [57] A. Bazavov *et al.* [Fermilab Lattice and MILC Collaborations], “ $B_{(s)}^0$ -mixing matrix elements from lattice QCD for the Standard Model and beyond,” Phys. Rev. D **93**, no. 11, 113016 (2016) [arXiv:1602.03560 [hep-lat]].
- [58] J. L. Rosner, S. Stone and R. S. Van de Water, “Leptonic Decays of Charged Pseudoscalar Mesons - 2015,” [arXiv:1509.02220 [hep-ph]].
- [59] M. Carpentier and S. Davidson, “Constraints on two-lepton, two quark operators,” Eur. Phys. J. C **70**, 1071 (2010) [arXiv:1008.0280 [hep-ph]].
- [60] L. Maiani, G. Parisi and R. Petronzio, “Bounds on the Number and Masses of Quarks and Leptons,” Nucl. Phys. B **136**, 115 (1978).
- [61] N. Cabibbo and G. R. Farrar, “An Alternative To Perturbative Grand Unification: How Asymptotically Nonfree Theories Can Successfully Predict Low-energy Gauge Couplings,” Phys. Lett. **110B**, 107 (1982).
- [62] L. Maiani and R. Petronzio, “Low-energy Gauge Couplings and the Mass Gap of $N = 1$ Supersymmetry,” Phys. Lett. B **176**, 120 (1986) Erratum: [Phys. Lett. B **178**, 457 (1986)].
- [63] A. A. Andrianov, D. Espriu, M. A. Kurkov and F. Lizzi, “Universal Landau Pole,” Phys. Rev. Lett. **111**, no. 1, 011601 (2013).

- [64] G. Parisi, “On the Value of Fundamental Constants,” *Phys. Rev. D* **11**, 909 (1975).
- [65] T. Eguchi and H. Sugawara, “Extended Model of Elementary Particles Based on an Analogy with Superconductivity,” *Phys. Rev. D* **10**, 4257 (1974).
- [66] K. R. Dienes, “String theory and the path to unification: A Review of recent developments,” *Phys. Rept.* **287**, 447 (1997) [hep-th/9602045].
- [67] Y. Yamada, “Two loop renormalization of gaugino masses in general supersymmetric gauge models,” *Phys. Rev. Lett.* **72**, 25 (1994) [hep-ph/9308304].
- [68] M.E. Machacek and M. T. Vaughn, “Two Loop Renormalization Group Equations in a General Quantum Field Theory. 1. Wave Function Renormalization,” *Nucl. Phys. B* **222**, 83 (1983).
- [69] I. Antoniadis, C. Kounnas and R. Lacaze, “Light Gluinos in Deep Inelastic Scattering,” *Nucl. Phys. B* **211**, 216 (1983).
- [70] The ATLAS collaboration [ATLAS Collaboration], “Search for squarks and gluinos in final states with jets and missing transverse momentum using 36 fb^{-1} of $\sqrt{s} = 13$ TeV pp collision data with the ATLAS detector,” ATLAS-CONF-2017-022.
- [71] CMS Collaboration [CMS Collaboration], “Search for vector-like quark pair production $T\bar{T}(Y\bar{Y}) \rightarrow bWbW$ using kinematic reconstruction in lepton+jets final states at $\sqrt{s}=13$ TeV,” CMS-PAS-B2G-17-003.
- [72] N. Arkani-Hamed, T. Han, M. Mangano and L. T. Wang, “Physics opportunities of a 100 TeV proton-proton collider,” *Phys. Rept.* **652**, 1 (2016) [arXiv:1511.06495 [hep-ph]].

- [73] S. Bhattacharya, J. George, U. Heintz, A. Kumar, M. Narain and J. Stupak, “Prospects for a Heavy Vector-Like Charge $2/3$ Quark T search at the LHC with $\sqrt{s} = 14$ TeV and 33 TeV.” A Snowmass 2013 Whitepaper”, arXiv:1309.0026 [hep-ex].
- [74] T. Golling *et al.*, “Physics at a 100 TeV pp collider: beyond the Standard Model phenomena,” Submitted to: Phys. Rept. [arXiv:1606.00947 [hep-ph]].
- [75] C. Liu and Z. h. Zhao, “A Realization of Effective SUSY with Strong Unification,” Phys. Rev. D **89**, no. 5, 057701 (2014) [arXiv:1312.7389 [hep-ph]]; C. Liu, “[SU(3) x SU(2) x U(1)]² and strong unification,” Phys. Lett. B **591**, 137 (2004) [hep-ph/0405271].
- [76] B. S. DeWitt, “Quantum Theory of Gravity. 1. The Canonical Theory,” Phys. Rev. **160**, 1113 (1967).
- [77] M. Faraday, T. Martin (ed.), Faraday’s Diary of Experimental Investigation 1820-1862, Vol. V, entries 10018, 10061, The Royal Institution of Great Britain, HR Direct, (2008).
- [78] K. Akama, “An Attempt at Pregeometry: Gravity With Composite Metric,” Prog. Theor. Phys. **60**, 1900 (1978).
- [79] K. Akama, Y. Chikashige, T. Matsuki and H. Terazawa, “Gravity and Electromagnetism as Collective Phenomena: A Derivation of Einstein’s General Relativity,” Prog. Theor. Phys. **60**, 868 (1978).
- [80] D. Amati and G. Veneziano, “Metric From Matter,” Phys. Lett. B **105**, 358 (1981).
- [81] D. Amati and G. Veneziano, “A Unified Gauge and Gravity Theory With Only Matter Fields,” Nucl. Phys. B **204**, 451 (1982).

- [82] J. M. Maldacena, “The Large N limit of superconformal field theories and supergravity,” *Int. J. Theor. Phys.* **38**, 1113 (1999) [*Adv. Theor. Math. Phys.* **2**, 231 (1998)] [hep-th/9711200].
- [83] E. P. Verlinde, “On the Origin of Gravity and the Laws of Newton,” *JHEP* **1104**, 029 (2011) [arXiv:1001.0785 [hep-th]].
- [84] J. Maldacena and L. Susskind, “Cool horizons for entangled black holes,” *Fortsch. Phys.* **61**, 781 (2013) [arXiv:1306.0533 [hep-th]].
- [85] C. Cao, S. M. Carroll and S. Michalakis, “Space from Hilbert Space: Recovering Geometry from Bulk Entanglement,” *Phys. Rev. D* **95**, no. 2, 024031 (2017) [arXiv:1606.08444 [hep-th]].
- [86] S. Weinberg, ”Critical Phenomena for Field Theorists”. In Zichichi, Antonino, *Understanding the Fundamental Constituents of Matter. The Subnuclear Series.* **14**, pp. 152. ISBN 978-1-4684-0931-4 (1978), S. Weinberg, ”Ultraviolet divergences in quantum theories of gravitation”. In S. W. Hawking; W. Israel. *General Relativity: An Einstein centenary survey*, Cambridge University Press, pp. 790831 (1979).
- [87] D. N. Page and W. K. Wootters, “Evolution Without Evolution: Dynamics Described By Stationary Observables,” *Phys. Rev. D* **27**, 2885 (1983).
- [88] S. Weinberg and E. Witten, “Limits on Massless Particles,” *Phys. Lett. B* **96**, 59 (1980).
- [89] C. D. Carone, T. V. B. Claringbold and D. Vaman, “Composite graviton self-interactions in a model of emergent gravity,” arXiv:1710.09367 [hep-th].
- [90] K. Akama and T. Hattori, “Dynamical Foundations of the Brane Induced Gravity,” *Class. Quant. Grav.* **30**, 205002 (2013) [arXiv:1309.3090 [gr-qc]].

- [91] M. Suzuki, “Composite gauge-bosons made of fermions,” *Phys. Rev. D* **94**, no. 2, 025010 (2016) [arXiv:1603.07670 [hep-th]].
- [92] A. Karam and K. Tamvakis, “Dark matter and neutrino masses from a scale-invariant multi-Higgs portal,” *Phys. Rev. D* **92**, no. 7, 075010 (2015) [arXiv:1508.03031 [hep-ph]]; “Dark Matter from a Classically Scale-Invariant $SU(3)_X$,” *Phys. Rev. D* **94**, no. 5, 055004 (2016) [arXiv:1607.01001 [hep-ph]].
- [93] H. Davoudiasl and I. M. Lewis, “Dark Matter from Hidden Forces,” *Phys. Rev. D* **89**, no. 5, 055026 (2014) [arXiv:1309.6640 [hep-ph]].
- [94] C. W. Chiang, T. Nomura and J. Tandean, “Nonabelian Dark Matter with Resonant Annihilation,” *JHEP* **1401**, 183 (2014) [arXiv:1306.0882 [hep-ph]].
- [95] G. D. Kribs, T. S. Roy, J. Terning and K. M. Zurek, “Quirky Composite Dark Matter,” *Phys. Rev. D* **81**, 095001 (2010) [arXiv:0909.2034 [hep-ph]]; J. L. Feng and Y. Shadmi, “WIMPless Dark Matter from Non-Abelian Hidden Sectors with Anomaly-Mediated Supersymmetry Breaking,” *Phys. Rev. D* **83**, 095011 (2011) [arXiv:1102.0282 [hep-ph]]; K. K. Boddy, J. L. Feng, M. Kaplinghat, Y. Shadmi and T. M. P. Tait, “Strongly interacting dark matter: Self-interactions and keV lines,” *Phys. Rev. D* **90**, no. 9, 095016 (2014) [arXiv:1408.6532 [hep-ph]]; L. Forestell, D. E. Morrissey and K. Sigurdson, “Cosmological Bounds on Non-Abelian Dark Forces,” *Phys. Rev. D* **97**, no. 7, 075029 (2018) [arXiv:1710.06447 [hep-ph]]; M. A. Buen-Abad, G. Marques-Tavares and M. Schmaltz, “Non-Abelian dark matter and dark radiation,” *Phys. Rev. D* **92**, no. 2, 023531 (2015) [arXiv:1505.03542 [hep-ph]].
- [96] E. Witten, “An $SU(2)$ Anomaly,” *Phys. Lett. B* **117**, 324 (1982)

- [97] E. Aprile *et al.* [XENON Collaboration], “Dark Matter Search Results from a One Tonne×Year Exposure of XENON1T,” arXiv:1805.12562 [astro-ph.CO].
- [98] R. Agnese *et al.* [SuperCDMS Collaboration], “Low-mass dark matter search with CDMSlite,” Phys. Rev. D **97**, 022002 (2018).

VITA

Shikha Chaurasia

Shikha Chaurasia was born on August 17, 1991 in Lawrence, Kansas, but basically grew up in Olney, Maryland. She was always fostering an affinity for math and science, but didn't realize it till she tried to step away from it and felt a bit lost. And so she chose to major in physics, astrophysics and math at the College of Charleston, where her passion for these subjects blossomed. She earned her Bachelor of Science degree in May of 2014 and joined the College of William & Mary the following fall for her graduate studies. She obtained her Master of Science in physics in 2016 and began working with Dr. Christopher D. Carone in the theoretical high energy group, where she studied physics beyond the standard model.